UCRL-53179-81

Fire-Protection Research for Energy-Technology Projects

FY 1981 Year-End Report

H. K. Hasegawa

N. J. Alvares

A. E. Lipska-Quinn

D. G. Beason

K. L. Foote

S. J. Priante

July 20, 1982

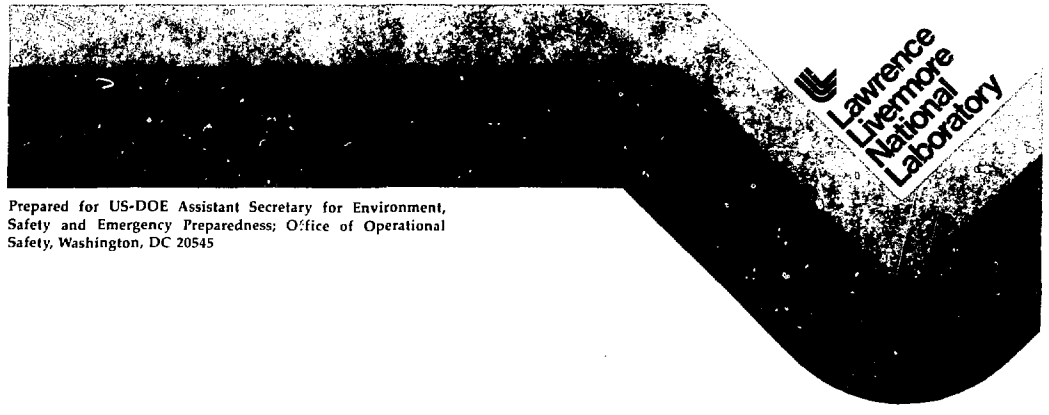

Prepared for US-DOE Assistant Secretary for Environment, Safety and Emergency Preparedness; Office of Operational Safety, Washington, DC 20545

Work performed under the auspices of the U.S. Department of Energy by Lawrence Livermore National Laboratory under Contract W-7405-Eng-48.

UCRL-53179-81
Distribution Category UC-20,20D,41

Fire-Protection Research for Energy-Technology Projects

FY 1981 Year-End Report

H. K. Hasegawa

N. J. Alvares

A. E. Lipska-Quinn

D. G. Beason

K. L. Foote

S. J. Priante

Manuscript date: July 20, 1982

LAWRENCE LIVERMORE LABORATORY
University of California • Livermore, California • 94550

Available from National Technical Information Service • U.S. Department of Commerce
5285 Port Royal Road • Springfield, VA 22161 • $12.00 per copy • (Microfiche $3.50)

CONTENTS

LIST OF FIGURES

LIST OF TABLES

Fire Protection Research for Energy Technology Projects
FY 1981 Year-End Report

H. K. Hasegawa, N. J. Alvares, A. E. Lipska-Quinn
D. G. Beason, K. L. Foote, and S. J Priante

ABSTRACT

This report summarizes research conducted in fiscal year 1981 for the DOE-supported project, "Fire Protection Research for Energy Technology Projects." Initiated in 1977, this ongoing research program was conceived to advance fire protection strategies for Energy Technology Projects to keep abreast of the unique fire problems that are developing with the complexity of energy technology research.

We are developing an analytical methodology through detailed study of fusion energy experiments at Lawrence Livermore National Laboratory (LLNL). Employing these facilities as models for methodology development, we are simultaneously advancing three major task areas:

- Determination of unique fire hazards of current fusion energy facilities.
- Evaluation of the ability of accepted fire management measures to meet and negate hazards.
- Performance of unique research into problem areas we have identified to provide input into analytical fire-growth and damage-assessment models.

INTRODUCTION

This document accounts for work done in fiscal year 1981 for a DOE-funded study entitled, "Fire Protection Research for Energy Technology Projects." Originally, the scope was limited to fusion energy research facilities, but it is now expanded to include other selected forms of energy research. As our study progressed we felt that logic and analytical methodologies developed for fusion facilities could be applied to a range of emerging and established energy technologies.

Figure 1 is a general schematic of the overall logic of the fire safety evaluation and Table 1 lists tasks we are advancing to achieve our major

goals. An ultimate output of this study is to assess potential fire damage in these facilities. To accomplish this, three parameters must be evaluated: (1) fire threat potential to the facility, (2) response and effectiveness of fire management systems, and (3) resultant fire-related damage.

We continued to modify and refine room-filling models in our efforts to predict potential fire/smoke threat to these facilities. In FY'81 we conducted a series of semi-ideal forced ventilation enclosure fire tests designed to produce data to compare to analytical results from room-filling codes. We also performed a series of large-scale cable fires (prototype) and magnetic tape fires. Furthermore, we expanded our cable library by 20 generic types of insulation and continue the analysis of their thermal degradation kinetics. Chemical analysis of acid ion release mechanisms continues to progress. Since our findings indicate that extensive damage to sensitive electronics and optics can be caused by corrosive combustion products, even from small fires that do not create substantial thermal hazards, this portion of the research is of primary importance.

Parameters evaluations of detection and suppression hardware were conducted to establish the commercial state-of-the-art, and we made studies of unique components of generic polymers to use as specific tracers for fire source and location detection. The first mailing of the off-site survey questionnaires was returned and evaluated during this period. Discussion and analysis of these materials reveal that the survey format and content raised more questions than it provided insight to off-site fire management procedures.

History and background for this report are contained in previous publications.[1,2,3]

Our accomplishments for fiscal year 1981 are listed below. Specific topics are described in detail in the text of the report.

CHEMISTRY

- LLNL electrical cable stock delineation and reduction to 20 generic types of insulation.
- Thermogravimetric and differential scanning analyses of generic cable insulation types and identification of similarities and differences.
- Comparison of thermal properties of cable insulation types with pure polymer (neoprene and PVC) to identify effects of plasticizers and additives.
- Chemical analysis of acid ion release mechanisms.

- Comparison of kinetics of thermal degradation of cable insulation types with pure polymer (neoprene and PVC) to identify effects of plasticizers and additives.

PHYSICAL SMOKE

- Established calibration procedure for aerosols used in dilution studies.
- Adapted porous tube sampling probe to produce aerosol dilution without changing aerosol distribution.

LARGE-SCALE EXPERIMENTS AND MODELING

- Magnetic tape fire experiments.
- Fire tests for model studies.
- Model-fire test correlation studies.
- Developed and tested algorithms for correlation studies.
- Preliminary large-scale cable experiments.

EXTINGUISHANT STUDIES

- AFFF application to gasohol fires.
- Effectiveness of gaseous extinguishants on magnetic tape fires.

DETECTOR STUDIES

- State-of-the-art survey of the operation and reliability of early warning detection systems.

FIRE RISK ANALYSIS

- Preliminary application of risk assessment protocol to a LLNL fusion facility.
- First mailing and evaluation of the off-site fire management system questionnaires.

This report is structured so that progress in the above listed items will be described in major sections as listed below:

(1) Large-Scale Experiments
- Magnetic tape studies
  - (a) Analysis for acid ion (see Ref. 4)
  - (b) Portable extinguishers
  - (c) Total-flooding extinguishant
- Prototype large-scale cable burns

(2) Off-Site Questionnaires Review

(3) Fire Risk Analysis (see Appendix A)

(4) Fire Modeling (see Appendices B and C)

(5) Fire Chemistry
- Detailed thermal degradation of polymeric electrical insulations

(6) Physical Smoke Studies (see Appendix D)

(7) Smoke Detector Survey (see Appendix D)

(8) Conclusions and Future Work

A major advancement in FY'81 was the performance of a number of large-scale fire experiments which are presented in the first section.

MAGNETIC TAPE FIRE EXPERIMENTS

The following study was pursued in two parts. The research presented below was the second phase dealing with magnetic tape fire dynamics and the effectiveness of extinguishants. Initially, a short experimental series was completed to evaluate the corrosive effects of the combustion gases, the results of which were presented in Reference 4.

Potential high-loss areas in energy technology projects include experiment control rooms and computer facilities. In this case, high loss is a combination of expensive computational and diagnostic electronics along with sizeable "down time" for the facility resulting in lost research time. The majority of these areas, especially computer centers, house great numbers of magnetic tape reels commonly encased in polymeric covers of ABS or polypropylenes. Furthermore, normal storage protocol is to stand or hang tapes vertically with a uniform space between each. In terms of fire spread, this configuration combines maximum surface-to-volume ratios with near optimal air entrainment resulting in very fast fire spread if a fire were to occur.

Both particulate and corrosive components of the combustion gases from a moderate fire would have damaging effects on electronic equipment. This would also be true of portable extinguishers which discharge a particulate extinguishant on fires; e.g., dry chemical. Since tape storage normally shares the same space with computers or spaces which communicate with computer rooms, without timely and effective extinguishment sensitive computational and diagnostic electronics could suffer major smoke and fire damage.

Due to the above reasons, we conducted a research program to evaluate the fire potential of tape reels and the effectiveness of appropriate countermeasures. We investigated and evaluated the fire suppression effectiveness of:

- 7.7-kg (17-lb) Halon 1211 portable extinguisher.
- 2.25-kg (5-lb) Halon 1211 portable extinguisher.
- 6.8-kg (15-lb) carbon dioxide (CO_2) portable fire extinguisher.
- Fixed wet pipe sprinkler.
- Halon 1301 total flooding system.

Following a visual survey of various types of tape storage racks used at LLNL, we fabricated the unit shown in Fig. 2. Due to the following design features, we felt that this configuration would enhance the growth rate and severity of the fire:

- It is a free-standing open rack which allows maximum air entrainment to all tape reel surfaces.
- The rack provides positive support to hold the tapes upright throughout the burn with a uniform space between each which ensures that they remain in place and burn with maximum surface-to-volume ratios.

This three-level rack, containing nine tapes per shelf, was used throughout the series. Each test was initiated with a low bunsen burner flame and was allowed to develop to one of two stages: (1) a low-level fire, defined as fire involvement of the tapes on the lowest shelf and partial involvement of those on the second shelf, or (2) a high-intensity fire, defined as the full involvement of all three shelves.

In our efforts to reproduce these two fire conditions, we supplemented our visual judgement of fire size by monitoring temperatures at each level on the rack. Reproducibility of the two fire intensities from test to test was imperative to conduct a proper comparison of the various modes of extinguishment (i.e., the respective agents had to be applied to as near to the same fire conditions as possible.)

PORTABLE FIRE EXTINGUISHER EXPERIMENTS

For the portable extinguishers (CO_2 and Halon 1211) the research plan was to test their effectiveness on the low-intensity fire and, if successful, repeat the experiments with the high-intensity fire. However, the first experiment in the series was to determine the time-dependent processes occurring during the development of a deep-seated, fully involved fire and to monitor the following:

- The time at which a 165°F fusible link sprinkler, mounted directly above the fire, would activate and its effectiveness in knocking down the fire.
- The length of time for an ionization-type smoke detector located in a remote corner of the test cell ceiling to activate.
- Temperatures at different levels on the rack.
- Dynamic mass-loss rate of fire.
- Fire development diagnostics.

This first experiment served as a baseline fire exposure which enabled us to define the levels of low- and high-intensity fires. After reviewing videotapes of magnetic tape burns we had performed previously, we decided that the bunsen burner was an appropriate ignition source for this application. The low intensity of the burner produced a very slow initial fire development which enabled us to pick a number of points in time to apply extinguishant for the low-intensity fire.

Figure 3 is a photo of the experimental set-up with the location of the sprinkler head and smoke detector. Both devices were approximately 2.1 m - 2.4 m (7-8 ft) above the top of the rack.

Pertinent observations for this experiment were the following:

- The gas to bunsen burner turned on to preset level and ignited at t_o.
- The gas to burner shut off at t_o + 210 s.
- The smoke detector sounded at t_o + 223 s.
- The sprinkler head fused and discharged water at t_o + 402 s.

As can be seen from the temperature plots of the middle and top racks (Fig. 4), the fire was deep-seated when the sprinkler discharged. The single sprinkler head at a flowrate of 136 l/min (36 gpm) at 496 kPa (72 psig) produced a coverage of about 23 l/min/m^2 (.57 gpm/ft^2) which did not extinguish the fire. Although the sprinkler's response time was minimized by positioning it directly over the fire, its effectiveness was reduced due to the sparseness of droplets in the center of the spray pattern (Fig. 5 shows

the air temperature next to the sprinkler head). Furthermore, because it was a three-tier rack, water penetration to the middle and bottom levels would be difficult. Fig. 6 is a photo of the fully developed fire and Fig. 7 shows the post-test remains. The total mass loss for the burn was a little less than 2 kg which is not a lot of fuel relative to the size of the resultant fire.

From the video records and temperature plots of this initial fire, we picked a low, medium, and high fire intensity. We then reproduced these levels and tested the effectiveness of the portable extinguishers on them.

The second experiment involved a 6.8-kg (15-lb) CO_2 extinguisher on the low intensity fire. In this test the burner was turned off at t_o + 120 s and the CO_2 was applied at 263 s. The extinguisher had no problem knocking down the fire in approximately 2 s.

The third experiment tested the effectiveness of a 6.8-kg CO_2 on a medium-intensity fire. In this case the burner was turned off at approximately 150 s and the CO_2 applied at 280 s. For this fire the extinguisher nozzle had to be positioned very close to the flames, about 15.2 cm (6 in.), and CO_2 discharged for 10 s before the fire was put out. The CO_2 was nearly depleted at extinguishment.

We decided to skip the low-intensity fire and test the 7.7-kg (17-lb) Halon 1211 directly on the high-intensity fire. The bunsen burner was shut off at approximately t_o + 90 s, and the fire was fully involved and deep-seated at 315 s (see Fig. 8 temperature plot). Halon 1211 was applied at 375 s at an approximate distance of 6 ft which knocked the fire down completely in around 4 s, using only 2.73 kg (6 lb) of Halon.

This experiment was so successful that we wanted to evaluate the effect of extinguisher size and tried a 2.25-kg (5-lb) 1211 unit on the fully involved fire--it did not terminate the fire. Even though it was only .45 kg (1 lb) less than that used by the 7.7-kg size, apparently the rate of application due to residual Halon and pressure was the margin that affected extinguishment. Consequently, the 2.25-kg unit didn't have sufficient backup "punch" to tackle a fire of this magnitude.

This experimental series dramatically illustrated that the 7.7-kg Halon 1211 extinguisher was far superior to CO_2 and, possibly, sprinkler water spray for this application. The fact that 1211 starts out in liquid form, then vaporizes when it hits the fire, allows the user to effectively apply Halon from a safe distance.

TOTAL-FLOODING HALON 1301 EXPERIMENTS

To complete this experimental series we also conducted two large-scale magnetic tape burns to evaluate the effectiveness of a fixed, total-flooding Halon 1301 system. As in the previous series, we used two different fire intensities:

(1) An incipient fire with Halon discharged shortly after the firing of two cross-zone smoke detectors.

(2) A deep-seated fire of approximately the same intensity as the deep-seated fires in the portable fire extinguisher experiments.

Unfortunately, we had only a limited quantity of Halon 1301--two spheres containing 6.8 kg (15 lb) each (see Fig. 9). Our calculations showed that a volume of approximately 14.15 m^3 (500 ft^3) would retain a Halon concentration of 5% to 6% for the amount of extinguishant in each sphere. Therefore, we constructed the 2.4 m × 2.4 m × 2.4 m (8 ft × 8 ft × 8 ft) high compartment shown in Fig. 10. The .91 m × .61 m (3 ft × 2 ft) opening in the ceiling was added in an attempt to aid visual observations by venting a portion of the smoke. Our calculations for Halon concentration included the leakage through this hole which had only a negligible effect on the concentration.

The experimental configuration and location of instrumentation are shown in Fig. 11. In addition, Figs. 12, 13, and 14 show the tape rack set-up, location and configuration of Halon nozzle, and view through compartment door, respectively. As in the previous burns, a bunsen burner was used as the ignition source as shown in Fig. 15. In conjunction with evaluating the effectiveness of 1301, we also wanted to determine the effect of the decomposed extinguishant on the programming recorded on tapes which were not directly involved in the fire. Four pre-programmed tapes were placed on a rack in a remote corner of the compartment and shielded from the radiant component of the fire by a piece of gypsum wallboard as shown in Fig. 16. To insure that these tapes did not experience excessive air temperatures, we installed a thermocouple in this area.

In total, the following conditions were monitored during the experiments;

(a) Temperatures.

- At the various locations in the compartment.
- The four levels of the tape rack.

- In the remote corner near the pre-programmed tapes.
- In the ignition flame.

(b) Oxygen concentration.

(c) Halon 1301 concentration at several locations in the compartment.

(d) Heat fluxes from the burning computer tapes.

(e) A pressure transducer tied into the Halon discharge line to determine the exact duration of gaseous release (see Fig. 9).

The two detectors attached to the ceiling, shown in Fig. 17, were typical ionization-type used here at LLNL. Each was wired into its own zone as indicated by a standard Zone Indicating Unit (ZIU) and powered by a Fire Indicating Unit (FIU). Since the detectors were wired into separate zones they are referred to as "cross-zoned." Typically, 1301 systems under computer room floors will not discharge unless detectors from two different zones fire to avoid costly discharges due to false alarms. We wanted to duplicate this situation for the first experiment, which would also mean that the fire would be in its incipient stage, thereby testing the effectiveness of Halon on a low-intensity fire. As mentioned previously, the fully involved, deep-seated fire would be very near the same fire used in the portable extinguisher fires.

The following is a summary of the results for the two experiments.

Test #1. Halon 1301 discharged 20 s after the firing of the two cross-zoned smoke detectors.

(a) Ignition of bunsen burner: 0 s.

(b) First detector fires and ignition of first level of tapes on rack: +45 s.

(c) Second detector fires and ignition of second level: +120 s.

(d) Halon 1301 manually discharged: +140 s.

Results. Total discharge time of gas was 3 s. There was an immediate knockdown of the fire with an average Halon concentration of 5%.

Test #2. Halon discharged after the fire had become deep-seated.

(a) Ignition of bunsen burner: 0 s.

(b) Ignition of first rack: +30 s.

(c) First detector fires: +70 s.

(d) Second detector fires: +100 s.

(e) Ignition of the second level on the rack: +150 s.

(f) Burner shut off: +180 s.

(g) Ignition of third level on the rack: +205 s.

(h) Fire fully involved: +300 s.

(i) Halon discharged: +325 s.

Results. Discharge duration 3.75 s. Average Halon 1301 concentration 5%. The fire was knocked down immediately with the exception of slight, residual smoldering in the bottom level of the rack for about 15 min.

Discussion

After studying the videotape records and the time/temperature plots for the various rack levels (see Fig. 18), it can be seen that both fires had similar growth histories up until the point where the first fire was extinguished.

In both experiments the pre-programmed tapes in the remote corner were unaffected by the 1301 and retained their programming. This result is more significant for the deepseated fire, since it was longer in duration and, consequently, more intense. From the time/temperature plots in Fig. 18, it is more than likely that the 1301 decomposed in Test #2 which would mean the generation of hydrogen bromide. Literature[5] states that Halon 1301 begins to decompose above 485°C (~900°F) and the bottom level of the tape rack had achieved this temperature. It should also be noted that in the second run the air temperature around the pre-programmed tapes peaked at 60°C at extinguishment. Figs. 19 and 20 show the condition of the tapes after experiment #1 and #2 respectively. The difference in fire intensities is obvious in the two photos; experiment #1 shows very minor damage compared to the second run which illustrates almost total destruction.

Detector response for both devices was fairly rapid (120 and 100 s for the second detector) in these experiments. However, in both cases, it was the detector closest to the fire which was the last to key. This firing of the second detector was delayed because it was located too close to the corner in the compartment in addition to being in the direct path of the inlet air flow.

Nevertheless, both fires were extinguished immediately and effectively by the 1301, which is surprising for the deepseated fire because the Halon concentration was only at 5% and had a very short soak time (10-45 s depending on location in the compartment for both tests).

To ensure that the fire was not oxygen-limited at the time of extinguishment we monitored the O_2 concentration during the experiments. It can be seen in Fig. 21 that in neither instance did the O_2 drop below 20% before the extinguishant was expelled into the compartment, which is indicated by the drop at 215 s and 315 s respectively. These data show that the knockdown of the fire was not aided by the "smothering" effects of combustion gases. Finally, Figs. 22 and 23 are composite plots of temperatures at various locations in the compartment, showing relatively low air temperatures for both tests. Similarly, heat fluxes were very low.

Conclusions

Even though just two experiments were conducted in this series, the results were encouraging. Firstly, the calculations for Halon concentration gave an accurate prediction for the actual concentration in the compartment. Secondly, recommendations from Halon design manuals normally suggest a much higher concentration (>10%) and long soak times for "deepseated" fires. However, it may be argued that even a well-developed magnetic tape fire does not fit the classic definition of a deepseated fire. In any case, Halon 1301 concentrations above 7-8% are not recommended for spaces occupied by humans. Since most computer and control room facilities have personnel adjacent to or within tape storage areas, 1301 normally would not be recommended above the floor. This experimental series was not extensive enough to make any definite statements about lowering concentration and soak time requirements for these fires. Furthermore, other contents in these areas would have to be taken into account (i.e., computer printout, combustible furnishings, etc.) for the appropriateness of extinguishant. Nevertheless, a modest amount of further research in this area could prove to be valuable in the protection of tape storage facilities.

PROTOTYPE LARGE-SCALE CABLE FIRE EXPERIMENTS

In an effort to obtain design insights for a final experimental configuration, we performed a number of very crude exploratory large-scale vertical cable burns.

Fire performance properties that we eventually hope to evaluate with the final apparatus include, but are not limited to:

- Time to ignition.
- Mass-loss rate.
- Flamespread rate and extent.
- Mass balance; quantity of smoke in proportion to mass burning rate.
- Combustion-gas composition and rate of acid/ion generation.
- O_2, CO, CO_2, and hydrocarbon concentrations.
- Temperatures--
    1. Profile through cross-section of array as well as along cable.
    2. Throughout test cell.
    3. At combustion-gas sampling ports.
    4. Air inlet and outlet.
    5. Ignition source flame.
- Input and output heat fluxes.

The prototype set-up shown in Fig. 24 includes;

- A 30 cm (12 in.) by .91 m (3 ft) high pipe to maximize the re-radiative effects of the fire.
- A 30 cm (12 in.) diameter methane/air premixed gravel burner ignition source.
- A vent hood above the apparatus to create a vertical draft past the cable and to exhaust combustion products.

EXPERIMENTS

Four monitored burns were conducted in this apparatus. The first two tests utilized (1) a rubber-jacketed multi-conductor cable and (2) a rubber-jacketed stranded copper cable. Both cables were around 1.6 cm (5/8 in.) in diameter and cut to 1.5-1.8 m (5-6 ft) lengths and were threaded into an expanded metal grate (as shown in Fig. 25) which was clamped to the top of the pipe. This grate held the 20-30 cable lengths in a vertical orientation and kept a uniform space between them which also helped duplicate the set-up from test to test.

The second two experiments tested a 2.54-cm (1-in.) and a 1.04-cm (.41-in.) diameter polyvinyl chloride (PVC) jacketed co-axial cable. Fig. 26 shows the cross-sectional composition of both these cables which contain a large percentage of polyethylene dielectric. Both of these cable sizes were previously tested in the SRI International heat-release-rate calorimeter along with a neoprene welding cable (also in Fig. 26). The results of that

experimental series indicated that an input irradiance of approximately 5 W/cm^2 was a threshold flux for sustained burning and a rapid increase in heat-release rate of the cables.

Therefore, the gravel burner was calibrated to expose the horizontal portion of the cable to an irradiance of 5 W/cm^2 at a distance of about 15.3 cm (6 in.). The burner was fueled by a premixture of air and natural gas which produced a heat-release rate of 18.33 kJ/s at a methane flowrate of 0.5 l/s.

Temperatures within the pipe were monitored at four equidistant levels and in the exhaust duct. For visual observation of vertical flamespread, four 5-cm (2-in.) diameter holes were drilled about 18 cm (7 in.) apart. Our experimental protocol was to start the ventilation through the exhaust hood (causing a vertical draft past the cables), ignite the burner and continue this ignition fire until the cables exhibited sustained burning.

RESULTS FOR RUBBER-JACKETED CABLES

As mentioned previously, the first two experiments were both rubber-jacketed cables, one containing multi-conductors and the other containing stranded copper conductor. The pertinent observations for both experiments are listed below.

	Time (s)	
	Multi-Conductor	Stranded Copper
Ventilation started and burner ignited	0	0
Sustained ignition of horizontal section of the cable and burner shutoff	135	180
Vertical flamespread		
17.78 cm (7 in.)	135	180
35.6 cm (14 in.)	180	215
53.3 cm (21 in.)	225	225
71.1 cm (28 in.)	270	240
Out the top >1.02 m	285	245

Figures 27 and 28 which are composite plots of the temperatures recorded at four levels within the pipe substantiate the visual observations of

flamespread. There was a close similarity in the time/temperature histories between the two tests. Since both cables had the same jacket material and were of the same diameter, this similarity is not surprising, not to mention that flamespread rate is primarily a surface phenomenon after ignition. These points were substantiated from post-test weighings and examinations that indicated that very little of the rubber jacketing had actually burned off and the majority of damage was limited to the surface of the jacketing. A photograph of typical fire damage is included as Fig. 29, and Fig. 30 shows a test in progress.

RESULTS FOR PVC-JACKETED CABLES

The third and fourth burns tested two different size co-axial cables; RG 220 A/U and RG 11 A/U which are 2.54 cm (1 in.) and 1.04 cm (.41 in.) in diameter respectively. As shown previously in Fig. 26 they are of identical composition but the RG 11 A/U is about half the diameter of the larger cable. In terms of fire response, a significant characteristic of this cable is the large percentage of polyethylene dielectric.

The experimental protocol was identical to the previous burns and the results are presented below.

The third experiment was a test of the larger RG 220 A/U cable. As may be seen from the time-temperature plots (Fig. 31) we could not get the cable to ignite with this fire exposure and set-up, even after eleven minutes of constant fire exposure.

However, the test of the RG 11 A/U had a different outcome. The pertinent observations are listed below.

	Time (s)
Ventilation started and burner ignited	0
Sustained ignition of horizontal section c cable and burner shut-off	125
Vertical flamespread	
17.78 cm	125
35.6 cm	315
53.3 cm	335
71.1 cm	350
Out the top >1.02 m	355

The temperature rise shown in Fig. 32 demonstrates ignition and flame-spread on the cables. The primary difference between the previous burn and this one is the size and mass of the two cable types. The RG 220 A/U has approximately 7 times the mass of the 11 A/U which makes the former much more resistant to ignition from this fire exposure. It is very resistant to ignition in the tight bundle configuration used in this experimental series. This finding is no surprise, but it is one of the fire performance characteristics that we will be evaluating in the final experimental apparatus.

Comparison of the temperature plots shows that the above three tests have very similar histories once self-sustained ignition has been established (i.e., once a drastic change in slope begins). It appears that this similarity is caused by the pipe enclosure, which means that it is doubtful this apparatus would produce enough resolution to adequately evaluate different cable types.

However, we have gained enough insight from these preliminary burns to begin designing the formal experimental apparatus in the next fiscal year.

OFF-SITE QUESTIONNAIRE REVIEW

During the previous fiscal year our efforts included structuring and distributing sample questionnaires to fire protection professionals with responsibility for fire prevention and fighting at each DOE experimental fusion facility. Besides those specific facilities, other experimental facilities involved in "nuclear technology" were also queried. Responses from these sources were received and provided additional response information. Within the mainline DOE fusion experiment alternatives, both ICF and MFE experiments were queried and responses were obtained. Our effort this year consisted of receiving and reviewing these questionnaires and optimizing the structure and content to facilitate information content and transfer. The following paragraphs describe our response to the completed questionnaires and some suggestions for improvements.

First, through our review it became apparent that our original general questionnaire needs to be shortened and focused. One approach to shortening this general questionnaire can be accomplished by requesting that respondents provide building fire protection system blueprints for detection and suppression subsystems, thereby conveying the general building system structure. Alternatively, a generalized input/output diagram showing building

fire protection subsystems and their interconnections can be provided. The benefit provided by this option is threefold:

- Brevity.
- Uniformity of subject focus.
- Uniformity of response.

Second, throughout the review of sample questionnaire responses, it was apparent that respondents were not attributing any strategic emphasis from location to location within the experimental facility. As a result, specific questions regarding operational experiment availability and fire protection could not be addressed for lack of information. An approach to this concern would be to provide a request that fusion experiment staff identify specific pieces of equipment or subsystems whose loss or damage would result in excessive program delay or in excessive additional operational funding. With this information questions involving localized fire protection system behavior could be solicited from the responsible fire protection professional. The usage of the same input/output or stimulus/response building fire protection system diagram could be used to describe strategically critical fusion equipment and its building compartments. To further describe critical compartments, a request for photographs would also assist us in determining pertinent fire protection equipment and local fuel loading.

DETAILED FIRE RISK ASSESSMENT OF THE SHIVA EXPERIMENT (PRELIMINARY)

In FY '81 our system safety consultant from Econ, Inc., performed a preliminary detailed fire risk analysis of the Shiva fusion facility. A draft report describing the analysis is attached as Appendix A. The steps followed in an attempt to provide a consistent basis for evaluating various levels of fusion-experiment fire protection are listed briefly on the next page.

The first major step in this assessment was to identify "critical" spaces and areas in the Shiva experiment. These spaces were identified by the Fire Science Group based on our perception of the importance of each area due to the economic value of its contents and its importance to the uninterrupted performance of fusion research.

Appendix A goes beyond this last step to identify equipment and hardware essential to Shiva system availability. Our consultant from Econ, Inc. went through this identification process by interviewing key programmatic and operational personnel and arriving at consensus opinions on what items were essential to Shiva system availability.

GENERAL FLOW OF SYSTEMS APPROACH TO FIRE RISK

1

DIVIDE BLDG. INTO ZONES

CRITERIA:

A. May Use Fire Protection Zones.
B. Natural Building Boundaries (Walls and Rooms).

2

SELECT CRITICAL AREAS FOR ANALYSIS

CRITERIA:

A. Capital Loss.
B. Programmatic Delay.

3

PERFORM ANALYSES TO DETERMINE FIRE HAZARD AND ZONE

CRITERIA:

A. Fire Growth Analysis.
B. Fire Protection System Analysis.
C. Research into Identified Problem Areas.

4

ASSESS POTENTIAL LOSS IN EACH CRITICAL ZONE

CRITERIA:

A. Programmatic Delay.
B. Capital Loss.

5

ASSESS EXPT. FIRE IMPACT ACCEPTABILITY AND COMPARE EACH ZONE

CRITERIA:

A. LLNL Guidelines.
B. DOE Guidelines.
C. Programmatic Delay.

6

IDENTIFY COST-EFFECTIVE SOLUTIONS TO INCREASE FIRE SAFETY OF FACILITY

CRITERIA:

A. Reiterate Loss Assessment With Recommended Changes.

FIRE MODELING

INTRODUCTION OF TEST SERIES

One goal of this project is to produce or adopt analytical procedures for predicting growth rate of fires leading to corresponding thermal and smoke exposure to components and structures in large experimental facilities. In FY 1980 we employed Cal-Tech's room-filling model[6] to estimate temperature rise, and particulate concentration and interfacial boundary of the ceiling layer, from a set of ideal steady-state fires of prescribed strength contained in various fusion energy experiment and support enclosures. Plausible analytical results were obtained relative to specified assumptions (instantaneous fires at specified strength, specified fire location, realistic room air leak, no heat sinks, and specified source aerosol concentration in combustion products). However, we had no means of testing these results to determine their proximity to conditions in real fires of similar characteristics (i.e., fires on high-volatility liquid fuel spills, high-pressure fuel sprays, or low-pressure gas leaks). Moreover, other national laboratories were very interested in developing fire-source-intensity terms for a variety of purposes. Their concern, like ours, was the lack of validation data for model correlation. A joint venture was presented* to conduct a set of ideal enclosure fire experiments at the LLNL fire test facility for the expressed purpose of developing calibration data for fire models.

The proposed test series conditions were distributed to as many enclosure fire modelers as we could so that they could cast predictions of enclosure fire conditions prior to the tests. Time constraints, however were such that only Cal-Tech, Los Alamos, and LLNL attempted pre-test estimates of enclosure fire conditions.

---

* Principal players in this activity were: LLNL--Fire Science Group, Los Alamos--Safety Assessment Fluid and Thermal Section Q6, Hanford Engineering Development Laboratory, Cal-Tech--Dept. of Engineering and Applied Sciences, University of California Berkeley--Department of Mechanical Engineering.

EXPERIMENTAL DESIGN

These tests were done in the enclosure shown schematically in Fig. 33. This test cell is ventilated by a negative-pressure system similar to HVAC circuits used in laboratories where containment of toxic materials is an issue. This system employs a centrifugal blower downstream of the test enclosure. Volumetric flow rate is measured by sharp-edge orifice at an appropriate distance upstream from the blower where the distance between sharp-edge orifice and test cell is large and potential temperature rise is low when fire experiments are performed.

Our philosophy in conducting these tests was to have uncomplicated fire and ventilation conditions covered by extensive--as complete as possible--measurements. Thus fuel geometry was simple; a small-cross-section natural-gas burner, or a heated .91-m (3-ft) diameter metal pan into which propyl alcohol or methyl alcohol was sprayed at calibrated rates to simulate conditions of pool fires. Source fires are located in the absolute center of the enclosure. Ventilation air is admitted by two 30.5-cm (12-in.) diameter ducts lying along the wall/floor interface of each long test cell wall. Side holes in each duct distribute opposed flow air to test cell bottom. Figures 34 and 35 schematically show pertinent dimensions of the test cell and spatial relationships of internal components.

Measured parameters are listed in Table 2 along with design fire strength and ventilation variations. Data derived from our measurements will define the response variables that we hoped to predict from our participating models. These "comparative parameters" are also listed last in Table 2. Figure 36 is a collage of four photographic views of test cell components and sensors: Plate "a" shows vertical thermocouple rake (Δ = 45 cm)* thermal radiation shield at foreground and visual reference board across the enclosure used for estimating descent of smoke level. Plate "b" is a direct view of the thermal radiation shield in center photograph including door side air inlet to left and radiometer station on floor right. Close-up of radiometer station is shown on Plate "c". Plate "d" shows test cell north side air inlet anemometer. The visible duct is attached to a sheet metal box that plugs into the test cell wall (box barely visible in back corner of photographed enclosure).

* Δ is distance between thermocouple stations along the rake.

Designed conditions of fire strength and ventilation rate were controlled by fuel-metering procedures and by balancing of inlet and outlet flow circuits respectively. Calibration of rotameters for liquid fuels (methyl and propyl alcohol) was done by direct volumetric procedures where fluids were decanted through metering circuits into a calibration volume. Liquid propulsion was provided by pressurizing fuel in a certified container with nitrogen gas, where volumetric flow rate was controlled by metering valve. When methane was employed for low-intensity fires, a gas rotameter calibrated for air was used by applying conversion factors for body and rotameter float assembly. We were not certain of correct designation for these parts but because of urgency, we opted to proceed with this approximate calibration with the intent of having absolute calibration performed post-test.

Variation in fan speed is used to provide two different ventilation rates through the test cell. Fan location is 15.25 m (50 ft) from exit to test cell. At this distance, exhaust gases are substantially cooled so that sharp-edge orifice measurements and fan characteristics are minimally effected. Temperature measurements taken at this station are applied to correct measured flow rate figures. Table 3 lists instrumentation type, calibration, and precision of devices used for sensing parameters of test cell fires and associated ventilation flow characteristics.

Because we used essentially non-smoky fuels we were able to view most fires throughout the term of specific experiments. Both video and photographic records were collected. Examples of these fires are shown in Fig. 37. Plates "a" through "d" show respectively: methane at nominally 50 kW, methyl alcohol at nominally 400 kW, and propyl alcohol at nominally 400 kW and 800 kW. Note that sprayed fuel is confined to .92-m (3 ft) pan dimensions by a radial spray nozzle. Spraying rate dictates fuel consumed which in turn controls heat-release rate. Thus, with a simple fuel we can duplicate enthalpy production properties of a variety of fuels of differing energy potential. Both methane (CH_4) and propyl alcohol ($CH_3CH_2CH_2OH$) flames have characteristic appearance of natural convection flames where color is mainly a phenomenon of incandescent soot particles resulting from production of longer-chain combustion product fragments heated in reaction regions. Methyl alcohol (CH_3OH) flames have a light violet hue which may be simply chemiluminescence of CH_3OH oxidation.

Figure 38 is a fire portrait of a 400 kW fire ventilated at 500 l/s. Inlet air flow, introduced at the bottom and on both sides of the test cell,

is recorded on channels 53 and 54. Exit air flow is recorded by channel 52. Since exit air flow measurement is taken closest to the pump, we designate it as forced flow, therefore exit flow measurements are given a negative sign. Conversely, inlet flow essentially motivated by pressure differential between the outside and interior of the cell is given a positive sign and designated as "free" ventilation. The characteristic pattern for air flow in enclosure fires where air is supplied at an initially defined rate is duplicated in the figure. Initial prefire data (at 10 s) shows inlet air (+) to be of slightly greater magnitude than out flow (-), hence net air flow is slightly positive, indicating minor leak paths. When the fire is dynamically growing (about 60 s), + flow is grossly curtailed because of gas expansion due to rapid temperature rise within the cell and in these data, net air flow is nearly zero. In 2 to 3 minutes, conditions in the test cell achieve a semi-equilibrium state, where again the net air flow is nearly balanced.

Table 4* shows air flow balance data for 200-, 400-, and 800-kW propyl alcohol fires ventilated at a design exit flow rate of 500 l/s (the inserted sketch illustrates air flow direction through the test cell). Net flow is always nearly balanced for initial conditions and after steady state has been achieved. But during the period of intense fire growth, fire size dictates the pattern of air flow in the system. These data show that large fast growing fires can cut off all air flow into an enclosure, and indeed cause heated combustion gases to flow out of inlet ventilation ports.

RESULTS

Figures 39 and 40 show specific temperature patterns measured by a thermocouple rake in test cell center regions. These temperature signatures are recorded here to illustrate changes in internal enclosure enthalpy relative to fire strength and initial ventilation setting. Figure 39 displays temporal increase of individual thermocouple stations along the rake. Temperature records from two topmost thermocouples are not included because we lacked capacity in computer readout for analog display. Omission of these data on Fig. 39 is irrelevant in defining the extent of hot layer after quasi-steady state conditions are achieved, since at fire strength greater

* Listed flow data given in grams/second (g/s) to facilitate mass balance correlations.

than 200 kW, upper test cell measured temperature magnitudes are coincident. Digital data collected from all stations are used for temporal variation information.

Figure 40 shows data from the thermocouple rake where fire strength varied from 200 to 400 to 800 kW in discrete steps. Between 200 and 400 kW, measurements were made of the cooling test cell for about 200 s as a check on instrumentation integrity. All temperature data exhibits monotonic decrease in this period except for channel zero (20 cm from floor) which increases, slightly, probably due to some mixing process and/or mass diffusion occurring during post fire plume conditions.

Fire intensity was increased from 400 to 800 kW without a cooling period between. Temperature rise in upper volume gases of test cell increases lineally with doubling fire strength. Achievement of nearly steady-state conditions occurs quite rapidly, usually within 150 s as indicated by established temperature levels within the enclosure. All parameters exhibit slight monotonically changing trends with time as second-order heat-transfer processes progress. However, primarily flow and thermal conditions are established from which pertinent information can be derived.

Figure 41 describes descent of 70°C temperature isotherm for fires of various strengths. These data show that rate of descent is relatively constant for fires burning at 200 kW or better. The largest variation in this group occurs upon approach to floor level. Time delay between start of this apparent descent from enclosure ceiling is directly related to fire strength. Note, these data were transcribed directly from individual temperature readings of the thermocouple rake.

Figures 42 through 44 show quasi-steady-state vertical temperature distribution ($t \simeq 480$ s) at thermocouple rake for the complete set of fires conducted in this series. These data show definite establishment of essentially constant temperature in upper enclosure volume for all fires. Shape of temperature distribution near the floor seems more dependent on fire strength, (i.e., for fire strength less than 200 kW, temperature gradient to floor is quite steep). Temperature slope above the steep portion is more gradual to the enclosure level where the upper volume temperatures become more or less constant. Breakpoint between these two temperature regimes ranges around 1.5 m from the floor. Ventilation effects are graphically illustrated in Fig. 44. The central curve (800 kW at 250 l/s, propyl alcohol) is displaced to lower temperatures because of inadequate air for complete

combustion. This fire visually produced many times the smoke concentration of adequately ventilated propyl alcohol fires.

Figure 45 is a composite of curves showing differences in vertical temperature gradient for spray fires at 500-l/s ventilation rate. Examples of heat transfer and combustion gas character are shown in Figs. 46 and 47 respectively. Figure 35 shows the plan view location of surface contact sensors and heat sensors recorded in Fig. 46. Temperature measurements on specific surfaces in Fig. 46 were made by thermocouples in compression contact with the surface. No attempt was made to shield thermocouple beads, consequently temperature measurement is not solely that of surface. Radiometer and calorimeter traces indicate flux levels at indicated locations. Decay of radiometer trace directly correlates to conditions of oxygen depletion shown in Fig. 47. Here two oxygen traces reflect oxygen concentration in both test cell and at duct gas pick-up station. Production of carbon dioxide, carbon monoxide and unburned hydrocarbons reflect the pattern of oxygen consumption. Test cell trace of oxygen depletion shows more sensitivity to internal test cell conditions than does data taken from the in-duct station. However, this is apparent only after termination of fuel spray. Up to this time the correlation is remarkable.

Table 5 summarizes experiments conducted during this test series. This list gives design heat-release rate and volumetric exit air flow rate. In addition fuel flow rate and initial observations are recorded.

A continuous color video monitor surveyed flame characteristics throughout each experiment. Recorded from these tapes are: flame height and flame appearance. One observation derived from these records was that during early fire stages, fuel over spray probably resulted in lower-than-design heat-release rate. Within 100 s of initiation, however, all indications of over-spray disappear and we are assured of total fuel spray contribution to the combustion process.

DATA ANALYSIS

Data analysis procedures have been in progress since the test series was completed in July 1981, and are not yet complete. Because we are attempting to develop data for model validation, we must understand and account for all anomalies and inconsistencies developed during experimental measurements and data reduction. We began to notice such anomalies (during low-fire tests with

methane as fuel) when attempting to resolve combustion enthalpy calculations with heat-release-rate determinations by oxygen depletion measurements.[6] Prior to obtaining absolute calibration of the methane rotameter, we found gross differences between heat-release-rate results calculations based on methane fuel flow rate, oxygen depletion, and CO/CO_2 production. After much agonizing, extensive cross checks, and ultimately an absolute calibration of the rotameter we determined that both our experimental fuel flow rates and oxygen depletion measurements were wrong because of experimental indiscretions and masking of true oxygen readings by water of combustion. Another possible anomaly is that equilibrium in oxygen is not achieved between fire plume and gas sampling station. Our major error in measuring gas flow rate was that we neglected to track gas pressure and temperature through the flow rater. Thus we cannot translate volumetric flow to mass flow for gaseous fuel measurements. We have made some reasonable estimates of mass flow rate which produce fuel enthalpy magnitudes that balance fairly well with heat-release-rate calculations based on CO/CO_2 formation. Fig. 48 shows this comparison in terms of elemental balance between input carbon from methane fuel and output carbon in form of CO, CO_2 and measured partially oxidized hydrocarbon fractions. The curve indicates incomplete combustion because net carbon input is greater than zero. However, design ventilation rate is about 50 times that necessary for complete combustion; so the only explanation of sense is that methane flow rate is substantially in error. Similarly, hydrogen and mass balance calculations give questionable results.

Calculational procedures of correction and balance equations are contained in Appendix B. All data were subjected to treatment by these factors, and were found in conformance with balanced conditions, especially after steady-state was approached. Precise measurement of volumetric fuel flow rate for liquid fuels absolved inaccuracies of energy input parameters, and combustion heat-release-rate measurements balanced (using CO/CO_2 production rate as a means of heat determination) in all but one test where fire was designed to be ventilation controlled.

Because we began to suspect the oxygen depletion measurements, oxygen balances contained in Appendix B are based on CO/CO_2 data. Figure 49 compares total combustion heat-release rate from: CO/CO_2 production measurements, O_2 depletion measurements, and O_2 depletion calculated from CO/CO_2 measurements. Oxygen heat-release-rate calculations from measured data exhibit extreme noise resulting from amplification of experimental

fluctuations by the heat of combustion multiplier. Data trends, however, are obvious showing major difference between CO/CO_2 and O_2 derived values.

Figure 50 is an example of elemental balance for sprayed propyl alcohol fuel, at a design rate of 440 l/s. Balanced conditions after quasi-equilibrium is attained show validity of balancing procedures and define the fire as being fully ventilated where all fuel is converted to simple products. Equations for balance parameters, BASIC program, and program notes are attached as Appendix B along with an example test series for comparative purposes. Table 6* and supplemental symbol glossary collect pertinent parameters of all tests conducted during this experimental series. Listed data was recorded after quasi-steady-state conditions were achieved. The first column lists parameters defined in attached glossary. The top row defines test sequence in terms of fire strength (1st number) and chronology (2nd number). In all, we conducted 12 separate experiments, 2 of which (2nd numbers 12I to 12III, and 13I to 13III) consisted of 3 changes in fire strength during the period of the test. Designed and corrected parameters, along with pertinent thermal energy data, estimated and measured temperatures, and thermal energy ratios complete the table.

A particularly interesting trend appears for all tests which indicates that most of the energy released by these fires in this test cell is absorbed by enclosure surfaces. Greater than 70 percent of released heat is absorbed in these surfaces where the trend of energy deposit is (slightly) inversely proportional to ventilation rate.

MODEL VALIDATION

Data in Table 6 were developed to check predictions of contemporary fire spread models. Predicted parameters are constrained to specific flow and temperature conditions described in Table 2. Interfacial height between hot and cool layer in a naturally ventilated room is well defined because of density and flow regimes established through enclosure openings. Fires in enclosures with forced ventilation will produce heated volumes of gas in ceiling regions. But (depending on forced ventilation patterns) distinct layers with sharp interfacial boundaries will not be established. Instead a

---

* Table 6 collects more than specific experimental data and corrections. These factors will be employed subsequently.

monotonic temperature gradiant will exist between a more-or-less uniform hot volume and the floor plane as indicated in Figs. 42 through 45.

For model validation, these data must be constrained to two layers separated by a definite interfacial boundary. Fortunately, this need was foreseen by Speckler at Harvard[7,8] who proposed a procedure of mass and energy conservation along the air-temperature gradient to force such data into two distinct layers.*

Figure 51 compares vertical temperature distribution. With Speckler's two-layer calculation, both simple and complicated integration procedures were used to establish Speckler's interface height and lower-layer temperature level. The simpler integration procedure is more than adequate for these calculations. Figure 52 is a display of the descent rate of the pseudo (Speckler) interface. Comparison of these estimates with Fig. 41 is reasonable. Table 7 compiles two-layer calculations for the range of fire strength data developed during this test series.

Our major goal in refining these data was to provide the best test data possible for model validation. Our adoption of Cal-Tech's† room-filling model for preliminary analysis was motivated by its ease of application and flexibility in terms of input modification practices.

Before experimental data was reduced to values contained in Table 6, the Cal-Tech model was applied to our proposed design conditions by several individuals at Los Alamos, LLNL, and Cal-Tech** along with an independent model developed at Los Alamos. Table 8 collects these predictions along with design test conditions and final corrected test data.

Bolsted, Creighton, and Zukoski applied the Cal-Tech model each with some variation of input parameters. Required data is: combustion heat release rate, enclosure ventilation rate and position of ventilation source and exhaust sites. Ad hoc heat transfer and fuel efficiency factors are applied by the user. Creighton did not apply any heat loss conditions and Zukoski

---

* Speckler's procedures, derived algorithms and BASIC program are attached as Appendix C.

† Model description and references are contained in Reference 3 (UCRL-53179).

**Los Alamos Modelers were John Bolsted and Fritz Krause. Livermore Modeler was John Creighton and Cal-Tech Modeler was Ed Zukoski.

included a set of enclosure surface heat loss values varying from 0.1 to 0.8 (results all contained on Table 8). Krause's model LAFM (Los Alamos Fire Model) uses mass burning rate, combustion product thermochemistry and volumetric flowrate, based on maximum ceiling temperature data from tests to predict compartment heat-release time histories. Bolsted uses some LAFM data for combustion heat-release input to his trials with the Cal-Tech model. We note that all models suffer from the fact that design and final corrected data differ for many of the tests, moreover, stepped fire strength data has not yet been modeled. Thus we display these comparisons in Table 8 for preliminary review only. Listed experimental data is adjusted to two-layer conditions via Speckler's procedures; T_U is an average of measured temperature in upper regions of the test cell where essentially uniform conditions are established after Quasi-Steady State is reached. From T_U, we employ Speckler's procedure to calculate T_L and H_L. Thus T_U is the only actual measured quantity on Table 8.

Cal-Tech and LAFM predict only steady-state T_U and H_L. Preliminary comparison of data and model predictions indicates trends only, e.g., enclosure heat loss considerations produce better model results at high fire strength, energy balance considerations between upper- and quasi-lower-layer may serve to bring predicted T_U to more realistic levels, and model H_L values bear small resemblance to either Speckler's calculation or the lower-region temperature gradient in the test cell.

FIRE CHEMISTRY: THERMAL DEGRADATION OF WIRE AND CABLE INSULATIONS

INTRODUCTION

Last year's study on thermal degradation of representative cable insulations showed that the mode of decomposition of the insulations is influenced by the antioxidants, plasticizers, stabilizers and flame retardants that are incorporated in the plastic formulations. Some of the additives enhance the rate of decomposition of the pure polymer and/or thermally degrade into flammable species which help to feed the flame.

We learned that the mode of thermal degradation also depends upon the radiant flux level used to irradiate the plastics. Low levels such as 2.5 W/cm^2 lead predominantly to low concentrations of cyclic and polycyclic

hydrocarbons; a flux of 5.0 W/cm^2 forms a great variety of compounds ranging from acid ions and simple saturated hydrocarbons to complex polycyclic compounds. An irradiance level of 8.0 W/cm^2 results mainly in acid ions and unsaturated hydrocarbons and polycyclic compounds.

This year we extended our study to a number of additional cable and wire insulations as well as to virgin polymers. Having subjected approximately 100 different insulations to thermogravimetric (TG) analysis and categorized them into 25 groupings, we performed an in-depth analysis on the thermal degradation of eleven such insulations. We subjected our samples to TGA and differential scanning calorimetric measurements (DSC) at different heating rates. We paid particular attention to the generation of corrosive substances during the different phases of pyrolysis, as these are detrimental to high-value instrumentation. In addition, we also looked at the kinetics of degradation of the insulations at the dehydrochlorination region, or acid ion producing region, and the non-corrosive thermal degradation products generated at the different phases. We compared our results to those obtained from virgin polymers.

EXPERIMENTAL PROCEDURE

In the first set of experiments, virgin polymers, several polyvinyl chloride insulations, and rubber insulations comprised of neoprene and chlorinated and sulfonated polyethylene were heated in our thermal gravimetric analyzer at a rate of 10, 20 and 40°C/min in air from ambient temperature to 900°C. We monitored the samples' weight as a function of temperature and their rate of weight change with a multichannel recorder. This information was also stored on a magnetic tape which was subsequently retrieved by our PDP-11 computer and used in calculating activation energies in the dehydrochlorination region. In addition, we also measured the generation of corrosive gases, mainly acidic components, as a function of temperature. This was done by directing the thermal degradation products formed by the samples in the TGA to a container filled with 200 ml of distilled water buffered to pH 6.8-7.0. The aqueous solution was gently stirred with a magnetic stirrer to achieve uniform mixing. The change in pH (predominantly caused by formation of HCl) was measured with a pencil-size pH reference electrode as a function of temperature and monitored by our multichannel recorder. This simple

approach gave us a visual correlation between weight loss, the generation of corrosive gases and the initial temperature at which these gases are formed.

All differential scanning calorimetric analyses were performed on a DuPont 900 Differential Scanning Calorimeter using a standard cell. Our samples weighed between 6 and 10 mg and were heated in air at 20°C/min.

In the second set of experiments we attempted to see if there are differences in the general types of products formed in the various phases of pyrolysis (as seen by our TGA measurements). Such information would aid us to better understand the mode of decomposition and thereby determine the differences in the formulations of the various composite polymers.

Such knowledge is particularly helpful in identifying those formulations which either contain highly flammable additives (e.g., phthalate plasticizers) or additives which in themselves are not flammable but at high enough temperature form either highly flammable species which will contribute to flame spread or degrade to highly toxic products which will create an extra health hazard to firefighters.

We used samples weighing between 10 and 25 mg to generate the degradation products. They were heated in air at 20°C/min in our TG apparatus and the resulting degradation products were collected on the TGA furnace tube at predetermined weight loss steps. Separate runs were made for each collection step. After each collection, the furnace tube was cooled to room temperature and then washed with methylene dichloride in preparation for GC/MS analyses. Each extractant was concentrated down to 0.5 ml and a 3-microliter aliquot was injected on a 25-meter Carbowax 20-M fused silica capillary column. The column oven was programmed from 70°C to 220°C at a rate of 10°C/min, helium flow rate was maintained at 6 ml/min, and the injection port, mass spec transfer line and jet separator were set at 250°C. The components comprising the separated peaks were identified with the help of our computerized spectral library system. In this system, the spectra of unknown compounds are compared to approximately 40,000 compounds stored on a library disk pack, and the 10 best matched compounds are printed out. These then are subjected to a spectral-compare program where the masses of the sample peak and those of the library hit were printed in graphic form for easier comparison of mass peak numbers and intensity.

EXPERIMENTAL RESULTS

Polyvinyl Chloride

The PVC insulation used in our experiments was designed for high-power electrical cables, multi-strand general-purpose cables and general appliances cables.

The TGA's of all formulations as well as of the pure polymer show three regions of decomposition. There is the initial rapid weight loss, which is primarily the result of a loss of HCl and the degradation of a plasticizer. The dehydrochlorination reaction leads to the formation of long, conjugated polyvinyl structures. The second region involves the decomposition of the residual cross-linked polymer chains and the third region is thought to be due to a very slow degradation of the polymer's charlike residue. The initial region of degradation is preceded by an induction period which had been attributed by Dresdow and Gibbs[9] to activation of weak links in the polymer.

We showed that the general shape of the curves changes with additives used in the formulations as well as heating rates. Figure 53 contrasts the thermograms of four different types of insulations and virgin PVC heated in air at 20°C/min. The greatest difference appears in PVC-104 which is an insulation used for high-voltage cable. We see that the induction phase begins at 40°C and phase one, which is associated with acid ion production, shows considerably lower overall weight loss as well as rate of weight loss in comparison to the other types of PVC insulation. The insulation which exhibits the largest amount of weight loss and the highest rate of degradation is PVC-3 which approaches the degradation rates of virgin PVC.

The effect of heating rates on the degradation of the various PVC formulations in the acid ion production phase are summarized in Table 9. As expected the higher heating rates lead to higher degradation rates and thereby faster production of acid ions. However, the faster heating rates do not increase the overall weight loss in the acid ion production phase and therefore the total production of acid ions remains constant with increased heating rates. We also found that higher heating rates lower the temperature responsible for the initial degradation of PVC-78 and PVC-95 but do not do so in the insulations labelled PVC-3 and PVC-104. This is most likely due to the different additives used in the different formulations. The different additives also influence the amount of char formed in the various polymers as

measured at 600°C. For example, PVC-3 shows a char residue of 12%, PVC-78 a residue of 33%, PVC-95 a residual char of 38% and PVC-104 left a char residue of 6%. In contrast, virgin polymer did not leave any residue at 600°C. The principal char-forming additives used in the PVC formulations, associated with fire retardance, are Sb_2O_3, alumina trihydrate, calcinated clay and phosphate esters. Depending upon the manufacturer, the commonly used PVC formulations contain anywhere between one and three of the above additives in a single formulation.

The activation energies for the different formulations were calculated according to the Arrhenius relationship and are based on the 1st-order kinetics in the dehydrochlorination region. The values obtained for PVC-95 and PVC-78 are 21.5 kcal/mol and that for PVC-104 is 33 kcal/mol. These activation energies are somewhat lower than those reported for pure PVC polymers,[10] which agrees with the literature findings that plasticizers decrease thermal stability of PVC.[11] Since PVC-3 did not generate acid ions via the 1st-order kinetics we did not calculate the activation energy for this insulation.

The presence of plasticizers in our PVC composites was confirmed by our DSC and GC/MS studies. Figures 54 and 55 show DSC curves of pure PVC polymer as well as polymer plastics heated in air at 20°C/min. PVC-3, 95, and 104 show an exotherm between 262-274°C which we attribute to the presence of a metal oxide such as zinc or ferric oxide. The broad endotherms showing two peaks between 280 and 330 in PVC's-3, 78, and 95 coincide with dehydrochlorination of the PVC insulation and the decomposition of the plasticizer dioctylphthalate (DOP). The fact that DOP is included in these formulations is attributed to the presence of acetic anhydride in the degradation products of PVC-3 and 78. Although at this time we did not analyze the degradation products of PVC-95 it is logical to assume that its endotherms at 295°C and 330°C are due also to dehydrochlorination of the insulation and decomposition of DOP. PVC-104 shows two endotherms at 105°C and 119°C which might be due to the melting of the crystalline regions of what seems to be a PVC composite. The exotherm at 268°C is again probably due to a metal oxide and the two endotherms at 280°C and 283°C are due to the presence of the plasticizers. From the GC/MS analysis of the thermal degradation products we feel that the plasticizers are probably calcium stearate as well as dibutylene dilaurate.

The thermal degradation products generated during and post the dehydrochlorination phase are included in Tables 10-14. The tables include only

those products which were condensed on the walls of the TGA glass tube; therefore the lighter-molecular-weight gaseous products are excluded from the table. In addition products retained on the Carbowax-20M capillary column are also excluded from the tables. As in our previous report we attempted to categorize the various compounds according to their probable health and flammability and reactivity hazards. The hazards, assigned according to the recommendations of the National Fire Protection Association (NFPA), are those that might be encountered by firemen fighting fires involving plastic insulation materials. The system used by NFPA identifies the hazards of a chemical in terms of three categories, namely, health, flammability and reactivity and it indicates the order of severity in each of these categories by five divisions ranging from four indicating a severe hazard to 0 indicating no special hazard.

An important observation pertaining to all these tables is that there is very little information on the hazards of the compounds formed during pyrolysis and combustion of these plastics.

The overall analysis of the tables shows that the degradation of the plasticizers occurs during the dehydrochlorination region and the components collected after the dehydrochlorination region consist mainly of the polynuclear hydrocarbons as would be expected from the decomposition of the residual cross-linked polymer chains.

Rubber Insulations

The rubber insulations were designed for high-power high-current cables, welding cables, single-conductor high-voltage cables, and multiconductor power cables.

The insulations consisted of neoprene, or polychloroprene, and chlorinated and sulfonated polyethylene.

Figure 56 shows thermograms of the various rubber formulations heated in air at 20°C/min as compared to the pure polychloroprene polymer. While the thermograms have notable differences they all exhibit to some extent three distinct weight-loss regions. The first phase shows a rapid loss in weight which is associated with the release of HCl from the polymer chain. Essentially all of the chlorine content is liberated at these temperatures. Good-quality compositions of neoprene and sulfonated and chlorinated polyethylene contain approximately 15% chlorine by weight, based on chlorine

contents of 37.5 and 35% for polymers of neoprene and chlorinated and sulfonated polyethylene. While HCl separates from the polymer chains, the degree to which it is released to the atmosphere is dependent on compound formulation as discussed later in the report. The second phase shows a gradual loss in weight which is attributed to gradual oxidation of the highly cross-linked carbonaceous residue of the polymer chain. At about 500°C we see another rapid-weight-loss region which some authors attribute to ignition of the carbonaceous residue.[12]

A study of the curves reveals distinct differences in starting temperatures leading to HCl formation, duration of HCl evolution and the rate of acid ion production. This is further substantiated by Figs. 57 and 58 which show the acid ion production along with the individual rubber insulation thermograms. The higher temperature leading to formation of HCl shown in neoprene-118, neoprene-435, and neoprene-007 might be due to presence of acid acceptors in the formulations such as ZnO, MgO or Sb_2O_3 reacting with the HCl evolved at lower temperatures. The weight loss occurring below 300 is attributed by some researchers to loss of water of hydration from the hydrated alumina present in many of the formulations. The incorporation of $CaCO_3$ in some of the formulation would lower the total ion production as $CaCO_3$ would wait with the formed HCl according to the following equation:

$$CaCO_3 + 2\ HCl = CaCl_2 + H_2O + CO_2.$$

The activation energies for the different formulations were again calculated according to the Arrhenius relationship and are based on the 1st-order kinetics in the dehydrochlorination region. The value obtained for neoprene-118 is 32 kcal/mol and for neoprene-435 it is 26 kcal/mol. These values are as observed in the PVC formulations somewhat lower from the values reported for pure polymers. Again we attribute this discrepancy to the presence of plasticizers such as alkylphthalates, dioctylphthalates, or calcium stearate. At this time we have yet to determine the activation energies of polychloroprene, rubber-134 and neoprene-84.

The effect of heating rates in the dehydrochlorination region of the rubber insulations are shown in Table 15. As observed in the various PVC formulations the higher heating rates result in higher degradation rates and therefore faster production of HCl. Of the insulations studied neoprene-435 degrades with the fastest rate and neoprene-84 degrades with the lowest rate

and the same time leaves the highest amount of char. We also observed that higher heating rates do not necessarily increase the overall weight loss in the dehydrochlorination region and with the exception of neoprene-118 do not lower the temperature responsible for the initial degradation of the insulations. As in the case of the PVC insulations, we attribute the above differences to the different additives used in the various insulations. For example plasticizers such as triisodecyl, in the absence of phosphate esters, would enhance the degradation rate of the insulation material and fail to substantially increase the final char residue. On the other hand the char residue would be increased and the rate of degradation decreased if a flame retardant such as tricresyl phosphate were included in a formulation containing a flammable plasticizer such as triisodecyl or dioctylphthalate.

Figure 59 further illustrates the effect of additives on the degradation scheme of the insulations. Thus, neoprene-118 shows two exotherms at 309°C and 325°C which we attribute to dehydrochlorination of the insulation and decomposition of a plasticizer used in the formulation. Neoprene-84 shows a sharp exotherm at 250°C which is probably due to decomposition of a metal oxide, an exotherm at 375°C which might be attributed to loss of water from $CaCO_3$ and an exotherm at 412°C which is in the dehydrochlorination and desulfonation region of this insulation. Neoprene-007 shows two exotherms at 330°C and 337°C which we again attribute to decomposition of metal oxides and dehydrochlorination of the insulation plastic. Neoprene cable-435 shows two exotherms at 331°C and 336°C which we attribute to degradation of the insulation and plasticizers, an exotherm at 375°C which is probably due to oxidation of the highly cross-linked region. In contrast, the DSC curve for polychloroprene shows an exotherm at 350°C which occurs at the dehydrochlorination region and several small exotherms between 425°C and 450°C which we attribute to the oxidation of the highly cross-linked region. Rubber-134 shows an exotherm at 250°C which again is attributed to the decomposition of a metal oxide; two exotherms at 375°C and 387°C which is in the dehydrochlorination region and which we attribute to decomposition of the insulator and plasticizer.

Tables 16-21 show thermal degradation products generated during and post the dehydrochlorination region of the different rubber insulations heated in air at 20°C/min. As in the case of the PVC formulations main components comprising the mixture of these degradation products are the higher-molecular-weight components as separated on Carbowax-20M capillary column. It is

conceivable, therefore, that the mixture contains other compounds which may have remained unresolved on this column.

The tables again show that although the dehydrochlorination region leads mainly to the production of HCl other products are also formed both from the decomposition of the insulation material and additives such as plasticizers, stabilizers and organic flame retardants that were included in the formulation. As previously noted with the PVC formulation, higher temperatures, as exhibited in the post-dehydrochlorination region, lead to the formation of various higher-molecular-weight compounds ranging from straight-chain hydrocarbons to long-chain acids and alcohols as well as polycyclic compounds. The nature of the mixture will depend upon the exact formulation of the insulator. We also observe that as with the degradation products from PVC there is very little information on the hazards of the compounds generated during pyrolysis and combustion of the various insulations.

CONCLUSIONS

The results of our study show that:

- The mode of thermal decomposition of the insulations is influenced by the composition of the formulations of the insulations. The presence of some plasticizers, such as dioctylphthalates or triisodecyl, will enhance the flammability of both PVC and rubber insulations and therefore if used in the formulation of either of these insulations should be accompanied by flame retardants such as tricresyl phosphate. The presence of acid acceptors (e.g., ZnO, MgO or Sb_2O_3 and $CaCO_3$) will influence how much HCl will be released into the environment.

- The acid ion production is enhanced by higher heating rates. However higher heating rates do not increase the total acid ion production nor decrease the final char residue.

- In general, flame retardants, e.g., Sb_2O_3, alumina trihydrate, and triaryl phosphates, increase charring and decrease the rate of degradation especially in the dehydrochlorination region.

- There is very little information on the hazards of the compounds formed during pyrolysis and combustion of the plastics.

PHYSICAL SMOKE STUDIES

A description of our efforts to design and construct a usable smoke dilution system is included as Appendix D.

Also included in Appendix D is a survey of state-of-the-art commercial fire detectors.

CONCLUSIONS AND FUTURE WORK

Table 1 lists the goals we have been pursuing since the beginning of the project and Fig. 60 maps our milestones for FY'82 and FY'83.

A significant advance in FY'81 is that we have begun preliminary validation of our experimental and analytical techniques. Furthermore, many of the component parts of the program are beginning to gel into the major goals listed in Table 1.

Some specific examples are the following:

Fire chemistry

- Acid ion analysis: the small-scale acid ion sampling technique has proven to be a very useful and efficient tool for screening cable types to be tested in our large-scale apparatus.
- In the next fiscal year we will be using this tool extensively for screening. More importantly, we will be sampling from the large-scale experiments in an attempt to obtain correlations (to small scale). Such a finding would validate the small-scale technique as a useful and inexpensive method for insulation specification (for corrosive potential).
- Identification of combustion-gas components and degradation mechanisms will give insights for formulation changes for improved fire performance.

Physical Smoke

Dilution system: although our attempts to construct a usable smoke dilution system to date have been frustrating, much has been learned from the experience. The design presented in Appendix D, however, shows a great deal of promise. The determination of size, quantity, and the rate of production of combustion particulates from specific fuels present in energy technology projects is essential to predict response times for fire detection devices, and damage to equipment.

Fire Modeling

Validation burns: the first series of semi-ideal burns presented in this report have yielded encouraging results for our modeling efforts. The modeling portion of this project is the heart of the methodology. This tool will predict the potential size and growth rate of a fire in specific energy technology facility spaces. It will also predict when fire detection and suppression systems will intervene. These are the primary components defining damage and loss and ultimately fire risk. More semi-ideal burns are planned in FY'82 and also large-scale vertical cable burns.

Large-Scale Cable Burns

Although the large-scale cable burns we have completed to date were very crude, they did provide us with sufficient insight for the design of an appropriate experimental apparatus. Moreover, we have been able to roughly contrast the effects of scaling on the results (i.e., heat-release rate and ease of ignition to large-scale tests). We will be performing a number of "second-generation" experiments in FY'82 utilizing those cable types tested in small scale. It is intended that we will be able to describe the burning characteristics of vertical cable arrays in terms which will provide relevant input into our fire modeling and fire chemistry. Hopefully, we will be able to see some correlation between the large- and small-scale results.

Risk Analysis

The preliminary risk analysis of Shiva experiment included as Appendix A, performed with Econ, Inc., is an illustration of how fire risk will be defined for fire protection decision-making purposes. In a general sense, it is fairly easy to see the impact of fire loss once monetary and programmatic delay times are placed on "critical" experimental spaces. In the next fiscal year we will expand this survey to other selected energy research facilities.

The milestones chart (Fig. 60) delineates the sub-tasks which must be completed to achieve the major goals for this program. These major goals are all necessary to produce the end result which is a standard guide of fire management tactics for large energy research facilities. It is appropriate to describe the significance of each of the major milestones as to their contribution to the ultimate goal. The tasks listed under "Fire Growth Parameters for Model Development" are a combination of small- and large-scale fire experiments to provide appropriate data input to our modeling efforts and

also as a particle model validation tool. Those tasks supporting "Smoke Aerosol Production and Transport; Physical and Chemical Characteristics," will help define two major phenomena:

- Potential corrosive and particulate damage to experimental components.
- Particulate analysis (size, distribution, etc.) will provide insight to the response times of smoke detection systems.

The next two milestones are probably the most significant components of the research program. The modeling technique will predict the rate and extent of fire development in these facilities and the work on fire management systems will hopefully define how detection and suppression efforts affect the degree of fire damage. The "Advanced Fire Management System Development" phase will concentrate on unique detection and suppression systems to deal with very specific fire problems in energy facilities which traditional countermeasures cannot negate.

ACKNOWLEDGMENTS

We would like to acknowledge the efforts of personnel from Hanford Engineering Development Laboratory and Los Alamos in the preparation and performance of the model validation burns. In addition, we would like to thank the fire modelers: Professor E. E. Zukoski of Cal-Tech., Professor P. J. Pagni of U. C. Berkeley, Fritz Krause of Los Alamos, and John Creighton of LLNL, all of whom spent many hours working on experiment design, modeling predictions, and data analysis. The authors also wish to acknowledge the fine support Geronimo P. Naanep of Econ, Inc., has provided us over the past several years in the areas of fire risk and systems analysis.

Finally, we acknowledge the many hours spent by Ms. Priscilla Kelly and Ms. Laura Colberg on the production of this report.

REFERENCES

1. N. J. Alvares and H. K. Hasegawa, "Fire Hazard Analysis for Fusion Energy Experiments," Fire Safety Journal, 191-211 (1979).
2. H. K. Hasegawa, N. J. Alvares, A. E. Lipska, H. W. Ford, and D. G. Beason, Fire Protection Research for Energy Technology Projects: FY'79 Year-end Report, Lawrence Livermore National Laboratory, Livermore, CA, UCID-18902 (1981).
3. H. K. Hasegawa, N. J. Alvares, A. E. Lipska, H. W. Ford, S. Priante, and D. G. Beason, Fire Protection Research for Energy Technology: FY'80 Year-end Report, Lawrence Livermore National Laboratory, Livermore, CA, UCRL-53179 (1981).
4. A. E. Lipska, S. Priante, D. Beason, H. Ford, and S. Stover, The Combustion of Reels of Magnetic Tapes, Lawrence Livermore National Laboratory, Livermore, CA, UCID-18976 (1981).
5. Halogenated Extinguishing Agent Systems Halon 1301, National Fire Protection Association, Boston, MA (1973), pp. 12A-46, 12A-47.
6. E. E. Zukoski, "Development of a Stratified Ceiling Layer in the Early Stages of Closed-Room Fires," Fire and Materials 2 (1978).
7. W. J. Parker, Calculations of the Heat Release Rate by Oxygen Consumption for Various Applications, U.S. Department of Commerce, National Bureau of Standards, Washington, D.C., NBSIR 81-2427 (1982).
8. P. J. Pagni, University of California, Berkeley, private communication (1981).
9. D. Dresdow and C. F. Gibbs, U. S. National Bureau of Standards, Circ. 525, p. 107; Mod. Plast. 31(6), 123 (1953).
10. R. R. Stromberg, S. Strauss, and B. G. Achhammer, J. Polym. Sci. 35, 355 (1959).
11. J. S. P. Rai and G. N. Mathers, "The Thermal Dehydrochlorination of Polyvinyl Chloride," Popular Plastic (July 1977).
12. C. E. McCormack, "Flame Resistance," Rubber Age (June 1972).

CJT/jvb

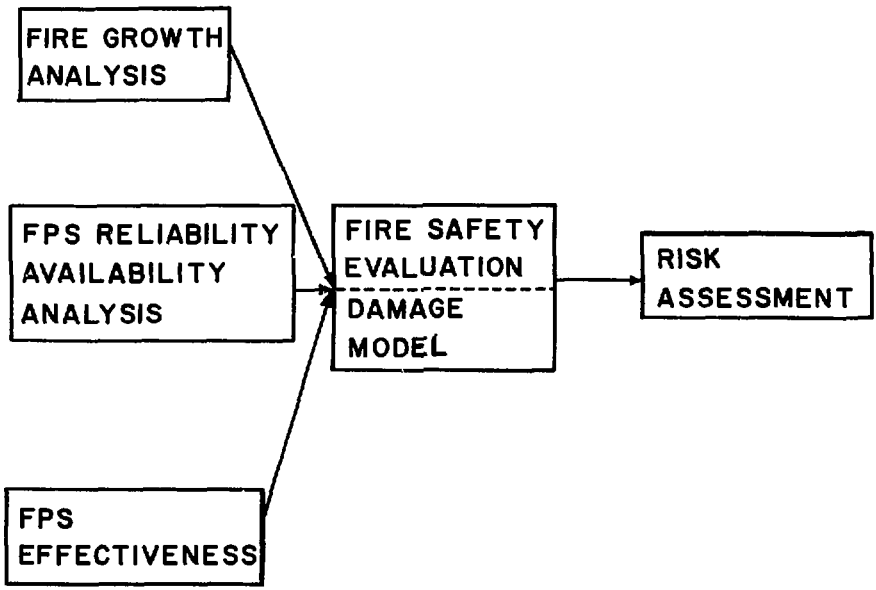

Figure 1. Schematic of overall logic of fire safety evaluation.

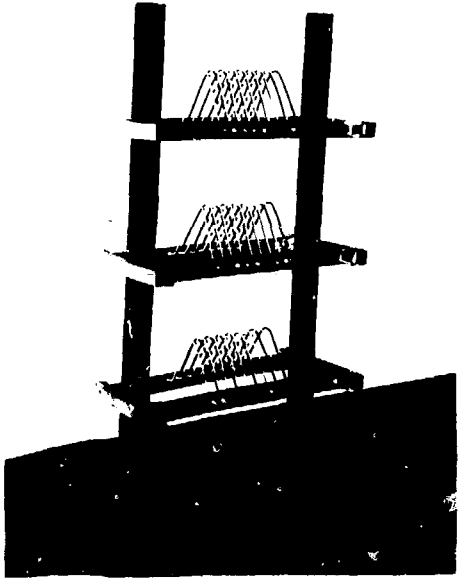

Figure 2. Photograph of magnetic tape rack.

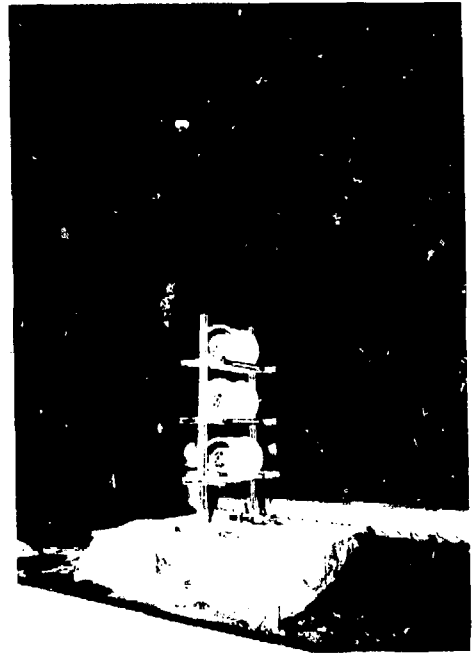

Figure 3. Photograph of magnetic tape set-up.

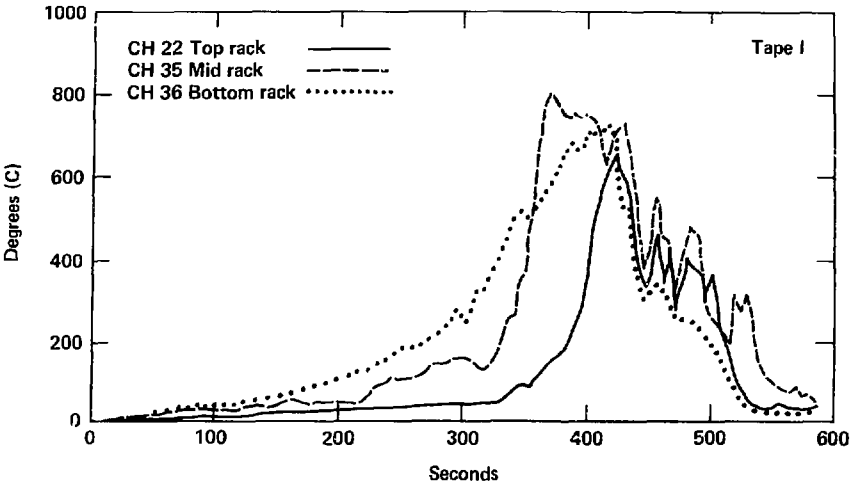

Figure 4. Temperature profiles for bottom, middle, and top racks of magnetic tape burn.

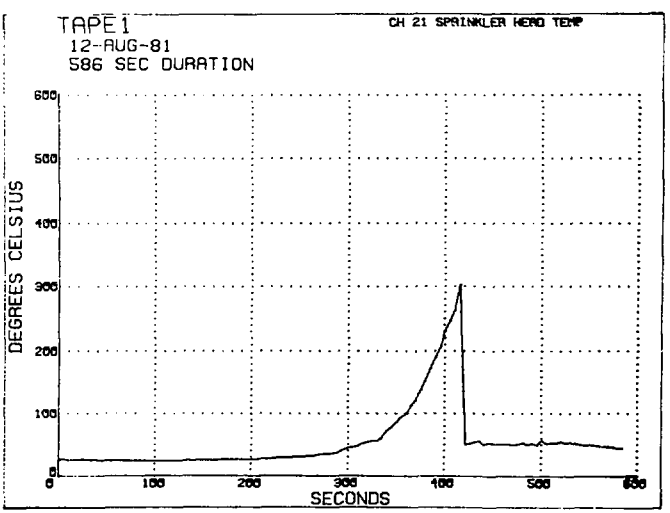

Figure 5. Plot of air temperature next to sprinkler head.

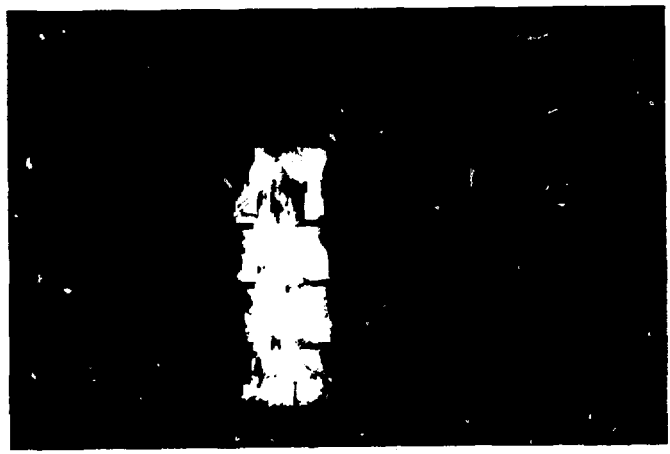

Figure 6. Photograph of fully developed magnetic tape burn.

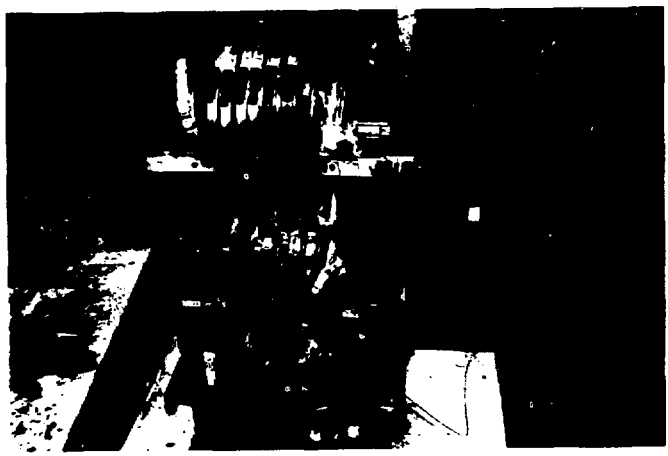

Figure 7. Post-test photo of magnetic tape burn.

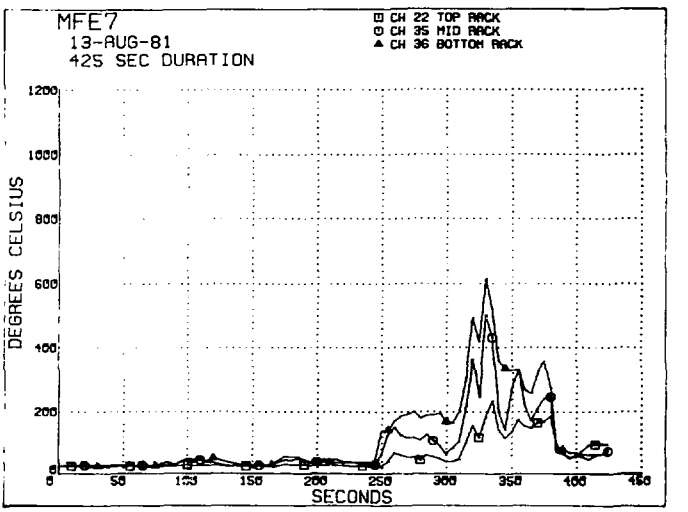

Figure 8. Composite temperature plot of fully involved magnetic tape burn.

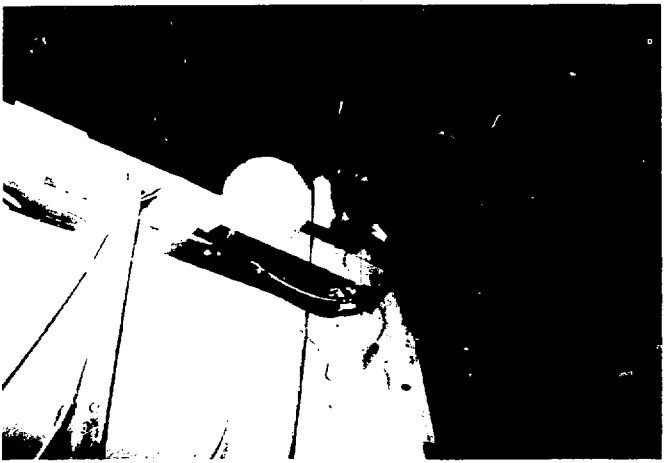

Figure 9. Photograph of Halon sphere set-up with transducer.

Figure 10. Photo of compartment set-up.

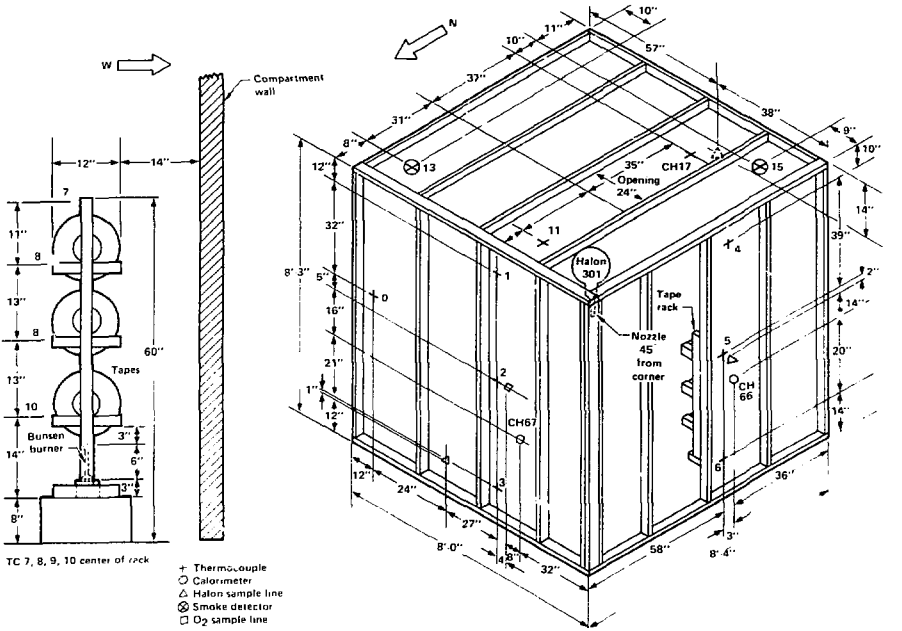

Figure 11. Diagram of compartment and associated instrumentation.

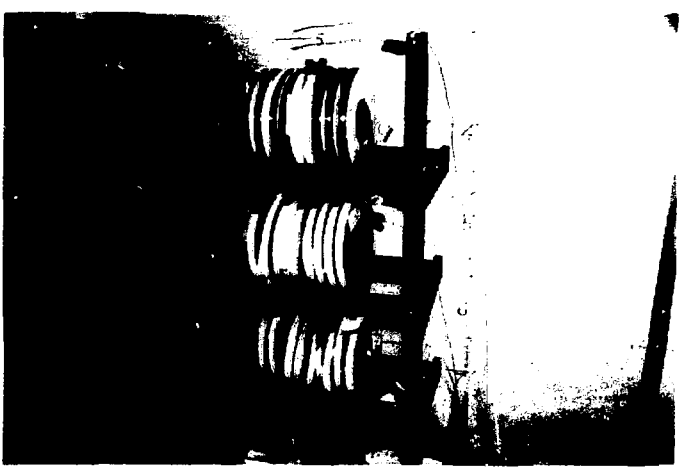

Figure 12. Photograph of typical tape rack set-up.

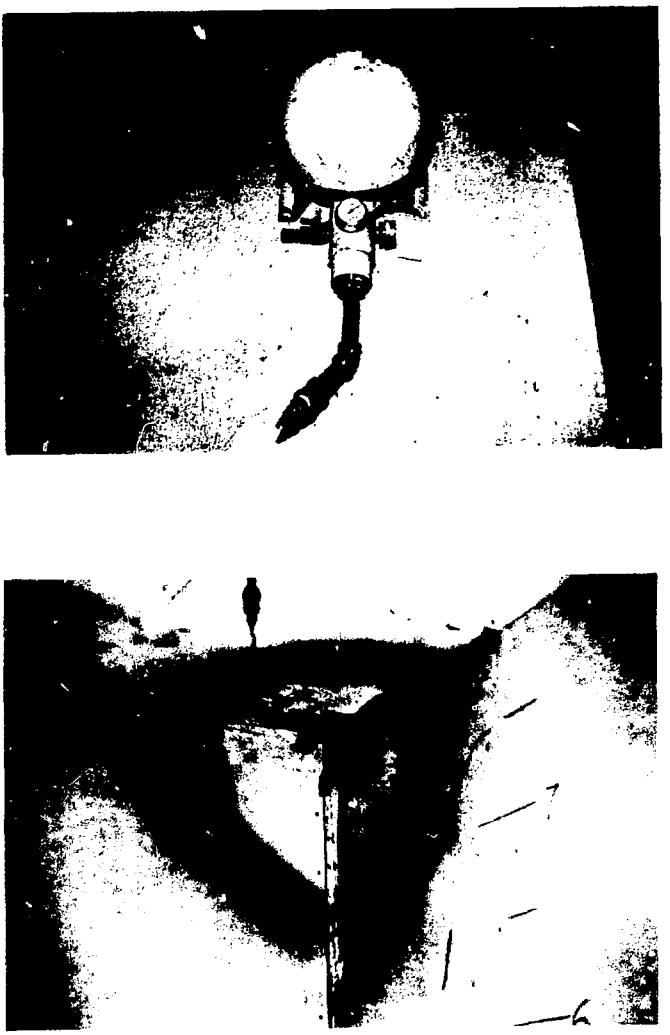

Figure 13. Halon sphere nozzle.

Figure 14. View of tape rack through compartment door.

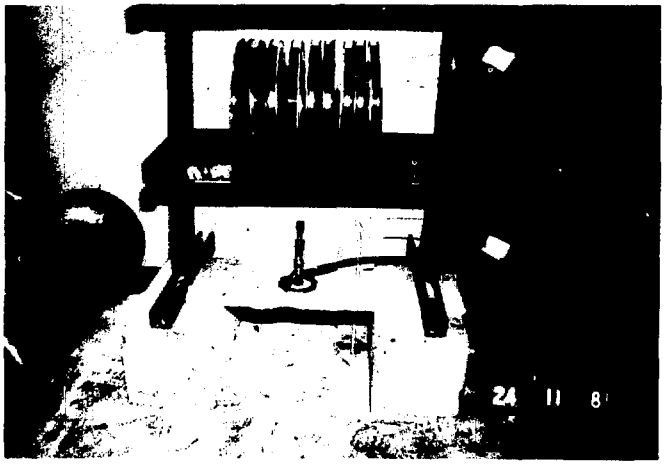

Figure 15. Bunsen burner ignition source.

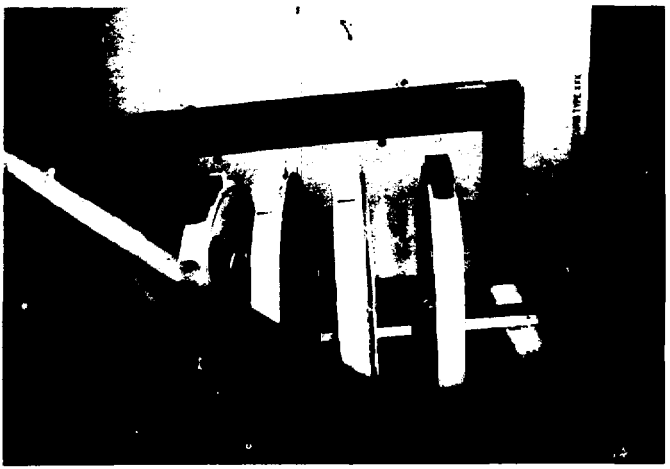

Figure 16. Gypsum wallboard shield of programmed tapes.

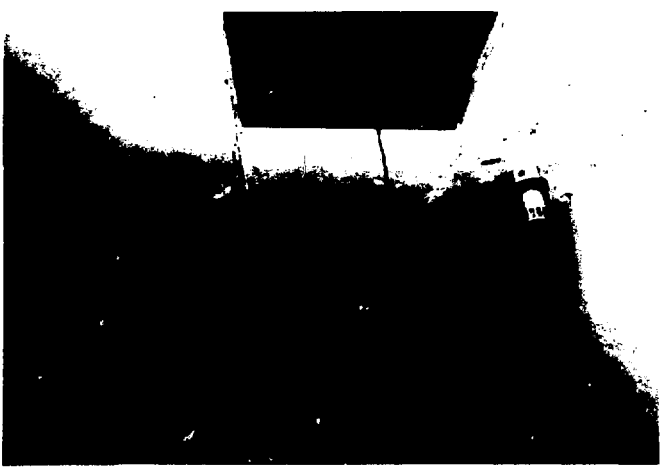

Figure 17. Detector.

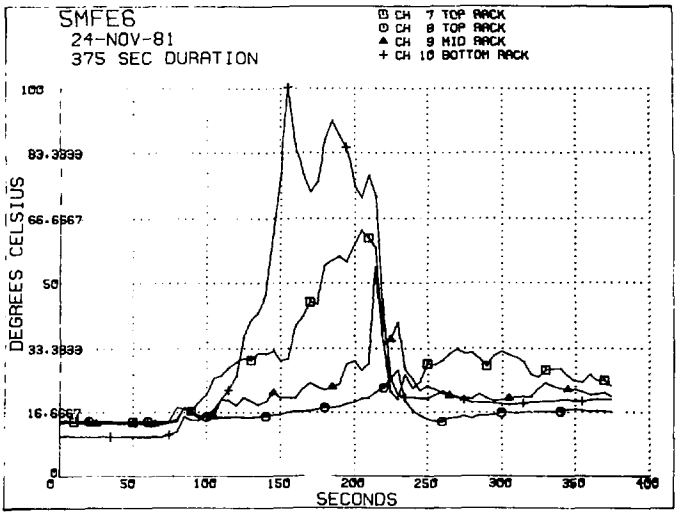

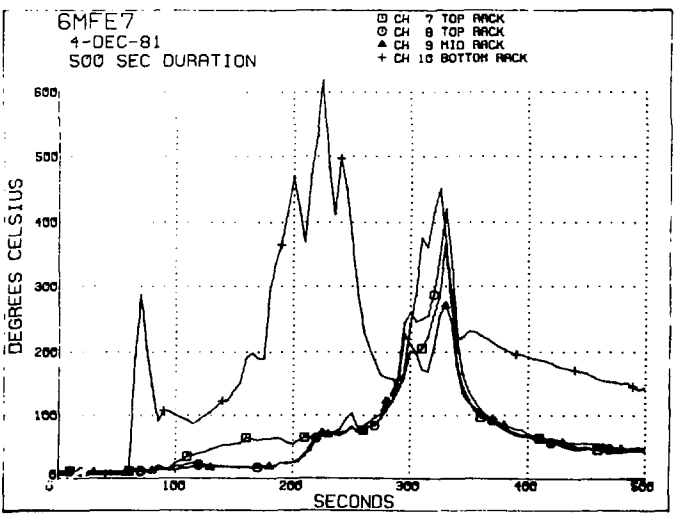

Figure 18. Multiple temperature plots of bottom and middle rack from pre-programmed tape burn.

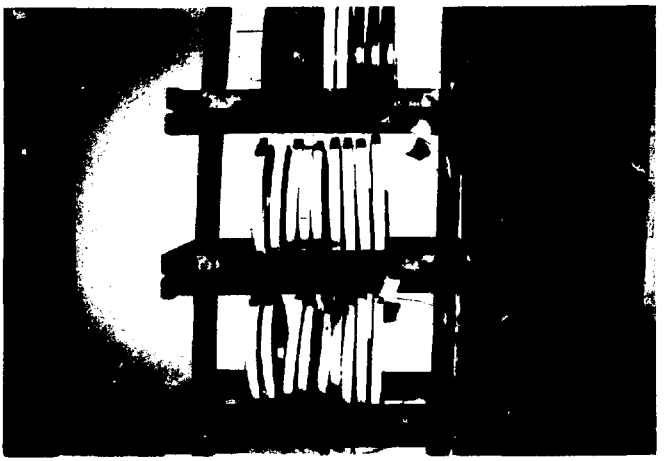

Figure 19. Post-burn photograph of preprogrammed tapes from Experiment #1.

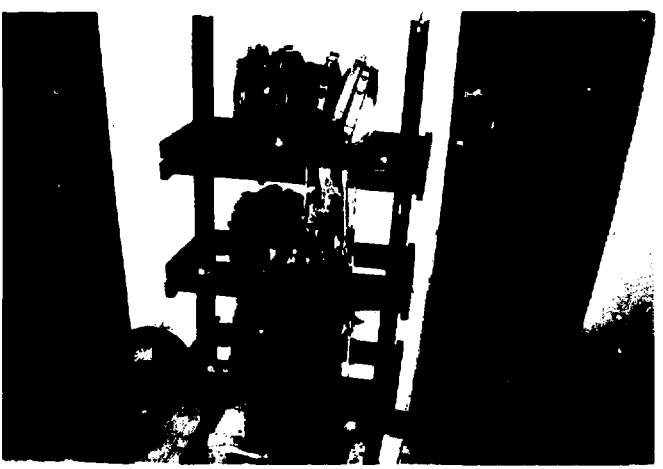

Figure 20. Post-burn photograph of preprogrammed tapes from Experiment #2.

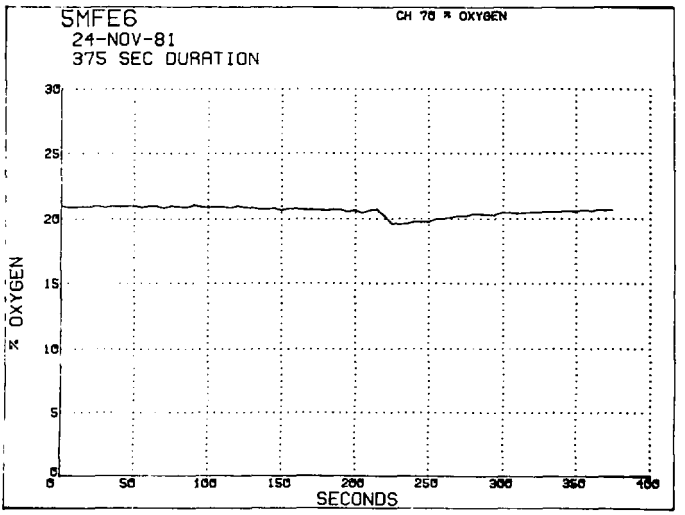

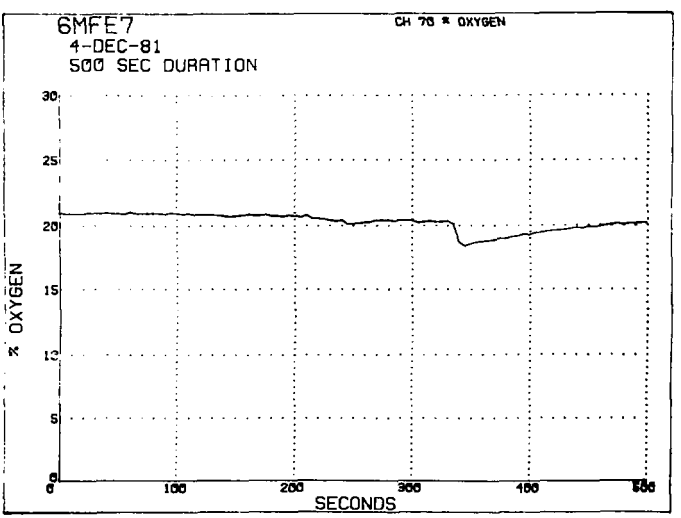

Figure 21. Composite plots of O_2 concentration for Experiments #1 and #2.

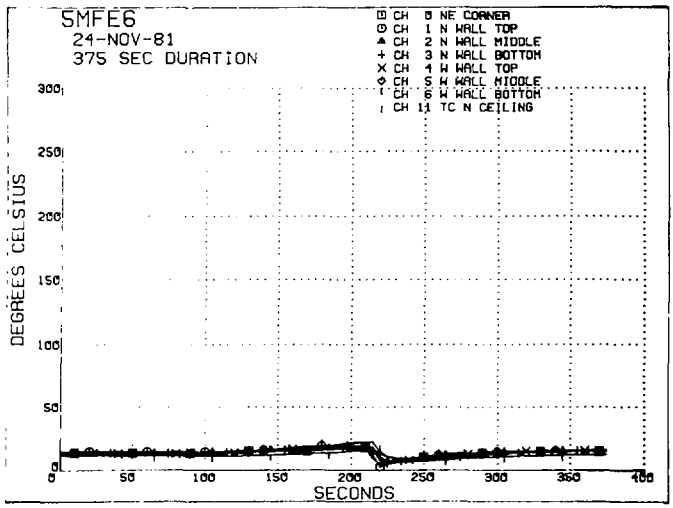

Figure 22. Temperature profile from compartment thermocouples--Experiment #1.

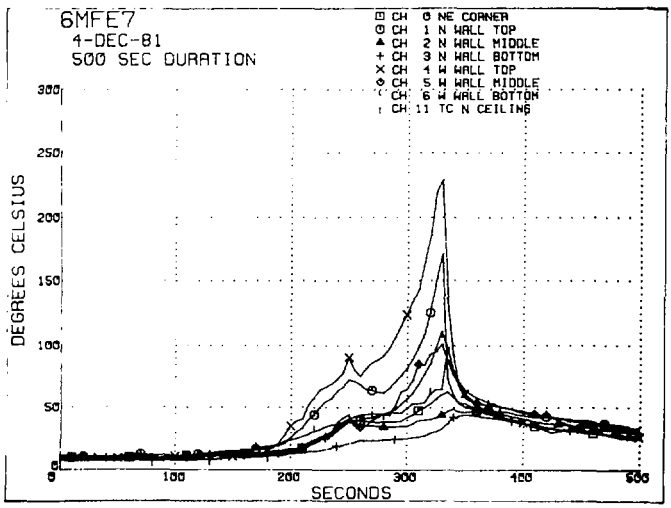

Figure 23. Temperature profile from compartment thermocouples--Experiment #2.

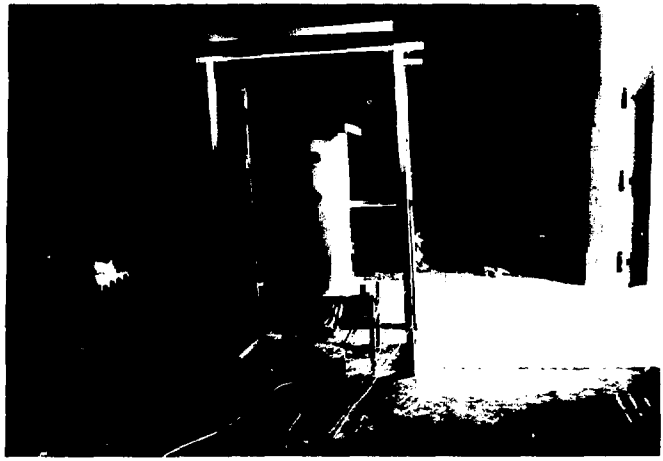

Figure 24. Prototype large-scale cable fire set-up.

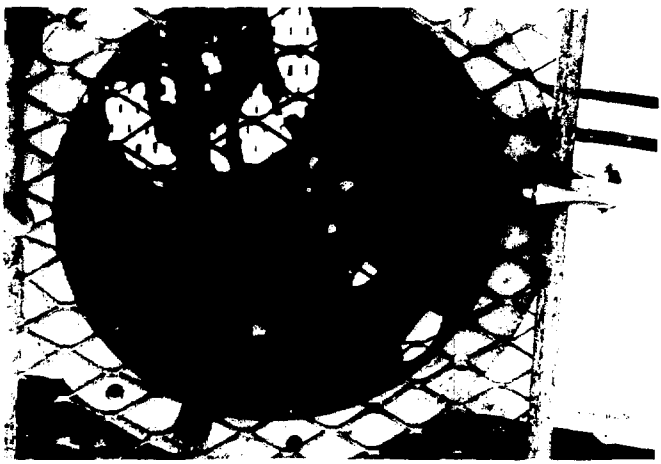

Figure 25. Expanded metal grate clamped to top of pipe.

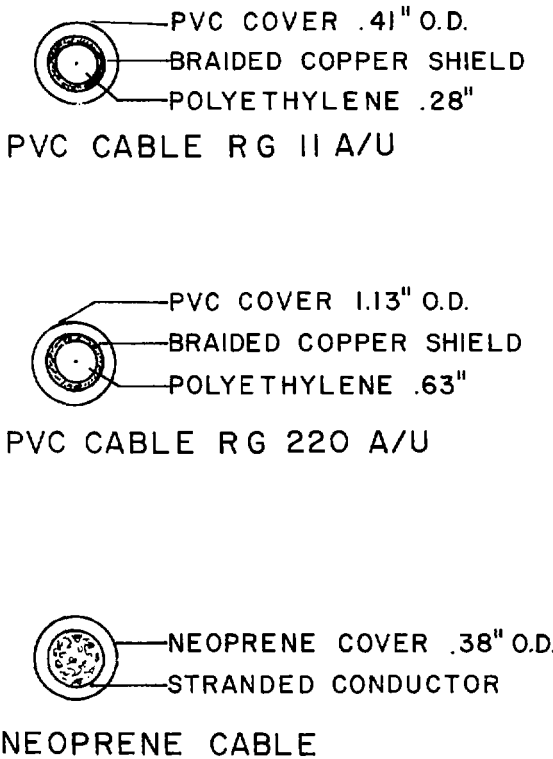

Figure 26. Cross-sectional composition of 1-in.- and 1/2-in.-diameter PVC-jacketed coaxial cable.

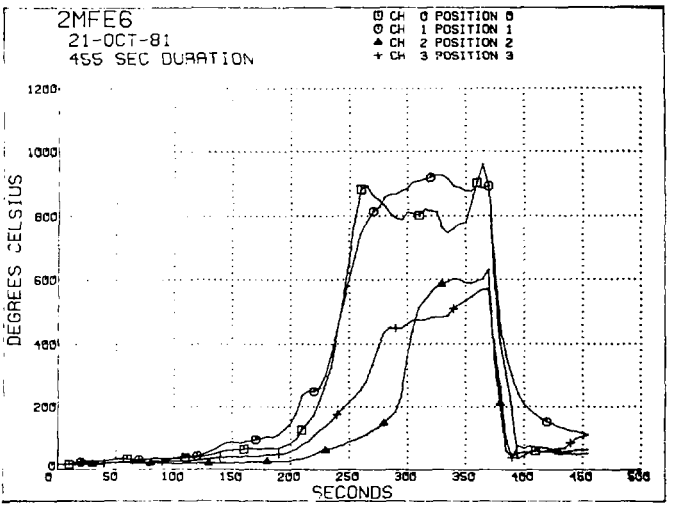

Figure 27. Composite plot of temperatures within the pipe, for rubber-jacketed multiconductor cable.

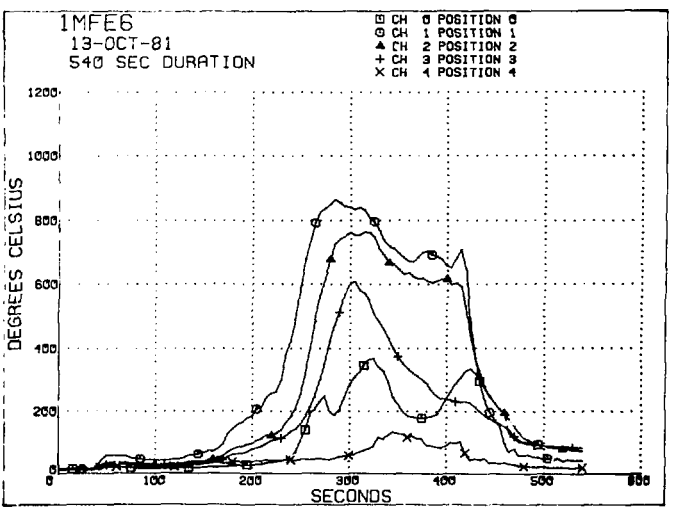

Figure 28. Composite plot of temperatures within the pipe, for rubber-jacketed stranded copper cable.

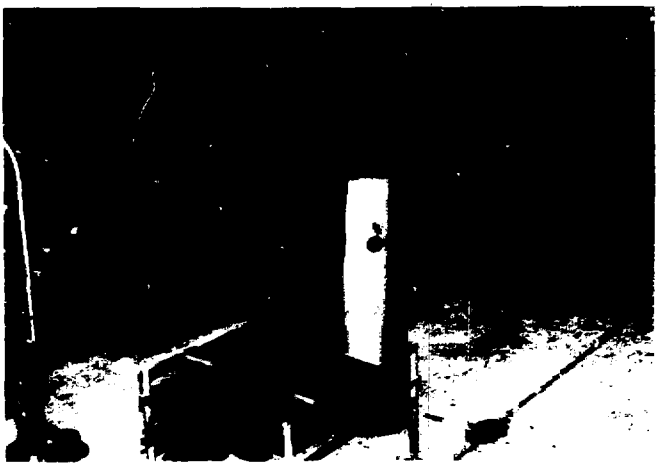

Figure 29. Post-test photograph of rubber-jacketed cable.

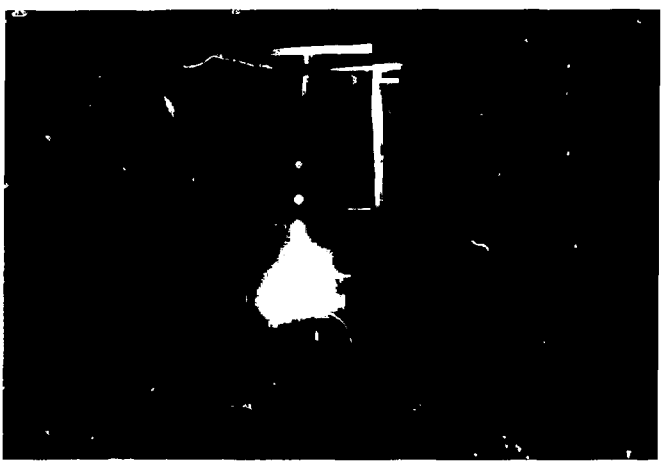

Figure 30. Photograph of test in progress.

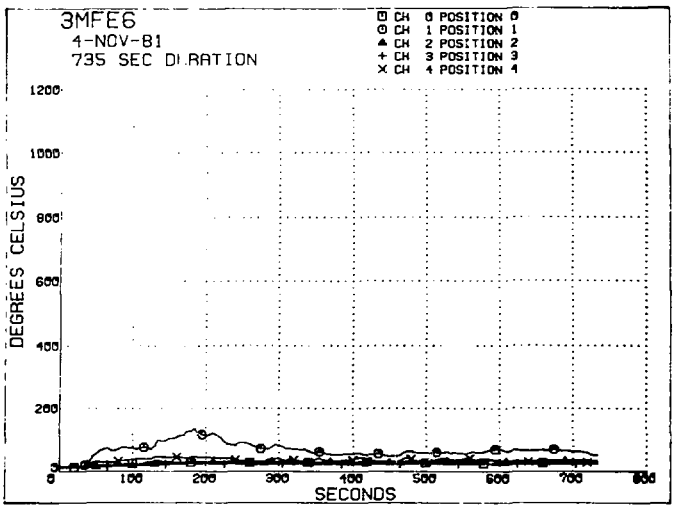

Figure 31. Temperature profile for RG 200 A/U cable burn.

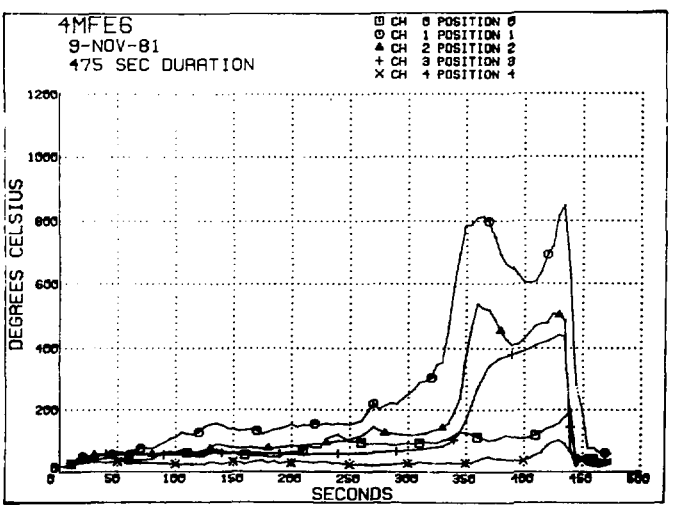

Figure 32. Temperature profile for RG 11 A/U cable burn.

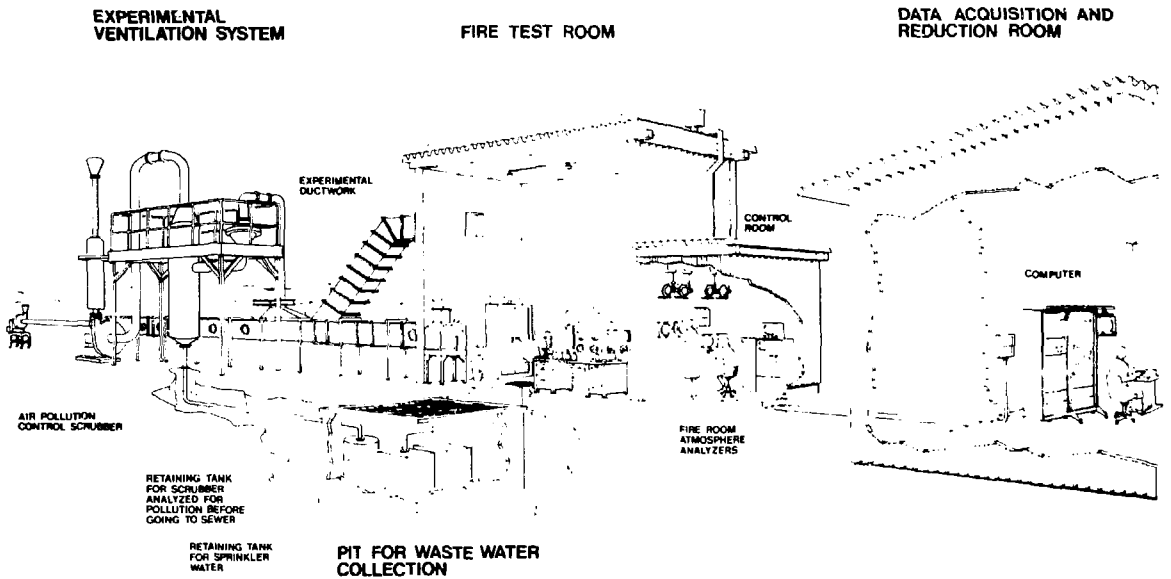

Figure 33. Schematic of test enclosure.

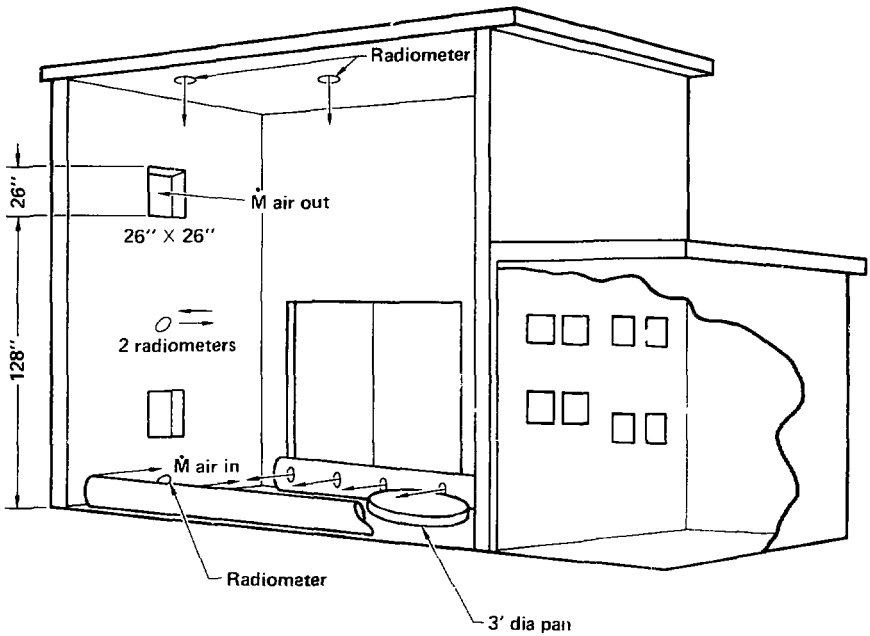

Room dimension 20' L X 13'6" W X 15' H
Door dimension 7' W X 8' H

Figure 34. Schematic presentation of pertinent test cell dimensions.

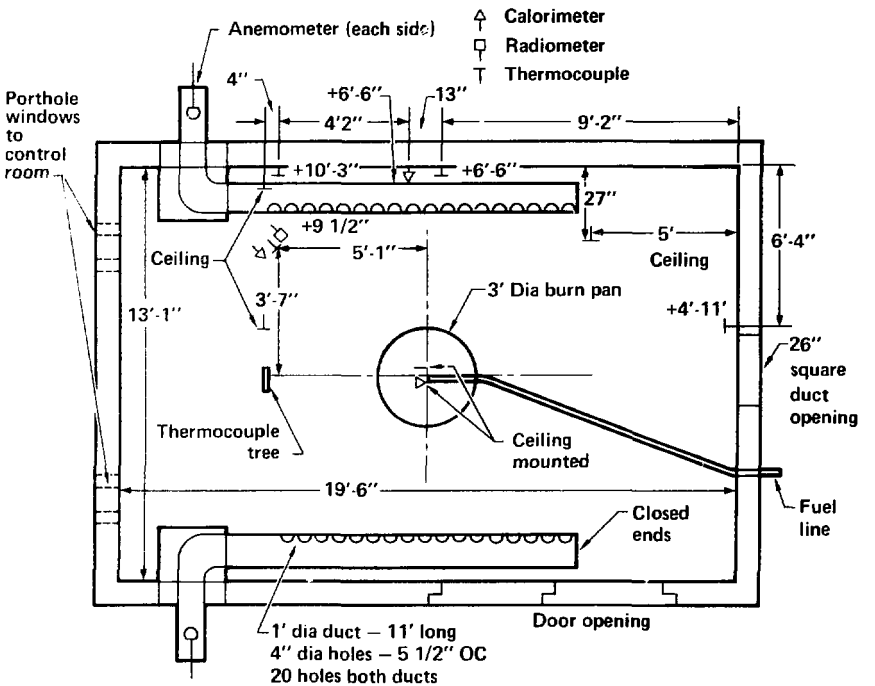

Figure 35. Schematic presentation of the spatial relationships of internal components.

a.

b.

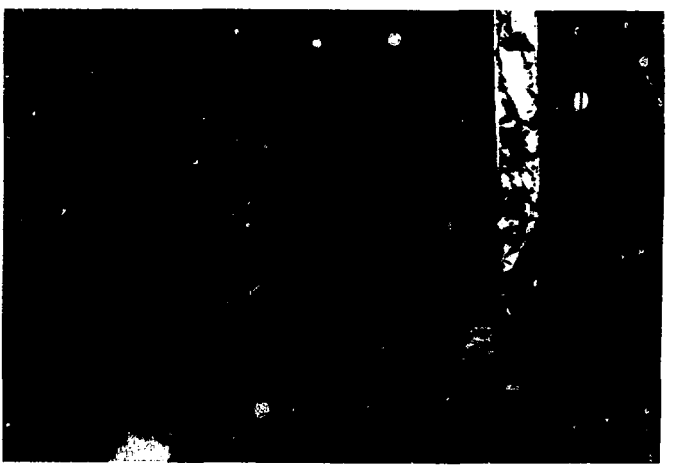

Figure 36. Photographic views of test cell components and sensors.

c.

d.

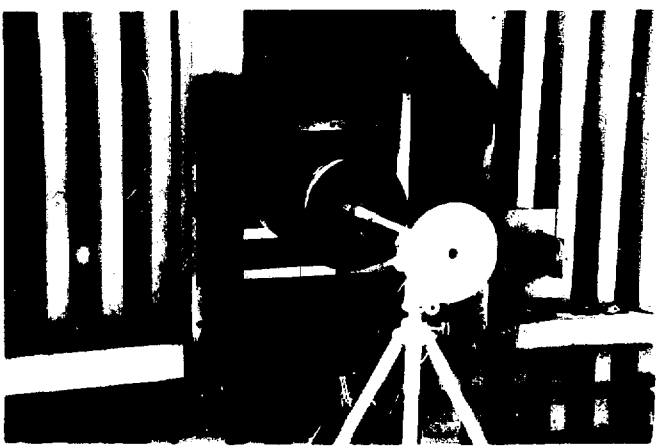

Figure 36. (Continued.)

a.

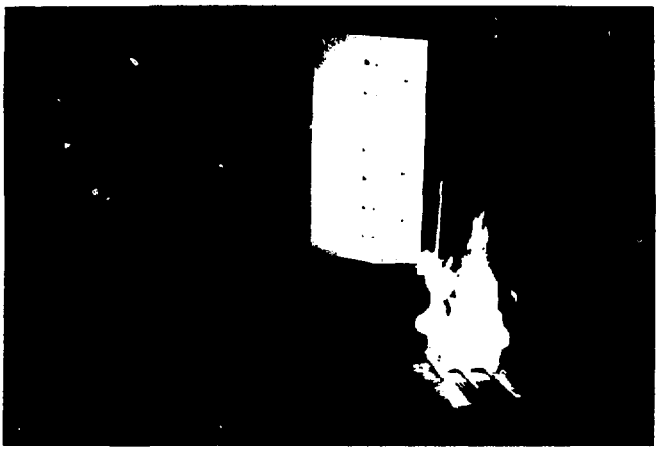

b.

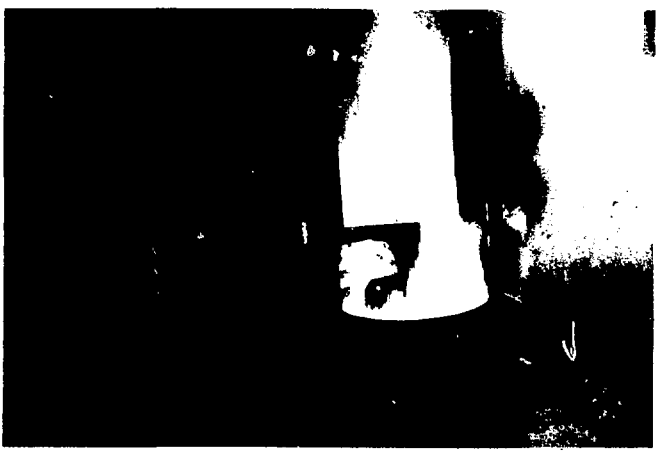

Figure 37. Examples of non-smoky fuel fires.

c.

d.

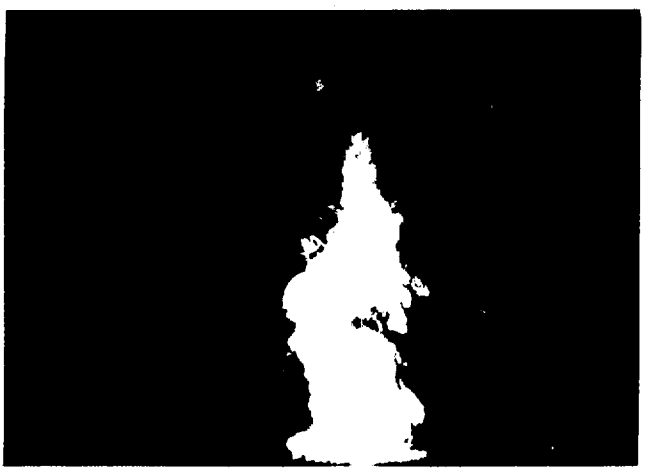

Figure 37. (Continued.)

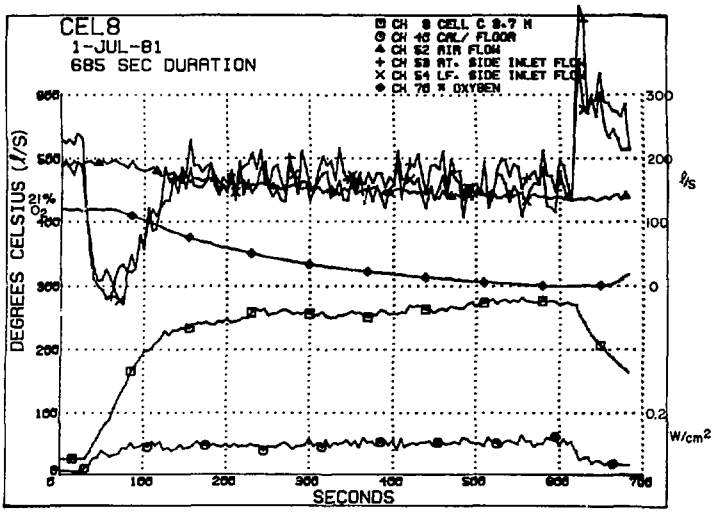

Figure 38. Fire portrait of a 400-kW fire, ventilated at 500 l/s.

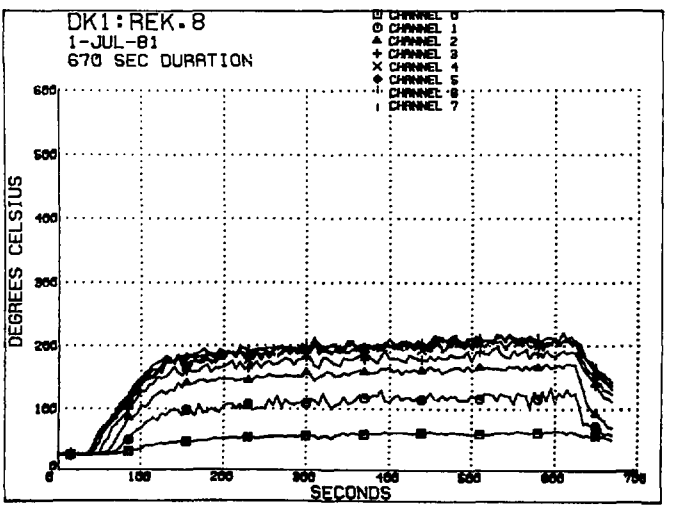

Figure 39. Temporal increase of individual thermocouple stations along rake.

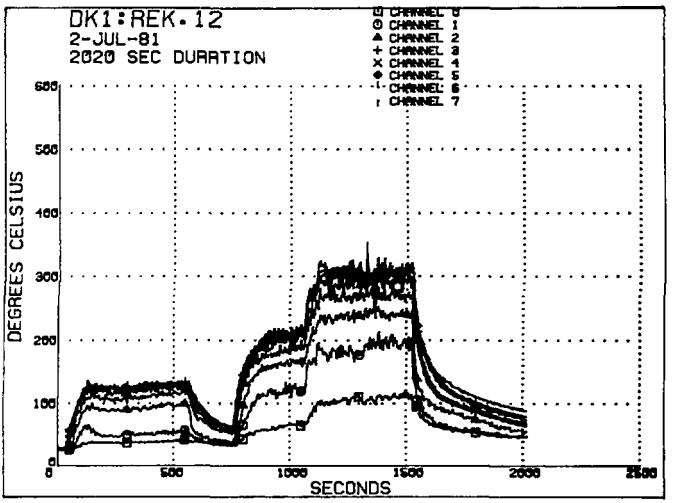

Figure 40. Data from thermocouple rake where fire strength varied from 200 kW to 400 kW to 800 kW in discrete steps.

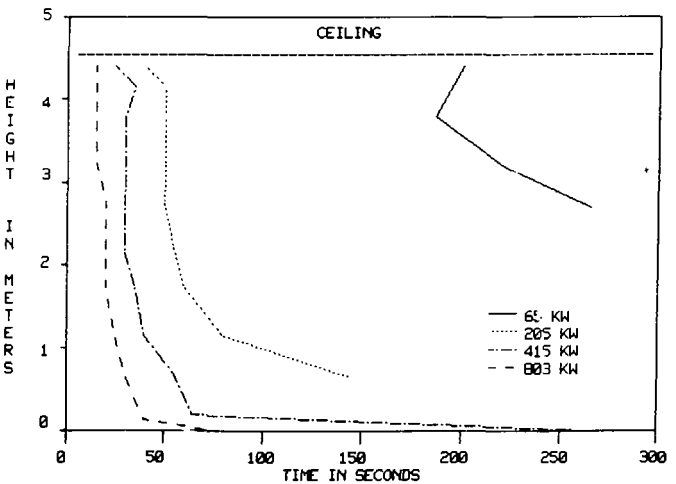

Figure 41. Descent of 70°C temperature isotherm for fires of various strengths.

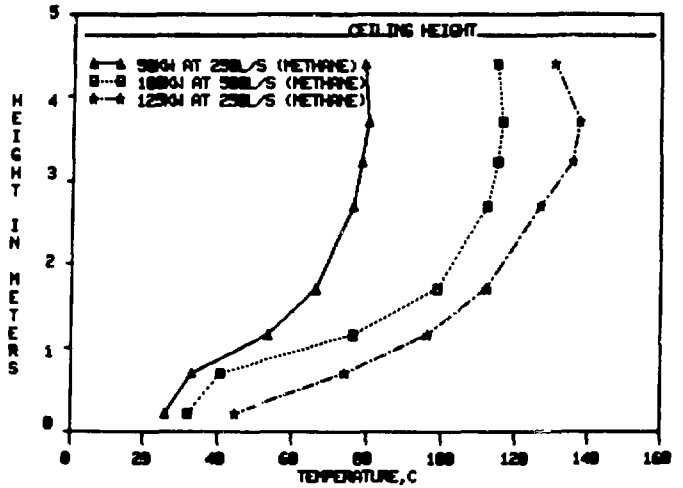

Figure 42. Quasi-steady-state vertical temperature distribution.

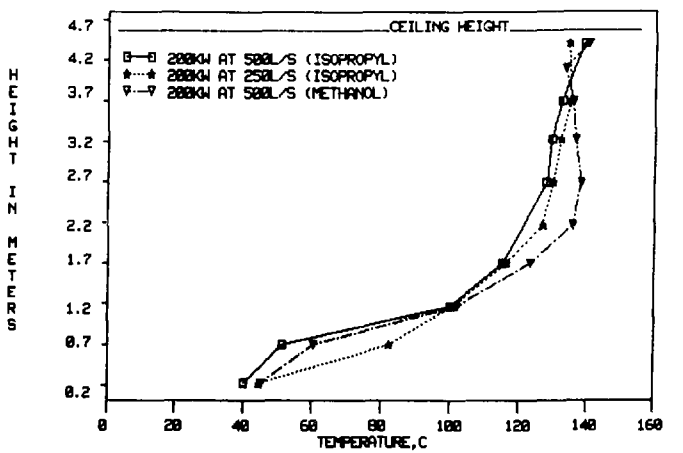

Figure 43. Quasi-steady-state vertical temperature distribution.

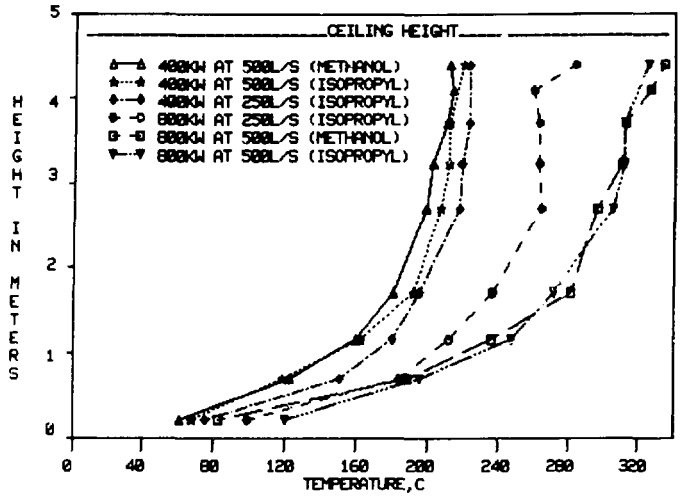

Figure 44. Quasi-steady-state vertical temperature distribution.

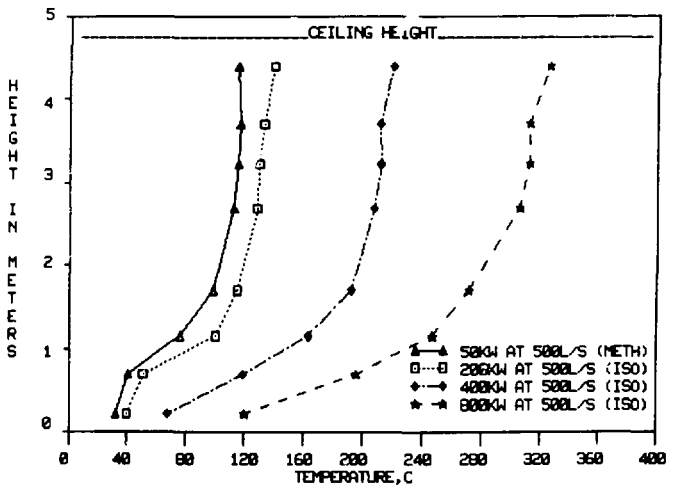

Figure 45. Composite of curves showing difference in vertical temperature gradient for spray fires at 500 l/s ventilation rate.

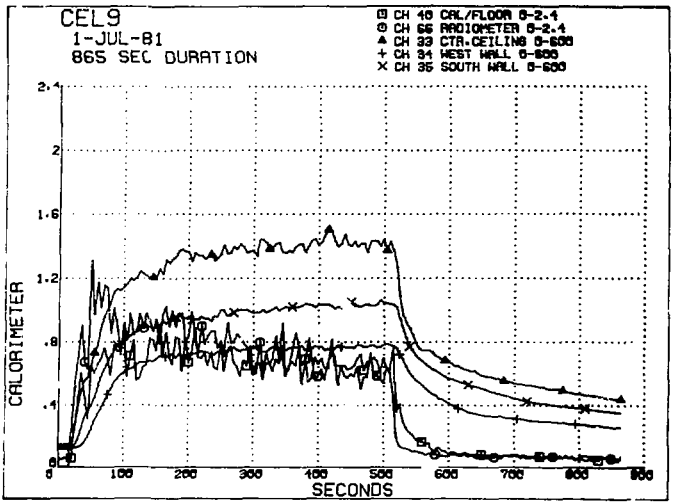

Figure 46. Specific surface temperature measurement as measured with thermocouples in compression contact with the surface.

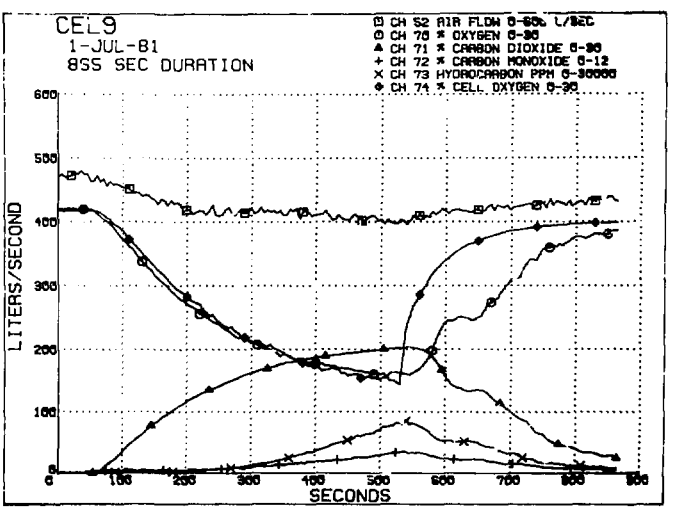

Figure 47. Computer plotting of O_2 depletion, CO, CO_2, and unburned hydrocarbon production.

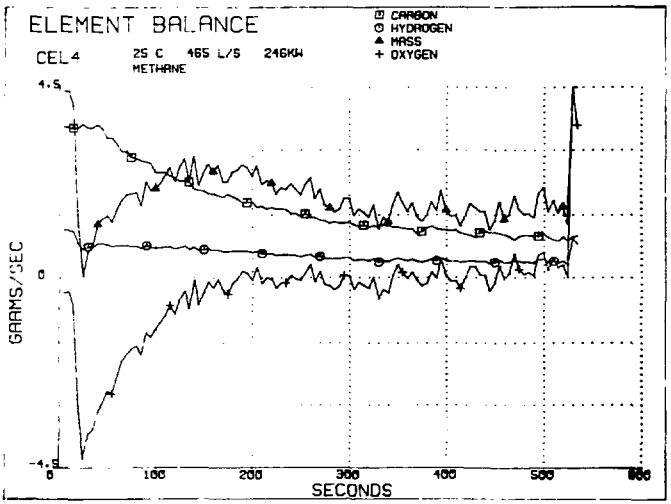

Figure 48. Elemental balance between input carbon from methane and output carbon in form of CO, CO_2, and measured partially oxidized hydrocarbon fractions.

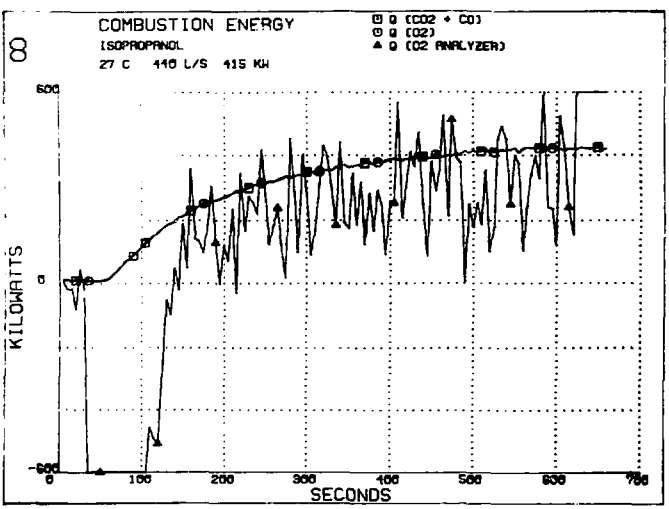

Figure 49. Comparison of total combustion heat-release rate from: CO/CO_2 production measurements, O_2 depletion measurements, and O_2 depletion calculated from CO/CO_2 measurements.

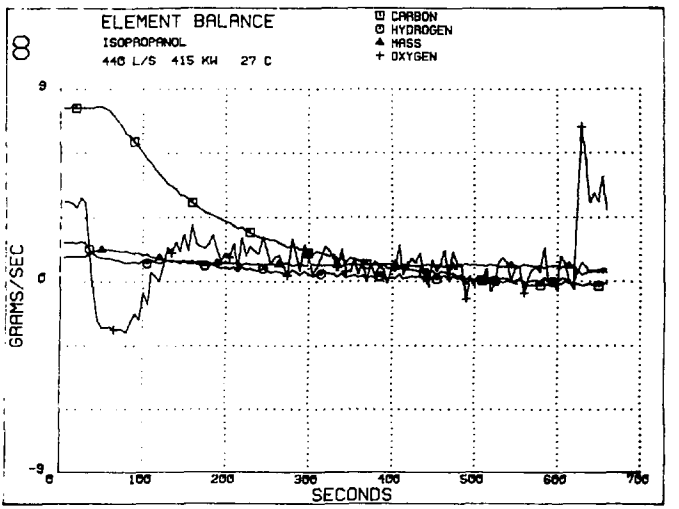

Figure 50. Elemental balance for sprayed propyl alcohol fuel, design ventilated at 440 l/s.

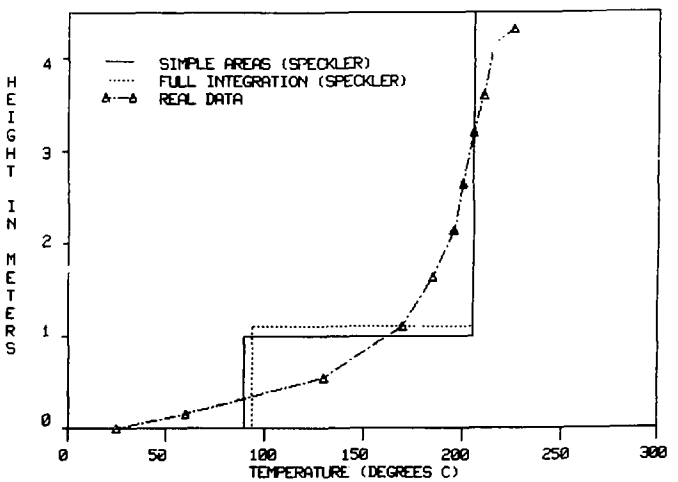

Figure 51. Comparison of vertical temperature distribution with Speckler's two-layer calculation.

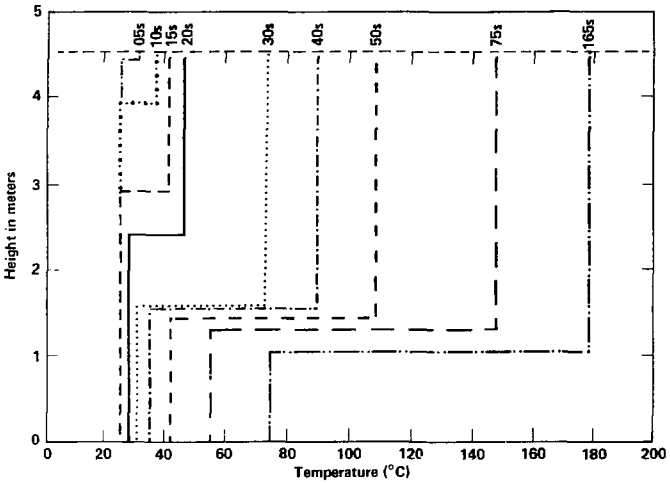

Figure 52. Display of descent rate of pseudo (Speckler's) interface.

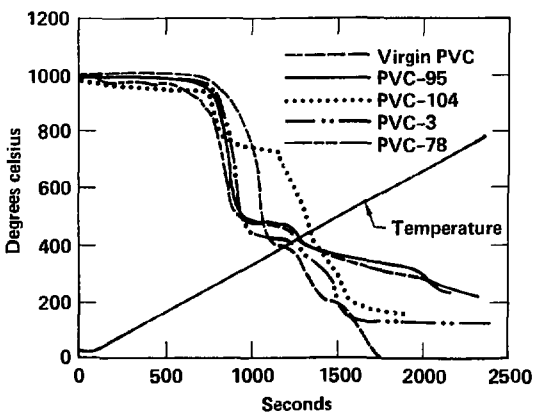

Figure 53. Comparison of thermograms of four different types of insulations and virgin PVC heated in air at 20°C/min.

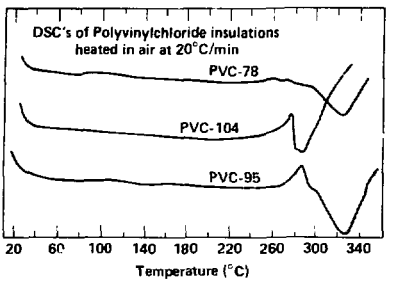

Figure 54. DSC curves of pure PVC polymer as well as polymer plastics heating in air at 20°C/min.

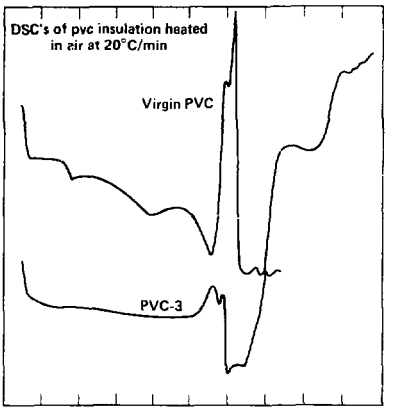

Figure 55. DSC curves of pure PVC polymer as well as polymer plastics heating in air at 20°C/min.

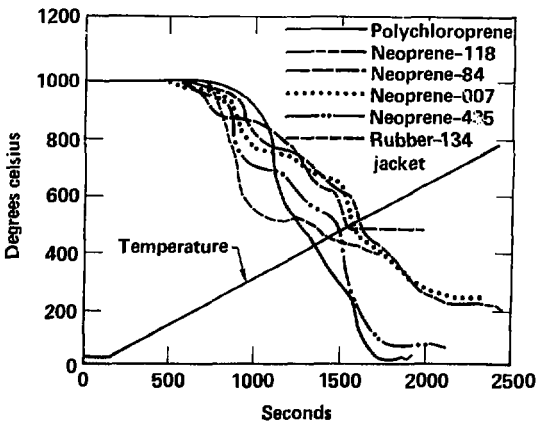

Figure 56. Thermograms of various rubber formulations heated in air at 20°C/min as compared to pure polychloroprene polymer.

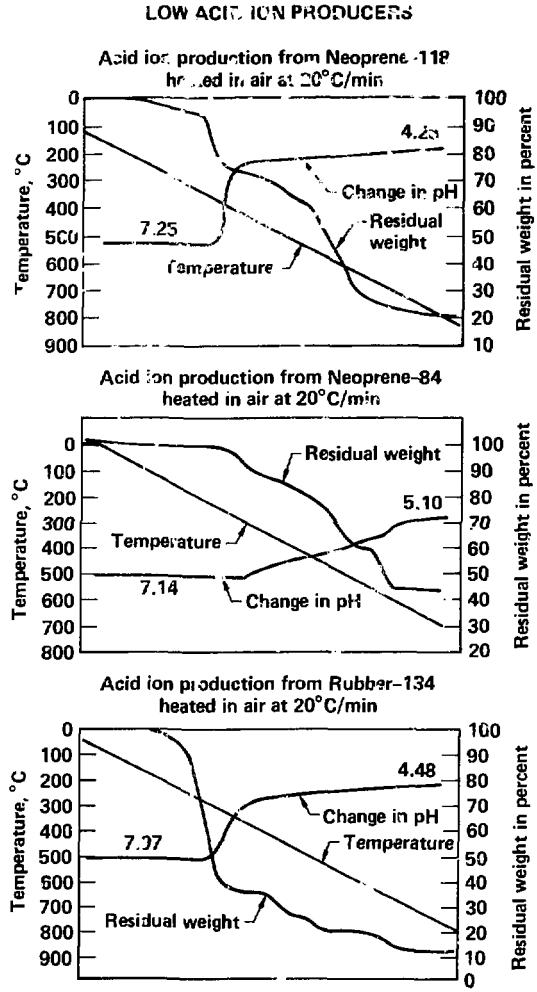

Figure 57. Acid ion production and thermograms for individual rubber insulations.

HIGH ACID-ION PRODUCERS

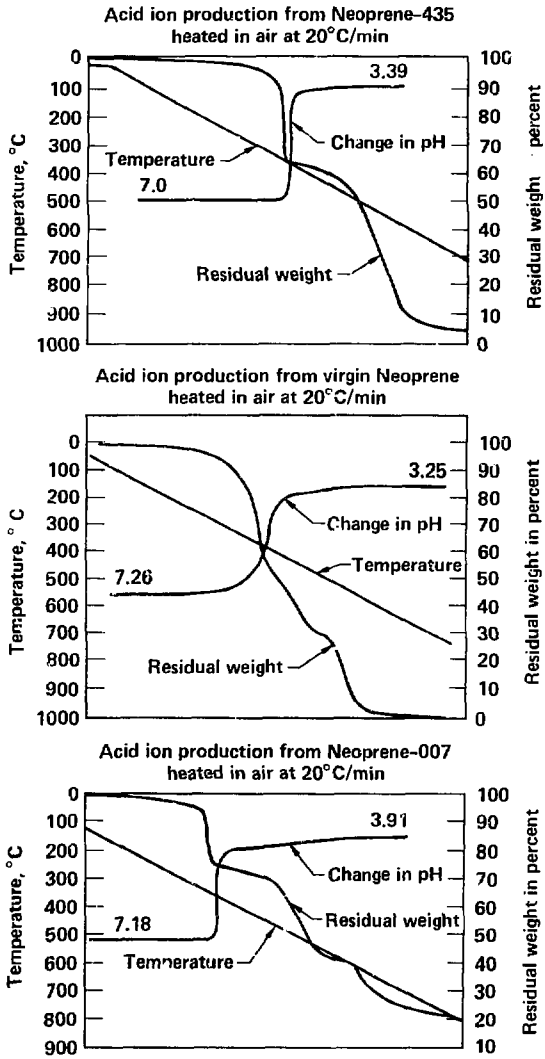

Figure 58. Acid ion production and thermograms for individual rubber insulations.

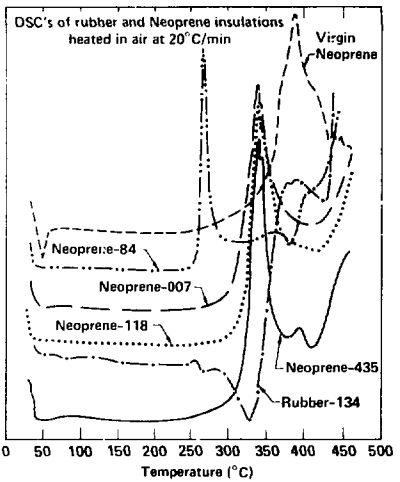

Figure 59. DSCs of rubber and neoprene insulations heated in air at 20°C/min.

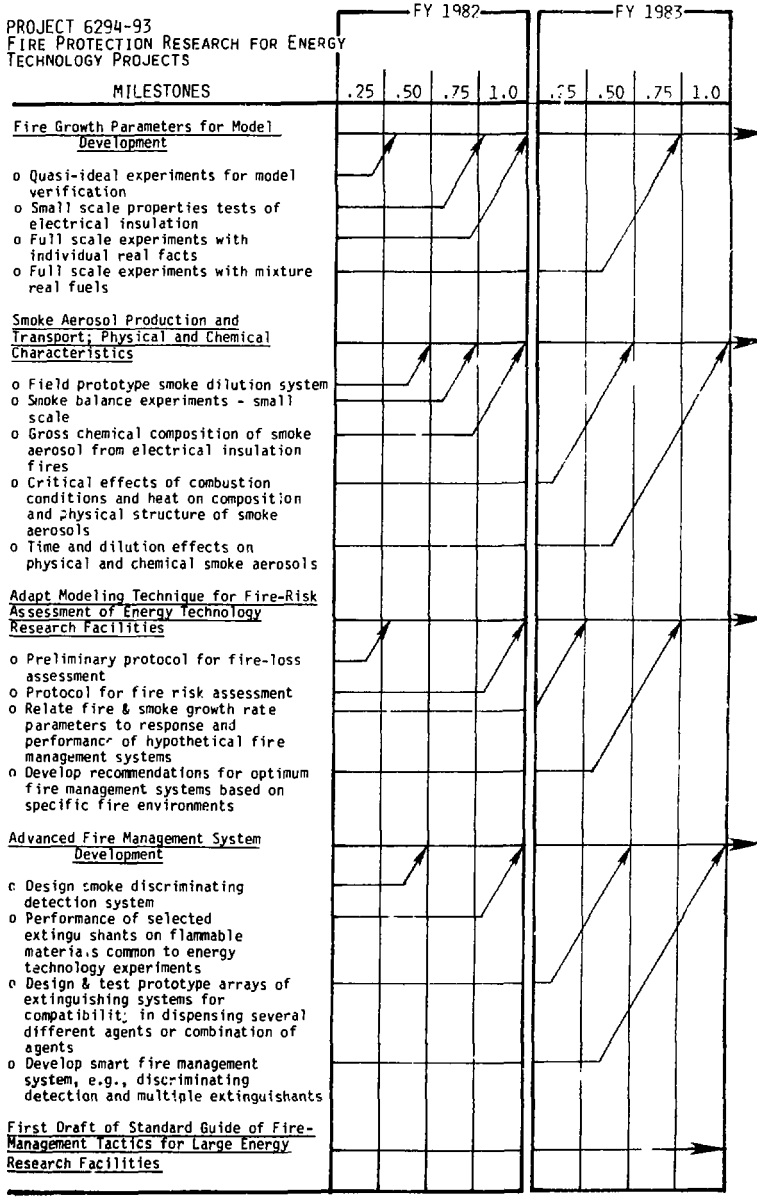

Figure 60. Milestones chart for FY'82 and FY'83.

Table 1. Program Objectives.

	A. Major goal: Parallel development of fire safety with fusion energy technology.
FAULT-TREE ANALYSIS	B. Define the engineering performance of state-of-the-art fire protection as applied to fusion energy experiments.
	C. Develop rational methods of assessing fault modes in fire protection systems.
	D. Develop techniques for defining fire hazards of fusion energy experiments.
FIRE GROWTH ANALYSIS	E. Couple hazards analysis with fire protection systems analysis for LLNL facilities.
	F. Develop survey protocol for fusion energy experiments at non-LLNL facilities and validate.
FIRE SAFETY EVALUATION	G. Analyze survey results and evaluate fire safety of each installation.
	H. Conduct research to solve identified problems.

Table 2. List of measured parameters along with design fire strength and ventilation variations.

Measured Quantities

- Fuel flow rate
- Inlet and outlet air flow rate
- Temperatures:
  - wall & ceiling
  - 3-D array - test cell (27 sites)
  - exhaust force stream
  - vertical rake (10 sites, 1-ft increments)
  - combustion plume
- Thermal measurements
  - wall radiation
  - ceiling radiation
  - plume radiation
- Enclosure pressure (temporal)
- Video of combustion plume
- Fixed gases (temporal) (in exit duct)
  - oxygen depletion
  - CO/CO_2 formation
  - total hydrocarbon
- Specific humidity (temporal) (in exit duct)
- Environmental conditions
  - relative humidity
  - ambient temperature
  - atmospheric pressure

Fire Strength Variation

50 kW, 100 kW, 200 kW, 400 kW, 800 kW

Ventilation Variation

250 l/s (500 cfm), 500 l/s (1000 cfm)

Comparative Parameters for Model and Experiment

- Ceiling layer growth
- Temperature rise in ceiling layer
- Inlet air flow rate as controlled by temperature and pressure condition in test cell

Table 3. Instrument type, calibration, and precision of devices used for sensing parameters of test cell fires and associated ventilation flow characteristics.

- Oxygen Depletion:
  Beckman model 402: 5ppm-1% accuracy, response time: 90%, 1 s

  Beckman model OM-11: ±5% full scale accuracy, response time: 90%, 80 us (exit duct)

- CO Formation:
  Beckman model 864: 1% full scale accuracy, response time: 90%, .5 s

- CO_2 Formation:
  Beckman model 864: ±1% full scale, response time: 90%, .5 s

- Ceiling, Wall Temp:
  Type K TCs (exposed bead, avg. 22, chromel-alumel)

- Rake:
  Type K TCs (exposed bead, chromel-alumel .005 diam)

- Outlet & Inlet Test Cell Ventilation Rate:
  Orifice differential pressure
  Vane anemometers - R. M. Young: very linear response above 1 m/s (2.2 mph). Threshold speed (lower) 0.2 m/s (0.4 mph) ±2% accuracy.

- Humidity: from wet bulb, dry bulb, relative humidity taken from stoichiometric chart in Industrial Ventilation from wet bulb, dry bulb values.

- Ambient Temperature: from initial conditions of rake, TC's where rakes not available (cell 1,7)

- Pressure: P24 Validyne transducers
  Range: ±.01 to ±3000 psia; 0.1 to 3000 psia full scale
  Stability: ±0.1%/supply voltage change from ±22 to ±35 VDC

- Radiant Energy: Hi Cal Radiometer and Calorimeters

- Liquid Fuel Flow: Flow rater FP-1/2-27-G-10/58. Calibration of constant pressure - where flow rate is metered by value

- Gas fuel flow: flow-rater factory calibrated for methane

Table 4. Air flow balance data for 200-kW, 400-kW, and 800-kW propyl alcohol fires ventilated at design exit flow rate of 500 l/s.

	Initial			Max. outflow			Steady-state		
	Forced (g/s)	Free (g/s)	Net (g/s)	Forced (g/s)	Free (g/s)	Net (g/s)	Forced (g/s)	Free (g/s)	Net (g/s)
200 kW	-496	+537	+41	-556	+ 89	-467	-434	+437	+3
400 kW	-512	+501	-11	-556	- 47	-603	-410	+389	-21
800 kW	-484	+468	-16	-557	-462	-1015	-355	+395	+40

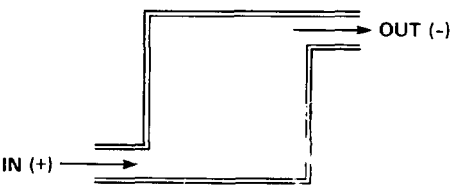

Table 5. Summary of tests conducted during the fire-modeling test series.

TEST SERIES	
CEL 1	43 kW/250 l/s Methane gas through "H" burner with flow rate set at 160 Fire strength calculated at 43kW
CEL 2	50 kW/250 l/s Methane gas through "H" burner with flow rate set at 191 @ 38 psig 30°C
CEL 3	25 kW/250 l/s Methane gas through "H" burner with flow rate set at 93 @ 14 psig (94 later)
CEL 4	50 kW/500 l/s Methane gas through "H" burner with flow rate set at 190 @ 33 psig 26°C
CEL 5	200 kW/250 l/s Isopropyl alcohol sprayed in 3-ft-diameter pan at 250 ml/min 15 on flowmeter
CEL 6	400 kW/250 l/s Isopropyl alcohol sprayed in 3-ft-diameter pan at 1040 ml/min 33 on flowmeter
CEL 7	200 kW/500 l/s Isopropyl alcohol sprayed in 3-ft-diameter pan at 520 ml/min 15 on flowmeter *No data on T/C Rek, no data on duct O_2 until last few seconds. First run with good CEL O_2 data (missing "O" ring in detector)
CEL 8	400 kW/500 l/s Isopropyl alcohol sprayed in 3-ft-diameter pan at 1040 ml/min 33 on flowmeter
CEL 9	800 kW/500 l/s Isopropyl alcohol sprayed in 3-ft-diameter pan at 2080 ml/min 63 on flowmeter

Table 5. (Continued).

CEL 10 and CEL 11 800 kW/250 l/s

Isopropyl alcohol sprayed in 3-ft-diameter pan at 2080 ml/min
63 on flowmeter

Moved O_2 (cell) to 28 in. from center line of pan and 15 in. above floor

*Reason for linking CEL 10 and CELL 11. Data acquisition stopped during CEL 10 restarted under CEL 11 on DKO. Later linked to a single file called CEL 10.

CEL 12 Step 200, 400, 800 kW/500 l/s

Isopropyl alcohol sprayed into 3-ft-diameter pan at 520 ml, 1040 ml, 2080 ml/min
15, 33 and 63 on flowmeter
air flow at 500 l/s
T/C at edge of pan was not in flame

*Changed CH 19 Ceiling at C1 (contact)
CH 20 Ceiling at C6
CH 21 Ceiling at B6
CH 22 Flame temp in pan at nozzle
CH 73 CH_4 at center of pan at nozzle

CEL 13 200, 400, 800 kW/500 l/s

Methanol sprayed into 3-ft-diameter pan at 6983, 1386, 2772 ml/min
21, 42, 84 on flowmeter
Air set at 500 l/s

*Returned CH_4 analyzer to duct stream

Table 6. Pertinent parameters of all tests conducted during the fire-modeling experimental series.

	Test														
	1/3	2/1	3/2	4/4	5/5	6/12I	7/13I	8/6	9/8	10/12II	11/13II	12/10	13/9	14/12III	15/13III
Fuel	CH_4	CH_4	CH_4	CH_4	C_3H_8O	C_3H_8O	CH_4O	C_3H_8O	C_3H_8O	C_3H_8O	CH_4O	C_3H_8O	C_3H_8O	C_3H_8O	CH_4O
$\dot{M}_d$ (l/s)	250	250	250	500	250	500	500	250	500	500	500	250	500	500	500
$\dot{M}_a$ (l/s)	250	250	245	465	245	445	440	230	440	420	430	230	405	475	420
$\dot{Q}_{cn}$ (kW)	65+	125+	130+	160+	205	205	179	415	415	415	354	830	830	830	750
$\dot{Q}_{c\Delta}$ (kW)	49	96	101	124	136	147	134	241	315	279	245	429	583	542	465
$\dot{Q}_{c\Delta}/\dot{Q}_{cn}$	0.78	0.78	0.78	0.78	0.67	0.73	0.73	0.58	0.76	0.67	0.70	0.52	0.70	0.66	0.62
T_u, (°C)	80	115	130	115	135	125	140	220	215	220	205	265	310	310	315
T_L, (°C)	50	50+	60	65	60	65	70+	90	110+	115	105+	120	195+	195	195+
T_∞, (°C)	20	28	30	25	30	28	32	30	25	28	32	32	30	28	32
$\dot{Q}_e$ (kW)	13	23	25	40	25	42	32	44	80	80	46	54	114	105	61
$\dot{Q}_w$ (kW)	36	73	76	84	111	105	104	197	235	199	199	375	469	439	403
$\dot{Q}_e/\dot{Q}_{c\Delta}$	0.26	0.23	0.23	0.32	0.18	0.29	0.24	0.18	0.26	0.29	0.19	0.12	0.19	0.15	0.13
$\dot{Q}_e/\dot{Q}_{cn}$	0.21	0.18	0.19	0.25	0.12	0.21	0.18	0.10	0.19	0.19	0.13	0.06	0.13	0.12	0.08
$\dot{Q}_w/\dot{Q}_{c\Delta}$	0.74	0.77	0.76	0.68	0.82	0.71	0.76	0.82	0.75	0.71	0.81	0.87	0.80	0.81	0.87
$\dot{Q}_w/\dot{Q}_{cn}$	0.37	0.58	0.58	0.53	0.54	0.51	0.57	0.47	0.57	0.48	0.56	0.45	0.57	0.53	0.54

\+ Estimated

* Since p^* = const., Q_{cell} = const., and $\dot{Q}_w = \dot{Q}_c - \dot{Q}_e$ $h_r = 4.5$

$\dot{Q}_e = \rho c_p (T_u - T_\infty)$ with $\rho c_p = 1 J/l_o K$

T_u = T upper

T_∞ = T inlet

Table 6. (Continued).

Symbol	Definition
1. Test	Experiments are listed in order of design combustion enthalpy, not chronologically.
2. Fuel	Self explanatory
3. M_d (l/s)	Uncorrected design pre-fire air flow rate.
4. M_a (l/s)	Measured air flow rate at 480 s after fire start; corrected for temperature.
5. $\dot{Q}_{cn}$ (kW)	$[M_f \cdot \Delta H_c]$ measured fuel spray rate times literature heat of combustion[1] (theoretical heat release rate).
6. $\dot{Q}_{c\Delta}$ (kW)	Heat release rate calculated from oxygen depletion at 480 s post fire start.
7. $\dot{Q}_{c\Delta}/\dot{Q}_{cn}$	Ratio of theoretical to calculated heat release rate (a chemical partition?)
8. T_u (°C)	Bulk temperature of upper (hot) zone.
9. T_L (°C)	Bulk temperature of lower (cold) zone.
10. T_∞ (°C)	Ambient temperature
11. $\dot{Q}_e$ (kW)	Enthalpy leaving enclosure in exhaust gases. $(\rho C_p [T_u - T_\infty])$ estimate ρC_p 1J/1 °K
12. $\dot{Q}_w$ (kW)	Enthalpy lost to enclosure walls and ceiling. $Q_w = (Q_{c\Delta} - Q_e)$; since P = const., Q cell = const.
13. $\dot{Q}_e/\dot{Q}_{c\Delta}$	Fraction of combustion enthalpy leaving enclosure in exhaust gases - (HRR by O_2 depletion).
14. $\dot{Q}_e/\dot{Q}_{cn}$	Fraction of combustion enthalpy leaving enclosure in exhaust gases - (HRR by $M_f \cdot \Delta H_c$).
15. $\dot{Q}_w/\dot{Q}_{c\Delta}$	Fraction of combustion enthalpy absorbed in walls (HRR by O_2 depletion).
16. $\dot{Q}_w/\dot{Q}_{cn}$	Fraction of combustion enthalpy absorbed in walls - (HRR by $M_f \Delta H_c$).

[1] W. J. Parker, An Investigation of the Fire Environment in an ASTM E-84 Tunnel Test, NBS Tech. Note 945 (Aug. 1977).

Table 7. Compilation of two-layer calculations for the range of fire strength data developed during the fire-modeling test series.

Run #	REK time (s)	Temp lower (°C)	Temp upper (°C)	Layer height (m)	5 points around time-averaged layer height (m)
2	500	59	127	1.11	1.08
3	485	31	74	1.17	1.17
4	500	41	107	1.21	1.21
5	625	65	133	1.07	1.05
6	600	109	219	1.00	.97
8	600	91	209	1.08	1.05
9	490	137	318	1.06	1.00
	500	156	317	1.35	1.33
10	600	140	262	1.07	1.04
	605	148	267	1.29	1.29
12A	550	55	130	1.15	1.14
12B	1050	94	213	1.09	1.09
12C	1475	146	300	1.05	1.05
	1480	160	311	1.29	1.29
13A	400	58	137	1.16	1.14
13B	825	85	199	1.07	1.08
13C	950	122	302	1.02	1.05
	955	136	310	1.27	1.28

Table 8. Corrected test data and fire-spread model predictions.

		Test													
		1/3	2/1	3/2	4/4	5/5	6/12I	7/13I	8/6	9/8	10/12II	11/13II	12/10	13/9	14/12III	15/13III
kW (est)		25	50	50	100	200	200	200	400	400	400	400	800	800	800	800
Exit Air (est)		250	250	250	500	250	500	500	250	500	500	500	250	500	500	500
kW (exp)		65	125	130	160	205	205	179	415	415	415	254	830	830	830	750
Exit Air (exp)		250	250	245	465	245	445	440	230	440	420	420	230	405	375	420
Experiment	T_U	74	-	127	107	133	130	137	219	209	213	199	262	318	300	302
	T_L	31	-	59	41	65	55	58	109	91	94	85	140	137	146	122
	H_L	1.17	-	1.08	1.21	1.05	1.14	1.14	.97	1.05	1.09	1.08	1.04	1.00	1.05	1.05
Bolstad	T_U	-	-	78	56	157	-	-	233	157	-	-	-	-	-	-
	H_L	-	-	1.2	1.6	1.6	-	-	2.0	2.2	-	-	-	-	-	-
Creighton	T_U	60	-	183	111	627	-	-	1270	681	-	-	-	-	-	-
	H_L	.8	-	.6	.8	.5	-	-	.4	.25	-	-	-	-	-	-
Krause	T_U	126	-	200	128	212	-	-	280	212	-	-	285	280	-	-
	H_L	4.5	-	0	4.5	0	-	-	1.6	0	-	-	0	0	-	-
Zukoski	.1	-	-	168	97	584	-	-	1156	586	-	-	-	-	-	-
Heat	.25	-	-	144	96	486	-	-	977	496	-	-	-	-	-	-
to T_U	.5	-	-	102	67	327	-	-	636	339	-	-	-	-	-	-
Walls	.7	-	-	72	52	210	-	-	393	216	-	-	776	408	-	-
	.8	-	-	57	43	144	-	-	253	153	-	-	516	280	-	-
	H_L	-	-	.7	1.4	.7	-	-	1.4	1.4	-	-	.7	1.4	-	-

All Temps in °Celsius

T_U = Hot layer temperature
T_L = Cool layer temperature
H_L = Height of interface between hot and cool layer

Table 9. Effect of heating rates on the degradation of various PVC formulations in acid ion production phase.

Insulation	Rate of heating (°C/min)	Rate of degradation (%/min)	Wt loss in dehydro-chlorination Region (%)	Temp of initial degradation (°C)	Char residue (%)
PVC-3	10	12.5	54	240	16
(High power	20	13.7	54	240	16
electrical cable)	40	55	58	260	12
PVC-78	10	6.3	44	200	32
(Appliance	20	8.3	46	60	33
cable)	40	21	42	60	33
PVC-95	10	8	56	210	38
(Multi-strand	20	12.6	48	205	38
signal cable)	40	27	49	80	38
PVC-104	10	5.6	22	100	16
(High voltage	20	10.6	22	60	16
cable)	40	20.9	24	220	6
Virgin	10				
PVC	20	30	60	220	0
	40				

Table 10. Thermal degradation products for PVC cable #3.

Degradation products	Flash point (°C)	Ignition temp. (°C)	Boiling point (°C)	Water soluble	Extinguishing method	NFPA HAZARD IDENTIFICATION		
						Health	Flammability	Reactivity
Acid Ion Stage								
Pentadecene								
6-methyl-1-heptanol								
phthalic anhydride	152	570	284	No	H_2O, Foam, Maybe	2a	1b	0c
benzoic acid	121	570	250	Slight	H_2O, CO_2, Dry Chem	2	1	
benzidine			400	Yes				
phenanthrene	171		340	No	H_2O-Foam		1	0
n-butyl-o-phthalate	171	399	340	Slight	CO_2-Dry Chem		1	
Post-Acid Ion Stage								
Phenanthrene	171		340	No	H_2O-Foam		1	0
n-butyl-o-phthalate	171	399	340	Slight	CO_2-Dry Chem		1	
3-methylphenanthrene								
4-methylphenanthrene								
2-phenylnaphthalene								
2,5-dimethylphenanthrene								
1,3,3,10B-tetrahydro-fluoranthene								

a. Chemical is hazardous when inhaled, but self contained breathing apparatus will protect against inhalation.
b. Chemical must be preheated to ignite. Water may cause frothing if it gets below the surface of the liquid and turns to steam.
c. Chemical is normally stable and therefore does not present any reactivity to firemen.

Table 11. Thermal degradation products for PVC cable #78.

Degradation products	Flash point (°C)	Ignition temp. (°C)	Boiling point (°C)	Water soluble	Extinguishing method	NFPA HAZARD IDENTIFICATION Health	Flammability	Reactivity
			Acid Ion Stage					
tridecanol	121		274	No	H_2O, Foam, Maybe	0	1c	0e
phthalic anhydride	152	570	284	No	H_2O, Foam, Maybe	2b	1	0
benzoic acid	121	570	250	Slight	H_2O, CO_2, Dry Chem	2	1	
phthalic acid	168		289			0a	1	0
phenanthrene	171		340	No	H_2O-Foam		1	0
2-methyl-pentanol	54	310	148	No		0	2d	
			Post-Acid Ion Stage					
1,1-diphenylethene								
2,3-diphenyl-thurene-1, 1-dioxide								
9-fluorenone								
butyl phthalate	-35	399	340	Slight				
2-methyl anthracene			Sub	No				
2-phenylnaphthalene								
1,3,3,10B-tetrahydro-fluoranthene								
dioctylphthalate	215	390		No	H_2O-Foam, Maybe	0	1	0

a. In a fire condition, chemical would pose the same health hazard as an ordinary combustible material.
b. Chemical is hazardous when inhaled, but self contained breathing apparatus will protect against inhalation.
c. Chemical must be preheated to ignite. Water may cause frothing if it gets below the surface of the liquid and turns to steam.
d. Chemical must be moderately heated to ignite.
e. Chemical is normally stable.

Table 12. Thermal degradation products for PVC cable #104 (acid ion stage).

Degradation products	Flash point (°C)	Ignition temp. (°C)	Boiling point (°C)	Water soluble	Extinguishing method	NFPA HAZARD IDENTIFICATION		
						Health	Flammability	Reactivity
3-chlorodecane								
2,6-di-T-butyl-1,4-benzoquinone								
methyl hexadecanoate								
1-hexacosene								
lauric acid			225	No			1b	
n-octadecanonitrile								
myristic acid			251	No				
decanoic acid			270	No				
oleic acid	189	363	286	No	CO_2, Dry Chemical	0a	1	0c
stearic acid								
palmitic acid			215	No				
dioctylphthalate	215	390		No	H_2O-Foam, Maybe	0	1	0

a. In a fire condition, chemical would pose the same health hazard as an ordinary combustible material.
b. Chemical must be preheated to ignite. Water may cause frothing if it gets below the surface of the liquid and turns to steam.
c. Chemical is normally stable and therefore does not present any reactivity hazard to firemen.

Table 13. Thermal degradation products for PVC cable #104 (post-acid ion stage).

Degradation products	Flash point (°C)	Ignition temp. (°C)	Boiling point (°C)	Water soluble	Extinguishing method	NFPA HAZARD IDENTIFICATION		
						Health	Flammability	Reactivity
1,7-octadiene								
1-methoxy-4-methyl-benzotriazole								
benzene	-12	498	80	No	H_2O, Maybe	4b	3d	0e
octadecanol		450	210	No		0		
stearic acid methyl ester								
(n-butylthio)cyclohexane								
2-methylcarbazole								
1-nonadecene								
phenanthrene	171		340	No	H_2O-Foam		1c	0
fluorenone			342	No				
2-methylphenanthrene								
dioctylphthalate	215	390		No	H_2O-Foam, Maybe	0a	1	0

a. In a fire condition, chemical would pose the same health hazard as an ordinary combustible material.
b. Chemical is an identified carcinogen and should be avoided.
c. Chemical must be preheated to ignite. Water may cause frothing if it gets below the surface of the liquid and turns to steam.
d. Chemical can be ignited under almost all normal temperature conditions.
e. Chemical is normally stable and therefore does not present any reactivity hazard to firemen.

Table 14. Thermal degradation products for virgin PVC.

Degradation products	Flash point (°C)	Ignition temp. (°C)	Boiling point (°C)	Water soluble	Extinguishing method	NFPA HAZARD IDENTIFICATION		
						Health	Flammability	Reactivity
Acid Ion Stage								
2-chloro-1-phenyl-2-butene								
diphenylacetylene			300	No				
phenanthrene	171		340	No	H_2O-Foam		1b	0c
8-mechylquinoline								
dioctylphthalate	215	390		No	H_2O-Foam, Maybe	0a	1	0
Post-Acid Ion Stage								
anthracene	121	540	340	No	H_2O, Foam, CO_2	0	1	
9-fluorenone								
2-methyl phenanthrene								
2-phenylnaphthalene								
pyrene			393	No				
dioctylphthalate	215	390		No	H_2O-Foam, Maybe	0	1	0
1,3,3,10-tetrahydro-fluoranthene								

a. In a fire condition, chemical would pose the same health hazard as an ordinary combustible material.
b. Chemical must be preheated to ignite. Water may cause frothing if it gets below the surface of the liquid and turns to steam.
c. Chemical is normally stable and therefore does not present any reactivity hazard to firemen.

Table 15. Effect of heating rates on thermal degradation of dehydrochlorination region in rubber insulations.

Insulation	Rate of heating (°C/min)	Rate of degradation (%/min)	Wt loss in dehydrochlorination region (%)	Temperature leading to initial degradation (°C)	Char residue (%)
Neoprene-118	10	1.75	18	260	29
(Multiconductor power cable)	20	5.60	22	170	23
	40	8.0	24	190	22
Neoprene-84	10	1.16	36	200	48
(Single conductor high voltage cable)	20	2.83	38	200	46
	40	544	38	200	46
007	10	2.0	24	200	26
(Welding cable)	20	9.0	24	200	25
	40	16.0	22	200	25
Neoprene-435	10	6.0	26	180	6
(High voltage, high amperage cable)	20	11.0	30	180	6
	40	60.0	46	180	6
Polychloroprene	10	6.40	42	180	0
(Virgin polymer)	20	9.0	44	230	0
	40	12.25	45	240	0
Rubber 134	10	5.8	50	240	25
(3-strand power cable)	20	8.8	46	240	30
	40	18.18	46	240	27

Table 16. Thermal degradation products generated during and post-dehydrohalogenation region of neoprene cable #007 heated in air at 20°C/min.

Degradation products	Flash point (°C)	Ignition temp. (°C)	Boiling point (°C)	Water soluble	Extinguishing method	NFPA HAZARD IDENTIFICATION Health	Flammability	Reactivity
			Acid Ion Stage					
3,3,6-trimethyl-1-indone								
1,2-benzoisothiazole-3								
4-methylbiphenyl								
squalene	200		285	No				
2,5'-dimethylbiphenyl								
triacontane			450	No				
nor-pentacosane								
3-ethyl-5-(2'-ethylbutyl)-octadecane								
n-dotriacontane			310					
dioctylphthalate	215	390		No	H_2O or Foam, Maybe	0a	1b	0d
phenyl B-naphthylamine			395	No			2c	
			Post-Acid Ion Stage					
n-octacosane								
3-ethyl-5-(2'-ethylbutyl)-octadecane								
n-hexatriacontane								
triacontane			450	No				
n-pentacosane								
di-(2-ethyl hexyl) phthalate	215	390	231	No	H_2O or Foam, Maybe	0	1	0
dioctyl phthalate	215	390		No	H_2O or Foam, Maybe	0	1	0

a. In a fire condition, chemical would pose the same health hazard as an ordinary combustible material.
b. Chemical must be preheated to ignite. Water may cause frothing if it gets below the surface of the liquid and turns to steam.
c. Chemical must be moderately heated to ignite.
d. Chemical is normally stable.

Table 17. Thermal degradation products generated during and post-dehydrohalogenation region of neoprene cable #118 heated in air at 20°C/min.

Degradation products	Flash point (°C)	Ignition temp. (°C)	Boiling point (°C)	Water solubility	Extinguishing method	NFPA HAZARD IDENTIFICATION		
						Health	Flammability	Reactivity
			Acid Ion Stage					
1,3-dimethylnaphthalene								
bis-trichloroethyl carbonate								
1,4-dimethyl-5-N-acetyl-naphtoalene								
1-n-butyl-2-cyclohexyl cyclohexane								
cis-9-octadecen-1-ol								
1-allylnaphthalene								
1,1,5,5-tetramethyl-2,3'-dimethylbiphenyl								
2-hexadecycloethanol								
2,4-dimethoxybenzaldehyde				No				
3,4,5,6-diphenylene-1-oxo-cycloheptane								
2,6-diisopropyl-1-chlorobenzene								
2,6,10,14,19-penta-methyleicosane								
anthracene	121	540	340	No	H_2O, Foam, CO_2	0a	1b	
4-methylfluorene								
1-methoxy phenazine								
diphenylethylene								
1,2-diphenylethylene			306	No				
4-methylphenanthrene								
2,3 dihydro-2-methyl-7-phenylbenzofuran								

Table 17. (Continued).

Degradation products	Flash point (°C)	Ignition temp. (°C)	Boiling point (°C)	Water soluble	Extinguishing method	NFPA HAZARD IDENTIFICATION		
						Health	Flammability	Reactivity
			Post-Acid Ion Stage					
n-dotriacontane			310					
nonacosanol								
triacontane			450	No				
hexatriacontane								
tetratetracontane								
tetratriacontane								
3-ethyl-5 (2-ethyl butyl) octadecane								
diisobutylphthalate	185	432	327	No	Alcohol Foam	0a	1b	0c
1,1-dichloro-2,2-bis (p-ethyl phenyl) ethane								
2,6,10,14-tetramethyl heptadecane								
4-methylphenanthrene								
7-N-butyldocosane								
2,6,10,15-tetramethyl heptadecane								
3,4-dichlorophenyl phenyl ether								
butyl (butoxycarbonyl) methyl phthalate								
2-chloromethylheptane								
2,4,5,7-tetramethyl-phenantrene								
dioctylphthalate	215	390		No	H_2O or Foam, Maybe	0	1	0

a. In a fire condition, chemical would pose the same health hazard as an ordinary combustible material.
b. Chemical must be preheated to ignite.
c. Chemical is normally stable and therefore does not present any reactivity hazard to firemen.

Table 18. Thermal degradation products generated during and post-dehydrohalogenation region of neoprene cable #84 heated in air at 20°C/min.

Degradation products	Flash point (°C)	Ignition temp. (°C)	Boiling point (°C)	Water soluble	Extinguishing method	NFPA HAZARD IDENTIFICATION Health	Flammability	Reactivity
			Acid Ion Stage					
1-octanol	81		194	No		1b	2e	0g
4,5-dimethyl-1-alpha-p-methoxy-benzoyloxy-p-methoxybenzyl.dene-1								
11-N-dicyclosane								
phthalic anhydride	152	570	284	No	H_2O or Foam, Maybe	2c	1d	0
n-nonacosane								
2 (methylthio) benzo-thiazole								
3-ethyl-5- (2-ethylbutyl) octadecane								
nonylphenol	141		295	Slight	Alcohol Foam		3f	1h
n-heptacosane			270	No				
1-methylbutyl isobutyrate								
dioctylphthalate	215	390		No	H_2O or Foam, Maybe	0a	1	0
phthalanil								
			Post-Acid Ion Stage					
palmitic acid			215	No				
n-hexadecane	>100	202	287	No		0	1	0
squalene	200		285	No				
7-N-butyldocosane								
3-ethyl-5- (2-ethylbutyl) octadecane								
nor-pentylthiol acetate								
phthalic acid	168		289			0	1	1
dioctylphthalate	215	390		No	H_2O or Foam, Maybe	0	1	0
diisobutyl phthalate	185	432	327	No	Alcohol Foam	0	1	0

a. In a fire condition chemical poses the same health hazard as an ordinary combustible material.
b. Chemical is only slightly hazardous to firemen.
c. Chemical is hazardous when inhaled, but self-contained breathing apparatus will prevent inhalation.
d. Chemical must be preheated to ignite. Water may cause frothing if it gets below the surface of the liquid and turns to steam.
e. Chemical must be moderately heated to ignite.
f. Chemical can be ignited under almost all normal temperature conditions. Water may not extirguish the fire because of the chemical's low flash point.
g. Chemical is normally stable.
h. Chemicals which are normally stable may become unstable in combination with other chemicals or at elevated temperatures and pressures. Normal precautions in approaching any fire should suffice.

Table 19. Thermal degradation products generated during and post-dehydrohalogenation region of neoprene cable #435 heated in air at 20°C/min.

Degradation products	Flash point (°C)	Ignition temp. (°C)	Boiling point (°C)	Water soluble	Extinguishing method	NFPA HAZARD IDENTIFICATION Health	Flammability	Reactivity
			Acid Ion Stage					
Acenaphthene			279	No		1b	1	
2-methylbiphenyl	137	502	255			2c		0e
4-phenyl-benzaldehyde								
1-(O-chlorobenzylidine-amino)-benztriazole								
2,3 ft-dimethyl biphenyl								
cyclopiazonic acid			270	No				
anthracene	121	540	340	No	H_2O, Foam, CO_2	0a	1d	
n-hexatricontane								
methylphenanthrene								
			Post-Acid Ion Stage					
2-2' methylenebis (4-methyl-6-tert-butyl phenol)								
3,3,4,5,5,8-hexamethyl-1-5-hydrindacenon								
1,6,8-trimethyl-I,2,3,4-tetrahydronaphthalene								
n-hexadecane	>100	202	287	No		0	1	0
1,1,9-trichlorononon-1-ene								
triacontane			450	No				
2:3,5:6-bisbenzotricyclo (2,2,2) octane 2-methyl octadecane								
2-methyltricosane								
2-methyl-4-heptanone								
7-ethoxy-8-(3-methyl-2-butenyl)								
dioctylphthalate	215	390		No	H_2O or Foam, Maybe	0	1	0

a. In a fire condition chemical poses the same health hazard as an ordinary combustible material.
b. Chemical is only slightly hazardous to firemen.
c. Chemical is hazardous when inhaled, but self-contained breathing apparatus will prevent inhalation.
d. Chemical must be preheated to ignite. Water may cause frothing if it gets below the surface of the liquid and turns to steam.
e. Chemical is normally stable.

Table 20. Thermal degradation products generated during and post-dehydrohalogenation region of polychloroprene cable heated in air at 20°C/min.

Degradation products	Flash point (°C)	Ignition temp. (°C)	Boiling point (°C)	Water soluble	Extinguishing method	NFPA HAZARD IDENTIFICATION		
						Health	Flammability	Reactivity
Acid Ion Stage								
2,3,4,5-tetramethyl-hexa-1,4-diene								
3,benzylidene-1,4,4-trimethyl bicyclo (3,2,0) heptan-2-one								
1,1,5,5-tetramethyl-4-acetyl-5-hydrindacene								
3,3,5,5-tetramethyl-1,7,S-hydrindacenedione								
1, methyl-7-isopropylphenanthrene								
dioctylphthalate	215	390		No	H_2O or Foam, Maybe	0a	1b	0c
Post-Acid Ion Stage								
7-hydroxy-5,6-benznorborene								
bicycloheptatriene								
2,2-prime-dimethylbiphenyl								
1,2-diphenylethylene								
4-methyl fluorene								
phenanthrene	171		340	No	H_2O - Foam		1	0
4-methylphenanthrene								
2-methylanthracene			Sub	No				
2,4,5,7-tetramethyl-phenanthrene								
di-(2-ethylhexyl) phthalate	215	390	231	No	H_2O, Foam, Maybe	0	1	0
pyrene			393	No				

a. In a fire condition chemical poses the same health hazard as an ordinary combustible material.
b. Chemical must be preheated to ignite. Water may cause frothing if it gets below the surface of the liquid and turns to steam.
c. Chemical is normally stable and therefore does not present any reactivity hazard to firemen.

Table 21. Thermal degradation products generated during and post-dehydrohalogenation region of rubber cable #134 heated in air at 20°C/min.

Degradation products	Flash point (°C)	Ignition temp. (°C)	Boiling point (°C)	Water soluble	Extinguishing method	NFPA HAZARD IDENTIFICATION Health	Flammability	Reactivity
			Acid Ion Stage					
2-methyl-4-hydroxy-pentanic acid lactone								
n-nonyl alcohol	74	100	178	No	Alcohol Foam	1b	2e	0f
2,5-dimethylhexene-1								
phthalic acid anhydride	152	570	284	No	H_2O or Foam, Maybe	2c	1d	0
benzoic acid	121	570	250	Slight	H_2O, CO_2, dry Chem	2	1	
phenanthrene	171		340	No	H_2O-Foam		1	0
			Post-Acid Ion Stage					
caproloctam			180	Yes				
phthalic anhydride	152	570	284	No	H_2O or Foam, Maybe	2	1	0
phenanthrene	171		340	No	H_2O-Foam		1	0
fluorenone			342	No				
methylphenanthrene								
2-phenylnaphthalene								
dimethylphenanthrene								
1,2,3,4-tetrahydrofluor-anthene								
methyl terephthalate								
dioctyphthalate	215	390		No	H_2O or Foam, Maybe			
pryene			393	No				
phenyl benzoate			314	No				
diiso octal phthalate	232		370	No	H_2O or Foam, Maybe	0a	1	0

a. In a fire condition chemical poses the same health hazard as an ordinary combustible material.
b. Chemical is only slightly hazardous to firemen.
c. Chemical is hazardous when inhaled, but self-contained breathing apparatus will prevent inhalation.
d. Chemical must be preheated to ignite. Water may cause frothing if it gets below the surface of the liquid and turns to steam.
e. Chemical must be moderately heated to ignite.
f. Chemical is normally stable.

APPENDIX A

EXPERIMENTAL FUSION FACILITY

FIRE RISK ASSESSMENT

1981

ECON, INC.

and

Lawrence Livermore National Laboratory

Fire Science Group

Special Projects

CONTENTS

PART I. GENERAL DISCUSSION

Over the last two years an objective of this effort has been the development of a risk analysis protocol for fire risk evaluation at experimental fusion facilities, built and operated by DOE at its member laboratories. Typically, when identifying the specific nature of fire risk at these facilities, we chose to assess these risks relative to the fusion program at each facility on an individual experiment, on a Division or Department level, and ultimately at the DOE level.

Unlike industrial or commercial settings,[1,2] fire risk requires slightly different ground rules. In research, moneys are made available to buy information in a timely manner as opposed to an industrial setting where fire risk assessments are made with regard to some uncertain impact on profit. With experimental fusion facility risk assessments we chose to reference or measure fire risks relative to their impacts on program schedules and budgets in the form of delays and marginal budget increases due to potential fire-related damage.

During the development of this effort we have had to integrate a number of different views of fire protection objectives. Foremost amongst these views are those oriented towards building fire protection and fire protection based upon threats to operational availability of critical system hardware and equipment for any given experiment. A more useful picture of program uncertainty is allowed for by using both perspectives

---

1 G. Ramachandran, Statistical Methods in Risk Evaluation, International Symposium on Fire Risk Evaluation 1979, ISBN 91-7144-138-7.

2 C.L. Farmer, A Probabilistic Risk Analysis Technique with applications to enclosure fires, International Symposium on Fire Risk Evaluation 1979, ISBN 91-7144-138-7.

in assessing fire damage risk and by identifying the uncertainty associated with various aspects of fire safe facility design and operation.

During previous efforts at formulating and applying a fire loss assessment, the following steps were undertaken to provide a consistent basis for ascertaining various levels of fusion experiment fire protection. This required the following steps:

- Defining the potential hazard and magnitude of fire in each critical zone, compartment, or area.
- Assessing the reliability and effectiveness of the fire protection system.
- Evaluating the interaction of the above two efforts to estimate the amount of damage to each area.

This update restates our previous findings for the Shiva Experiment and, together with a more critical review of operations, considers fire loss in terms of possible impacts on the experiment's programmatic budget and schedule. It is at the facility level that fire risk estimates should be made consistent with resident fire protection equipment, appropriate facility design criteria, contingency planning efforts, and budget and schedule objectives. The results of this brief study for Shiva should be useful to Novette and Nova operations personnel, as well as operations managers of other high cost, complex, multi-year and multi-objective experiments.

The next section presents a general discussion of the methodology and extension to our risk analysis procedure. The second section provides an analysis of the Shiva facility at LLNL. The last section consists of general comments.

PART II. GENERAL PROCEDURE

Because of budget and time constraints associated with this effort, a generalized assessment protocol needed to be developed. The assessment methodology needed to be both flexible and detailed enough so as to capture different important aspects of fire protection structure and intent at DOE's member laboratories participating in fusion experiments. The flexibility in detail was necessitated by our intent to perform a risk analysis exercise and to examine the possible impacts on three different levels of management.

Figure 2-1 is a logic diagram defining the general flow of our analysis. The assessment consists of two major parts. The first of these seeks to determine the specific location of facility vulnerability, the basis of which can be determined by general design criteria or by a recognition of high "value" equipment. Besides these previous criteria, the criterion "system operational availability" should be considered, since fire-related damage can be measured by its impact on system availability and cost.

The next major part consists of three separate but important views of the facility and the corresponding research program. Given information designating "critical" compartments within an experimental facility, the specific availability of fire detection and suppression equipment can be estimated using simple comparison and/or detailed fault tree analysis. The second aspect of these selected critical compartments is the issue of fuel load, both resident and transient etc. which effect fire growth. Given that critical equipment is vulnerable to external fires, and that the loss system capability is an issue, ignition and fire growth studies are necessitated in order to quantify the extent of possible damage. These evaluations would include the interaction of fire suppression and detection equipment resident in the building. The importance of the potential fire

EXPERIMENTAL FUSION FACILITY FIRE PROTECTION SYSTEM SURVEY

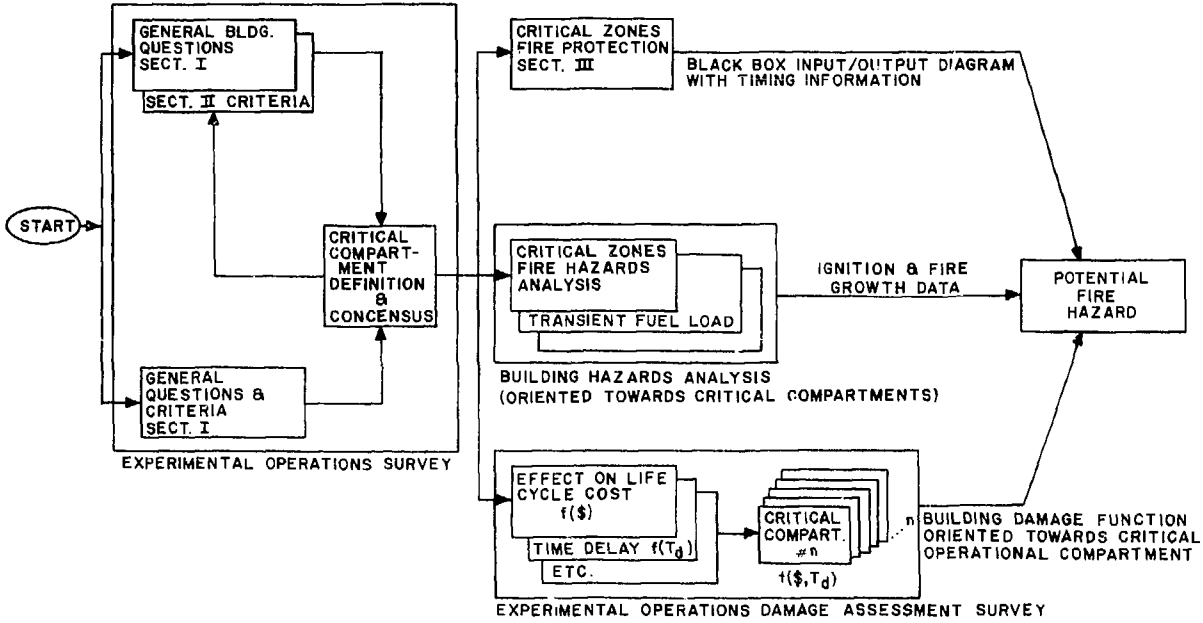

hazard in each compartment/building location is measured by its impact on the way the experiment is continued and by the amount of moneys paying for its continuation.

In order to derive information in these three areas a series of surveys are required. The first survey is directed at fire safety specialists and seeks information about the fire protection system and about fuel loads, etc. which effect fire growth. The second survey is directed at the operations manager/officer of the facility in question. The information sought by the second questionnaire relates to the costs in time and dollars of fire damage equipment and hardware essential to the operation of the system.

Figures 2-2 through 2-5 briefly delineate the tasks, their inputs, outputs and techniques associated with each level of analysis.

Figure 2-2. LEVEL I INVESTIGATION

STEPS	DERIVE DATA FROM
1. Decide upon criticality of specific pieces of equipment: (a) Program delay (b) Highly vulnerable	1. Program CPM chart, consider equipment required in critical path other resources as well.
2. Select pertinent zones.	2. Plant engineering drawings.
3. Examine entire fire protection system.	3. Questionnaire to: (a) Plant engineer (b) Operations engineer (c) Fire marshal/engineer
4. Construct fire protection system input/output diagram for zones with critical experiments. Importance - equipment.	4. Information derived from data Items 1, 2, and 3.
5. Examine pertinent parameters for each zone: (a) Ignition (b) Ventilation/wall penetrations, etc. (c) Accessability (time)	5. Questionnaire(s): (a) Site specific question (b) Fire hazards analysis
6. Draw control loop for specific area/zone in question and assign PDF's for failure of protection equipment, magnitude of response, response time, response effectiveness.	6. Derive information from data Items 4 and 5 opinion by Delphi, Emperical Performance Data.

Figure 2-3. LEVEL I INVESTIGATION

STEPS	DERIVE DATA FROM
7. Consider dynamics of fire for specific area/zone investigated.	7. Fire modeling.
8. Construct a series discrete damage functions (PDF's) as a f(p,t), etc., or assume a series of uniform distribution: (a) Construct a series for time delay (b) Construct a series for time and damage	8. Annual budget report: • Cost of line items • Replaceability of unique equipment • Delphi - opinion
9. Make qualitative observations.	
10. Run the model(s): • Use method of moments • Use Monte Carlo methods • Use statistical inference methods	
11. Go to next critical area/zone (Steps 1 - 10).	
12. Perform CPM analysis for expected impact on a site/experiment basis.	12. Level I Questionnaire.
13. Iterate if necessary.	
14. Compare with program budget constraints and milestones.	
15. Make specific observations and suggest implementable solutions.	

Figure 2-4. LEVEL II INVESTIGATION

STEPS	DERIVE DATA FROM
1. Level I investigation for all experiments separated by distance.	1. Questionnaire directed at programmatic people.
2. Derive from CPM chart importance of time delay/ increased funding requirements - consider program slack and depth of supporting resources. This includes contingency funds available from within the contracting laboratory. Also consider the possibility of other programs which use the same equipment.	2. Level II - Questionnaire.
3. Perform CPM analysis for expected impact on a lab basis.	
4. Iterate if necessary.	
5. Compare with program budget constraints and milestones.	3. Questionnaire.
6. Make specific observations and suggest implementable solutions.	4. Cooperation of management.

Figure 2-5. LEVEL III INVESTIGATION

STEPS

1. Level II investigation(s) for all laboratories with specific development work (state of art).
2. Derive from CPM chart the importance of time delay and increased funding requirements:
   - Contingency funds
   - Agency-wide and program-wide contingency funds
3. Perform CPM analysis for expected impact on DOE fusion program.
4. Iterate if necessary.
5. Compare with budget constraints and resolve to meet milestones.
6. Make specific observations and suggest implementable solutions.

DERIVE DATA FROM

1. Questions directed at programmatic people as well as policy makers.
2. Level III - Questionnaire.

PART III. SHIVA: A SPECIFIC APPLICATION

Recently completed applications of our fire risk assessment, which included the Shiva facility, were performed with the concept of a generalized fire in selected "critical" compartments. The simplifying assumption made during this previous effort was that if fire were prevented or significantly mitigated in a compartment, extensive fire losses resulting from equipment damage would correspondingly be minimized. In a number of compartments throughout the Shiva building, this approach provided an adequate level of detail, particularly in situations where critical system equipment was:

- Predominantly threatened by external fire damage; or
- where equipment was sufficiently hardened against damage from combustion products (e.g., soot, corrosive gases, aerosols, and heat).

However, in other instances the high vulnerability of specific building equipment, mandatory for system operation, forced a review of our procedures and methods. Increased detail requirements in our analysis resulted from focusing on the issue of Shiva system operational availability. As before, this was also measured in terms of marginal increases and schedule delay in project costs resulting from potential fire-related damages. This approach seemed to make sense, given that both time and budgetary resources were not unlimited. Also, the fact that fire-related experiment schedule delays caused by equipment repair or outright replacement costs were not insignificant when compared to what seemed acceptable.

It's significant to note that guaranteed high system availability generated more demands than the Shiva building's resident fire protection equipment alone could provide. However, when these facilities are initially

constructed, they are designed and built relative to usage requirements which are guaranteed to be fixed. Additionally, they are designed and constructed in agreement with one of several standards written to protect buildings and life safety (e.g., ERDA Facility Design Criteria, Appendix 6301; UBC Fire Code; and NFPA Guidelines).

Again, these standards, while necessary, are not entirely sufficient in themselves to guarantee high Shiva operational availability.

From the standpoint of Shiva's current schedule, a severe fire would most likely not impact the Shiva program schedule, since the experiment schedule for Shiva is near a conclusion. However, a fire involving any of the critical equipment required for Novette and Nova (e.g., capacitors, power supplies, target diagnostic equipment, alignment control electronics, etc.) would impact the cost and schedule of those respective efforts. Loss of this equipment at the Shiva experiment would presumably only impact the life cycle cost of the Shiva effort by way of reduced salvage value. However, in the case of special reusable equipment and hardware, fire loss may potentially be represented by replacement costs instead of their salvage value. Again, the impact on "near to end" Shiva program costs may be minimal, but the impact on the entire LLNL ICF effort may prove another matter.

In contrast, the impace of these potential losses may not be significant to the question of commercial electric generation via fusion, since recent experimental results have tended to favor alternative magnetic fusion approaches. In spite of this, potentially reduced funding caused by significant fire-related capital losses and long schedule delays does not seem likely since driver development and target interaction physics have important military applications.

If the same scenario involving the fire losses of critical operation equipment and hardware were to have occurred during the latter part of 1978, cost and schedule impacts on this Shiva program would certainly be more pronounced, delaying 1979's high density experiments, 1980's scaling experiments, and so on.

The accompanying Figure 3-1 illustrates a simplified representation of equipment and hardware essential to Shiva system availability. Critical amongst these are:

ESSENTIAL SHIVA SYSTEM AND HARDWARE AND EQUIPMENT SUBSYSTEMS

Control room

Special electronics
- Programmable switch
- Switch panels
- PDP 11/34's & 11/70
- Environmental control

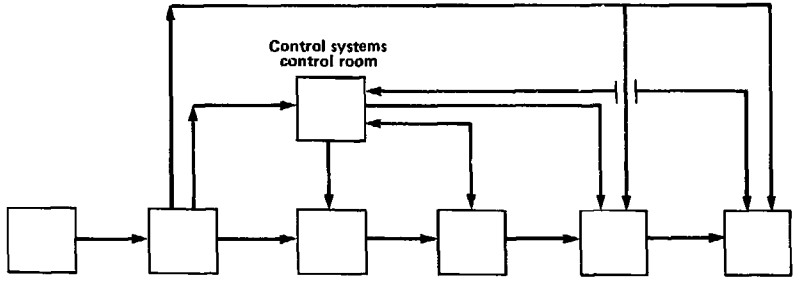

PG&E power	Power source conditioning	Capacitor banks	Laser bay	Target bay	Target room
• Power transformers	• Power sources • PS interface • Control room cable	• Spares • Special handling equipment • Power system interlocks • DAS	• Oscillator • Pre-amp/amp • N_2 blanket • Environmental control – Chillers – Air conditioning – Fans • DAS	• Vacuum system – Pumps – Control • DAS • Alignment • Equipment • Mirrors • Environmental control	• Target diagnostics electronics • DAS

- Power handling equipment
    - transformers
    - power supplies
    - capacitors
- Safety interlock
- Laser optics and electronics in the laser bay
    - pre-amplifiers and amplifiers
    - oscillator
    - optics
- Environmental control for laser bay
    - fans
    - chillers
- Target optics and electronics
    - target diagnostic electronics (switch panels, DAS)
    - optics
    - vacuum pump system
    - alignment computers
- Special electronics in the control room
    - programmable switches
    - switch panels
    - computers
- Control room environmental control

As indicated by the Figure 3-1, all these subsystems need to be operational for the facility to be fully operational. However, driver experiments can be conducted without the full use of the target room equipment. The results from previous efforts pointed out the vulnerability of the laser power cables and their through-floor penetrations and suggested that system optics were vulnerable to corrosion from combustion products. However, upon review this seems to be more approriate to the target room optical system since the laser train optics is protected by a nitrogen blanketing system. It's also interesting to note that the sprinkler system in these compartments is less than optimally located for early suppression. Less than optimal sprinkler head location is also a problem in the capacitor bank room. Sprinkler system spray may not be able to reach the necessary portions of the capacitor racks given a fire.

Appendix A is included summarizing a brief survey for various critical Shiva operational subsystems together with their potential dollar and schedule delay impacts given severe fire damage. Presumably if fire damage is minor, the schedule and cost impacts will be minimal. To some extent, adverse effects are prevented by some built-in system redundancy, (e.g., computers), and via a spares' inventory (e.g., capacitors and amplifier rods). In the case of Shiva spare capacitors kept in the same compartment with in-service units, this may defeat any advantages afforded by spares, given a severe capacitor bank fire. The risk of a major fire would likely be traded off against the convenience of nearby replacements.

As indicated earlier, Shiva system environmental control is essential to the operation of the system for driver and target experiments by virtue of its role in the laser alignment problem and clean room maintenance for the target bay, laser bay, control room, and the clean room.

To date our review has avoided addressing the vulnerability of the target fabrication activity and equipment to fire damage. Although we have not addressed this point, it's easy to see that target experiments would suffer a delay, given that targets needed to be manufactured somewhere else, or given the target fabrication equipment needed to be extensively repaired or replaced. Again, driver-related experiments could be rescheduled to compensate for any lost time.

Figure 3-2 is a map of critical compartments within Shiva's building 391. The darker shaded area represents those compartments which were previously considered critical areas/compartments selected for examination. The areas shown by the lighter shading represent those additional areas containing equipment previously mentioned, listed in Appendix A, and judged essential to Shiva system "Operational Availability".

Specific equipment not protected against internal fires includes:

- o control room electronic switch panels and programmable switches;
- o safety interlocks (internal fires caused by overheating, power surges, shorting, etc.);
- o target diagnostic equipment (internal fires);
- o vacuum pump subsystem;
- o power supplies;
- o oscillator and amplifier electronics; and
- o environmental control systems for the laser bay, target bay and control room.

In some cases (i.e., the last two) specific fire suppression equipment is not absolutely necessary by virtue of the absence of combustible fuel. The remaining items, however, possess ignition sources, fuel, high operational value, and are not directly provided with fire suppression devices. Hence, even though the general Shiva building fire protection system has a high general availability,* protection may not be adequate to guarantee a high measure of confidence against "severe" fire damage losses.

In other cases, fire damage probabilities may be relatively lower, by as much as an order of magnitude; yet because the fire damage consequences, measured either in time or dollars, are extremely high, the net risk may be worthy of concern. The concern might result in:

- a redesign or specification;
- a sparing policy;
- a contingency plan; or
- more comprehensive maintenance and inspection requirements.

The specific approach should be prescribed on the basis of its cost effectiveness. Examples of fire risks of this nature are represented by:

- transformer fire;
- capacitor bank fires; and
- target diagnostic electronic equipment.

---

*"Fire Protection Research for Energy Technology," FY 1980 Year-End Report, May 26, 1981, UCRL-53179; and "Fire Protection Research for Energy Technology Projects," FY 1979 Year-End Report, January 1981. UCID-18902.

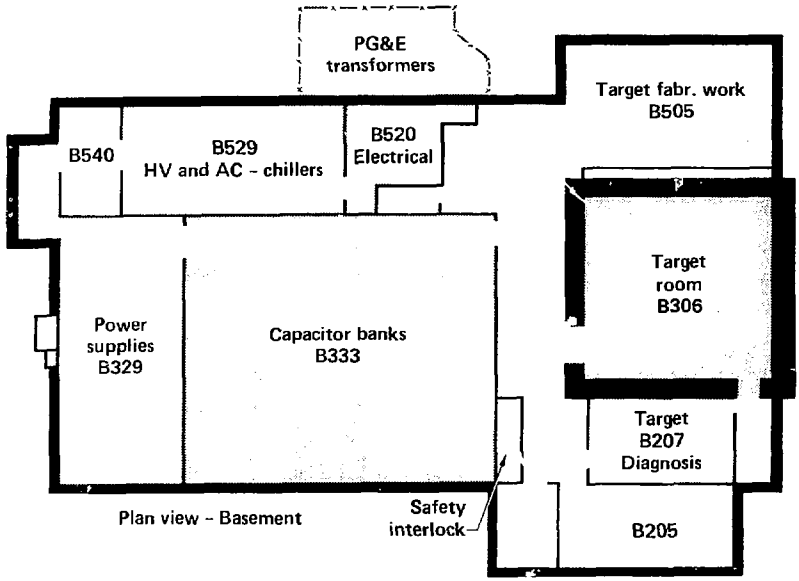

Plan view - Basement

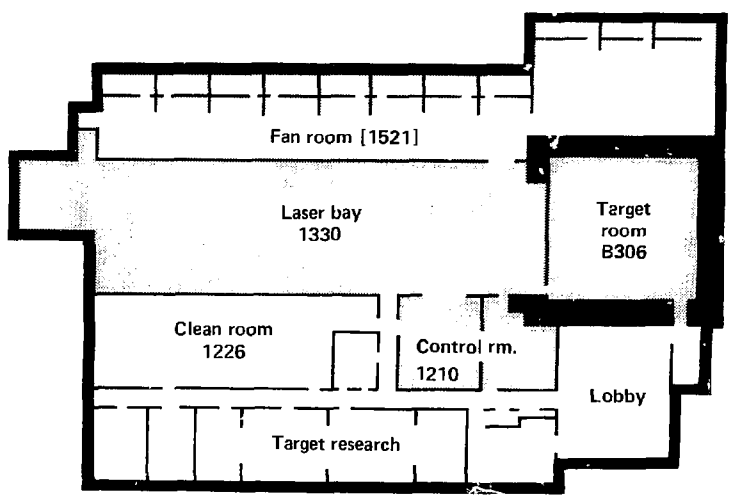

Plan view - 1st floor

There are a few cases where it is doubtful that fire protection/suppression will be effective in preventing fire damage. Specifically, the high expansion foam subsystem, originally specified and installed to protect the target bay, represents a subsystem which would be effective only after major damage to optics and electronic equipment has occurred because of operations personnel reluctance to use the system, its manual operation mode, and the cleaning effort required when it is used. Secondly, it is considered doubtful that the overhead sprinklers in the target and laser bays will be effective in preventing any major damage to system equipment. Damage is expected to occur early in the life of a fire.

By and large, the fire-related risks to the Shiva system are easily manageable or low to begin with. This is owed the minimization of the transient fuel load in the facility and to the clean room requirements of several essential areas. Two specific items deserve re-mentioning. First, there is a vulnerability in the power cables for the laser train. Second, the vulnerability of specially constructed electronic centers throughout the Shiva system could be specifically provided with both internal ignition design protection and individual fire suppression, since entire redundant units are not normally feasible.

PART IV. GENERAL COMMENTS

The general comments included in this section include two topics. The first comments on the evaluation of consequences. The second takes a broader view of program and risk analysis applications.

The evaluation of fire damage consequences can be more accurate than for the associated probability, since the former may involve a more predictable set of outcomes or less uncertainty. It was found, for instance, that the consequences of fire damage can differ by several orders of magnitudes in dollars (e.g., $5.5M for an entire rack station of diagnostic electronic equipment and $1K for specific pieces of electronic and mechanical equipment. The same is true of delay time). In these cases the relative significance of two problems is much more dependent on their consequences than the expected probability of occurrence. Hence, the quantitative measure of risk becomes more accurate than one might on the surface think.

Design risk analysis is most effective at helping to reduce risk via design early in a program. Specifically, fire protection system design risk trade-off studies can be employed to reduce fire damage consequences and probabilities during the conceptual system design phase, thus helping to reduce life cycle cost uncertainty. Further risk reduction can be achieved by testing and redesign as required during the development and test phases of a system like Shiva.

In the case of Shiva, this fire risk analysis provides no direct benefit to the Shiva project itself. However, it can provide a benefit to subsequent ICF projects by providing an assessment of specific design situations which may be used. Secondly, the procedure is a method of presenting design/cost trade-offs for management decisions.

APPENDIX A. SHIVA OPERATIONS SURVEY FORM

The following data was provided by knowledgeable operations personnel and represents our best state of current information as to the negative impacts on Shiva budget and schedule for fire-caused damages. More precise numbers for costs and schedule delay are recommended when doing a full analysis to support decisions for selecting or reviewing cost-effective fire protection. Penalty cost uncertainties can be estimated with the aid of the CPM chart analysis of recovery contingency plan along with equipment and hardware costs. Corresponding schedule delays can also be ascertained by analysis of this same CPM chart.

SHIVA OPERATIONS SURVEY FORM

Given layout and elevation plans of the experiment building, we need to enumerate specific areas/compartments of the facility which figure significantly into the uninterrupted progress of the program schedule.

The base assumption is that the experimental program only depends directly upon equipment availability.

Direct and indirect fire damage mechanisms should be accounted for in this operational readiness survey.

Direct Damage caused by combustion products and by fire

- o corrosive components
- o smoke (particulate)
- o heat (from external and internal sources)

Indirectly caused by structural failure

- o in-building equipment structure(s)
- o the building itself

TABLE 1

OPERATIONAL READINESS SURVEY FORM

CONTROL ROOM
LASER BAY

STRATEGIC BUILDING COMPARTMENT CONTAINING STRATEGIC EQUIPMENT	PROGRAMMATIC DELAY (Time/Days) L	E*	H	Contingency or Workaround Plan Y/N	REPLACEMENT COST (Cost 10^3 $) L	E*	H	Equip. Spares or Immediate Deliv. Y/N
Direct Damage								
1. Computers PDP 11/34 & Programs PDP 11/70	1	2	5	Yes	20K	40K	100K	Yes
2. Programmable Switches	3	5	10	No	--	70K	--	No
3. Switch Panels & Other Unique Electronic Assemblies	15	21	32	No	--	10.5K	--	No
4. Control Panels								
• Replacement Cards	0	0.2	1	Yes		- Small -		Yes
• Backplane (Wire Wrapped)	3	5	10	No	--	10.5K	--	No
Indirect Damage								
1. Air Conditioning				No		- Small -		Yes
2. Data Tapes		- Very Long -		Yes		- Minimal -		Yes
3. Floor				No		- Small -		Yes

L = Low
E* = Expected

TABLE 7

OPERATIONAL READINESS SURVEY FORM

LASER BAY

STRATEGIC BUILDING COMPARTMENT CONTAINING STRATEGIC EQUIPMENT	PROGRAMMATIC DELAY (Time/Days) L	E	H	Contingency or Workaround Plan Y/N	REPLACEMENT COST (Cost 10^3 $) L	E	H	Equip. Spares or Immediate Deliv. Y/N
Direct Damage								
1. Optics	0	1	2	Yes		Unknown*		Yes
2. Oscillator Controls (Unique)	20	22	30	No		High		No
3. Pre-Amp/Amplifiers Electronic Racks	10	15	25	No		High		Yes
Indirect Damage								
1. Structural collapse of								
Roof		Very Long		No		Very High		No
Crane								
Floor								

*Unknown to us at this time

TABLE 3

OPERATIONAL READINESS SURVEY FORM

TARGET BAY

STRATEGIC BUILDING COMPARTMENT CONTAINING STRATEGIC EQUIPMENT	PROGRAMMATIC DELAY (Time/Days) L	E	H	Contingency or Workaround Plan Y/N	REPLACEMENT COST (Cost 10^3 $) L	E	H	Equip. Spares or Immediate Deliv. Y/N
Direct Damage								
1. Electronics (Unique)								
• Diagnostics								
• Alignment (Front End)	15	22	33	No	10K	10K	20K	No
2. Optics (Few)								
• Mirrors*	0	1	2	Yes		- Unknown -		Yes
• Photomultiplier Tubes	0	1	2	Yes				
• Cameras Special	15	22	33	No				
3. Vacuum Control Area								
• Vacuum Pumps								
• Electronics	15	22	33	No	20K	25K		Questionable
Indirect Damage								
1. Crane Overhead								
2. Ceiling & Roof		Very Long		No		Very High		No

*NOTE: *Optics not protected by a nitrogen blanket.*

TABLE 4

OPERATIONAL READINESS SURVEY FORM

HEATING, VENTILATING AND AIR CONDITIONING

STRATEGIC BUILDING COMPARTMENT CONTAINING STRATEGIC EQUIPMENT	PROGRAMMATIC DELAY (Time/Days) L	E	H	Contingency or Workaround Plan Y/N	REPLACEMENT COST (Cost 10^3 $) L	E	H	Equip. Spares or Immediate Deliv. Y/N
Direct Damage								
1. Chiller(s)	Depends upon extent of damage			No		Unknown		No
2. Fan(s)								
• Target Bay		Same		No		Unknown		No
• Laser Bay								
Indirect Damage								
(None)		N.A.				N.A.		

TABLE 5

OPERATIONAL READINESS SURVEY FORM

POWER HANDLING, CONDITIONING, AND STORAGE

STRATEGIC BUILDING COMPARTMENT CONTAINING STRATEGIC EQUIPMENT	PROGRAMMATIC DELAY (Time/Days) L	E	H	Contingency or Workaround Plan Y/N	REPLACEMENT COST (Cost 10^3 $) L	E	H	Equip. Spares or Immediate Deliv. Y/N
Direct Damage								
1. Capacitor Room								
• Capacitors	0	Very Long		None at Present	2K		6M+	Yes(?)
• Capacitor Load Module & Fork Lift	0	Moderate		Yes	25K	30K	40K	No
2. Power Supply Area								
• Power Supplies & Control Circuits	0	Moderate		Yes (Spare)		- Small -		Yes
3. Power Interlock Conditioning Unit	1M**	2M**	3M**		5K Labor Costs		20K Hardware	No
4. P.C. Board Tester Electronics	0	0	Unknown	Yes		100K		Yes
Indirect Damage								
1. Flooding	--	30d*	--	No	Labor Cleanup Costs			N.A.
2. Ceiling Failure		- Very Long -		No		- Very Large -		No

NOTES: +Salvage Value of Capacitors
*See Seismic Experience
**M = Months

TABLE 6

OPERATIONAL READINESS SURVEY FORM

TARGET DIAGNOSTICS AREA(S)
(Outside Target Room)

STRATEGIC BUILDING COMPARTMENT CONTAINING STRATEGIC EQUIPMENT	PROGRAMMATIC DELAY (Time/Days) L	E	H	Contingency or Workaround Plan Y/N	REPLACEMENT COST (Cost 10^3 $) L	E	H	Equip. Spares or Immediate Deliv. Y/N
Direct Damage (Heat & Smoke)								
Electronic Racks	2M*	4M	6M		10K		5,500K 4 Million Labor 1.5 Million Hardware	No
Electronic Racks	5d		10d		Labor Costs			
Indirect Damage								
(None)								

NOTE: *M = Months

TABLE 7

OPERATIONAL READINESS SURVEY FORM

MISCELLANEOUS

STRATEGIC BUILDING COMPARTMENT CONTAINING STRATEGIC EQUIPMENT	PROGRAMMATIC DELAY (Time/Days) L	E	H	Contingency or Workaround Plan Y/N	REPLACEMENT COST (Cost 10^3 $) L	E	H	Equip. Spares or Immediate Deliv. Y/N
Direct Damage								
1. Outside								
- PG&E Transformers	1M	6M	18M	No		Unknown		
500 KEV/4 MVA				Defense Priority Possible				
Indirect Damage								
1. Minor Structural	- None -					Minor		

TABLE 8

OPERATIONAL READINESS SURVEY FORM

CLEAN ROOM

STRATEGIC BUILDING COMPARTMENT CONTAINING STRATEGIC EQUIPMENT	PROGRAMMATIC DELAY (Time/Days) L	E	H	Contingency or Workaround Plan Y/N	REPLACEMENT COST (Cost 10^3 $) L	E	H	Equip. Spares or Immediate Deliv. Y/N
Direct Damage								
1. Freon Spray System				Yes	0	3K	10K	Yes
2. Work Rack Fixtures				Yes			2K	No
Indirect Damage								
1. Heating, Ventilating and Air Conditioning		Uncertain		No			Unknown	N.A.

APPENDIX B

CALCULATIONAL PROCEDURES USED IN FIRE MODELING

Data from July 1981 LLNL idealized fire tests has been subjected to balancing criteria to assess potential error sources in measurement and state reduction procedures. We grouped our criteria into seven pertinent parameters of interest (see Table 1): total mass flow (in g/s), major species flow (O_2, N_2), major products flow (H_2O, CO_2), minor products flow (CO, CH_4), elemental balance (C, O, H), energy flow (kilowatts) and combustion energy (kilowatts). An example set of these seven plots for CEL8 is included along with an explanation of balancing relationships, terms, symbols and assumptions (Table 2). The BASIC programs "FIDO," "FANG," and "ROVER" (The Dog Files) that performed calculations and plotted the data can be found at the end of this appendix, along with some program notes that give detailed explanations of the "Dog Files" and how to run them.

TABLE 1

EQUATIONS

MASS BALANCE

$$Mass_{in} = \frac{1.176\ (300)}{(Temp_{in} + 273)}\ (Inlet\ Air_{north} + Inlet\ Air_{south})\ (1.03)$$

$$Mass_{out} = -\left(\frac{1.176\ (300)}{(Temp_{Hepa}^{*} + 273)}\right)\left(\frac{(Temp_{Hepa}^{*}) + 563}{662}\right)\ (Exit\ Air^{*})$$

$$Mass_{net} = Mass_{in} + Mass_{out} + Fuel_{in}$$

MAJOR SPECIES

$$N_{2in} = 0.76\ (mass_{in})$$

$$N_{2out} = 0.99\left(mass_{out} - O_{2out} - CO_{out} - CH_{4out} - CO_{2out} - (J3^{**} \cdot CO_{2out})\right)$$

$$N_{2net} = N_{2in} + N_{2out}$$

$$O_{2in} = 0.23\ (mass_{in})$$

$$O_{2out} = O_{2net} - O_{2in}$$

$$O_{2net} = -\ (J1^{**} \cdot CO_{2net}) + (J2^{**} \cdot CO_{net})$$

MAJOR PRODUCTS

$$H_2O_{in} = 0.01\ (mass_{in})$$

$$H_2O_{out} = (.01316 \cdot N_{2out}) + (J3^{**} \cdot CO_{2out})$$

$$H_2O_{net} = H_2Oin + H_2Oout$$

$$CO_{2net} = \frac{1.52\ (\%\ CO_2^{*})}{100} \cdot (mass_{out})$$

MINOR PRODUCTS

$$CO_{net} = \frac{0.966\ (\%\ CO^{*})}{100} \cdot (mass_{out})$$

$$CH_{4net} = \frac{0.552\ (ppm\ CH_4^{*})}{1000000} \cdot (mass_{out})$$

ELEMENT BALANCE

$$\text{Carbon} = (Z1^{**} \cdot \text{Fuel}_{in}) + \frac{12\,(CO_{2net})}{44} + \frac{12\,(CO_{net})}{28} + \frac{12\,(CH_{4net})}{16}$$

$$\text{Hydrogen} = (Z2^{**} \cdot \text{Fuel}_{in}) + \frac{2\,(H_2O_{net})}{18} + \frac{4\,(CH_{4net})}{16}$$

$$\text{Oxygen} = (Z3^{**} \cdot \text{Fuel}_{in}) + (O_{2net}) + \frac{16\,(H_2O_{net})}{18} + \frac{32\,(CO_{2net})}{44} + \frac{16\,(CO_{net})}{28}$$

$$\text{Mass} = \text{Fuel}_{in} + O_{2net} + (CO_{2net} + CO_{net} + CH_{4net} + H_2O_{net})$$

GAS ENERGY BALANCE

$$Q_{in} = 0.00102\,(\text{Temp}_{in} + 273) \cdot (\text{mass}_{in})$$

$$Q_{out} = 0.00109\,(\text{Temp}_{out} + 273) \cdot (\text{mass}_{out})$$

$$Q_{net} = Q_{in} + Q_{out}$$

COMBUSTION ENERGY

$$Q\,(CO_2 + CO) = V1^{**} \cdot (J1^{**} \cdot CO_{2net} + J2^{**} \cdot CO_{net})$$

$$Q\,(O_2) = V1^{**} \cdot O_{2net}$$

$$Q_{Wall} = -\,Q_{net} + Q\,(CO_2 + CO)$$

* Time delay/offset to account for transit down duct
** Value depends on fuel used

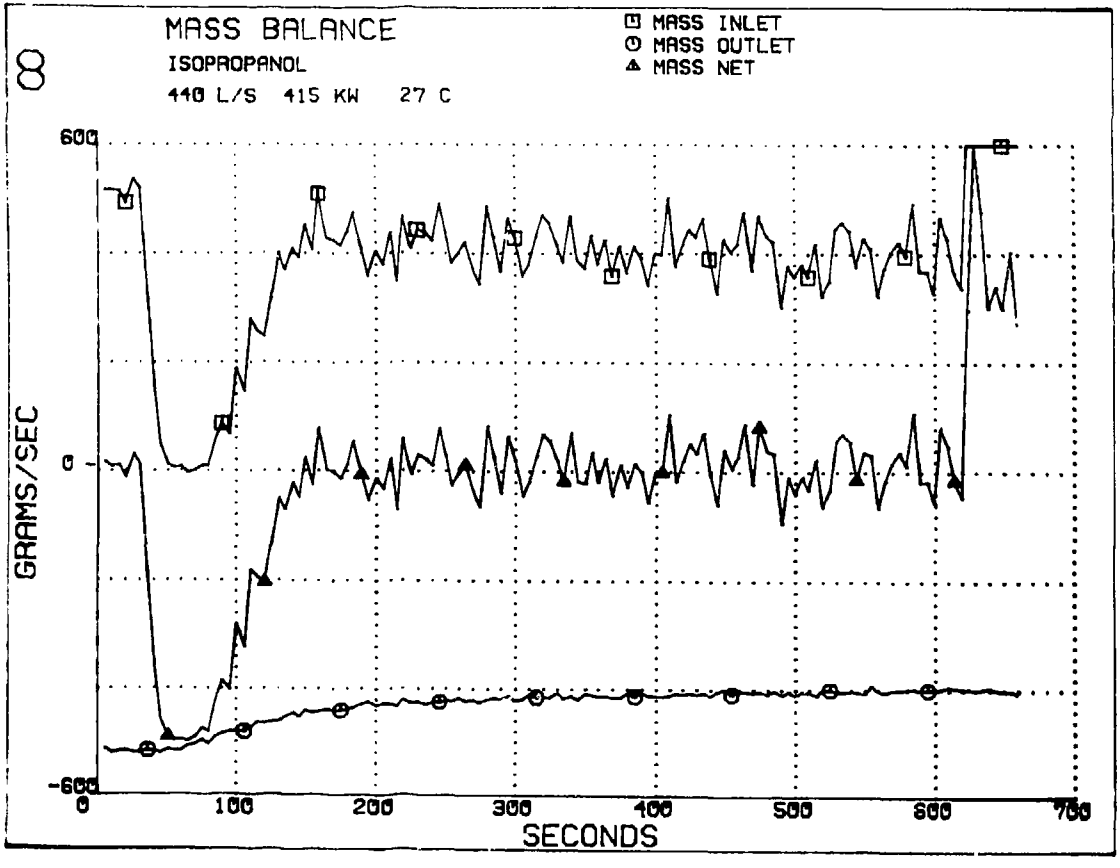
MASS BALANCE
ISOPROPANOL
440 L/S 415 KW 27 C
MASS INLET
MASS OUTLET
MASS NET
600
0
-600
GRAMS/SEC
0
100
200
300
400
500
600
700
SECONDS

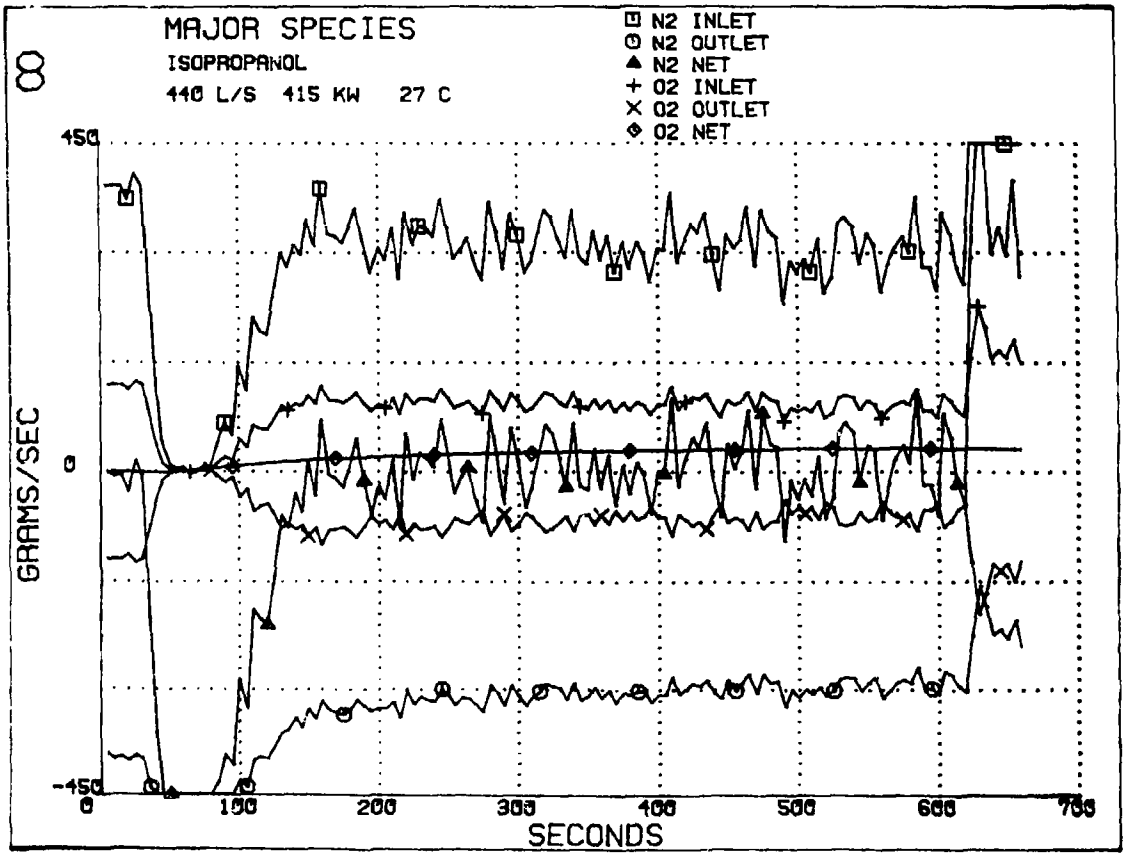
MAJOR SPECIES
ISOPROPANOL
440 L/S 415 KW 27 C
N2 INLET
N2 OUTLET
N2 NET
O2 INLET
O2 OUTLET
O2 NET
GRAMS/SEC
450
0
-450
0
100
200
300
400
500
600
700
SECONDS

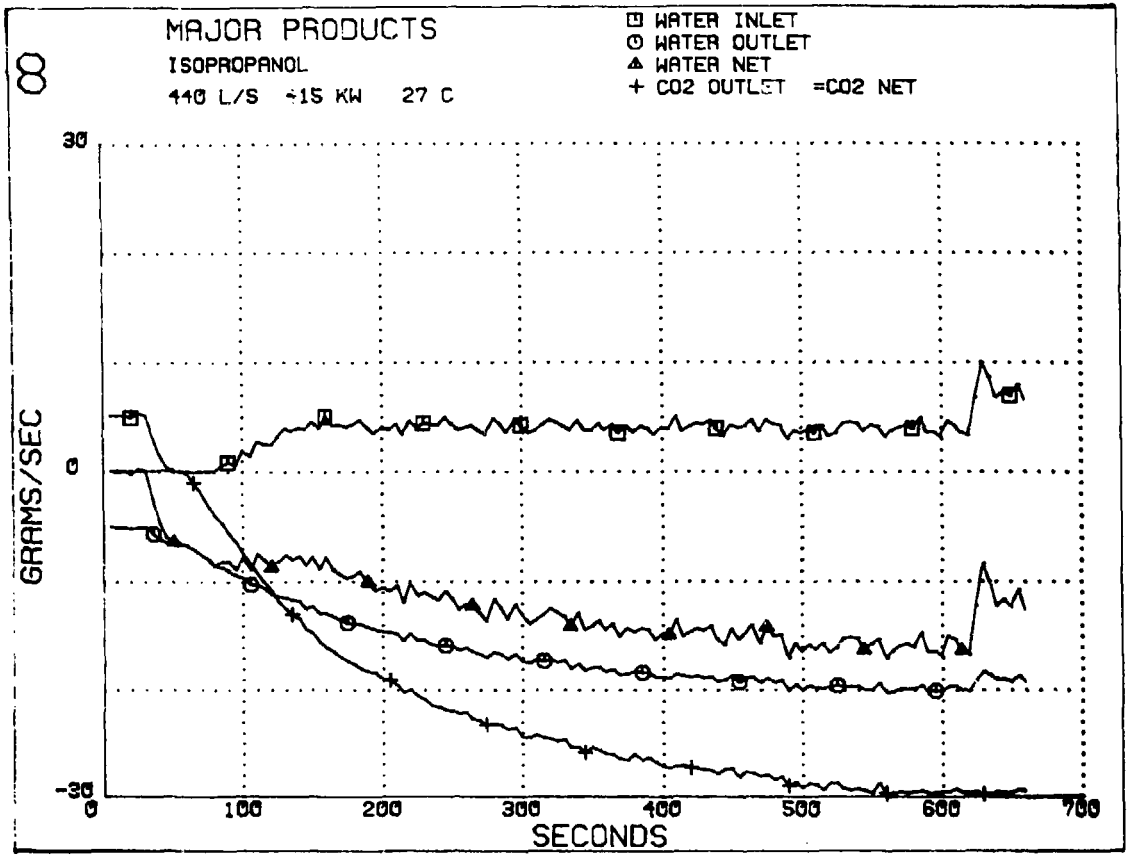
MAJOR PRODUCTS
ISOPROPANOL
440 L/S ÷15 KW 27 C
WATER INLET
WATER OUTLET
WATER NET
CO2 OUTLET =CO2 NET
GRAMS/SEC
30
0
-30
0
100
200
300
400
500
600
700
SECONDS

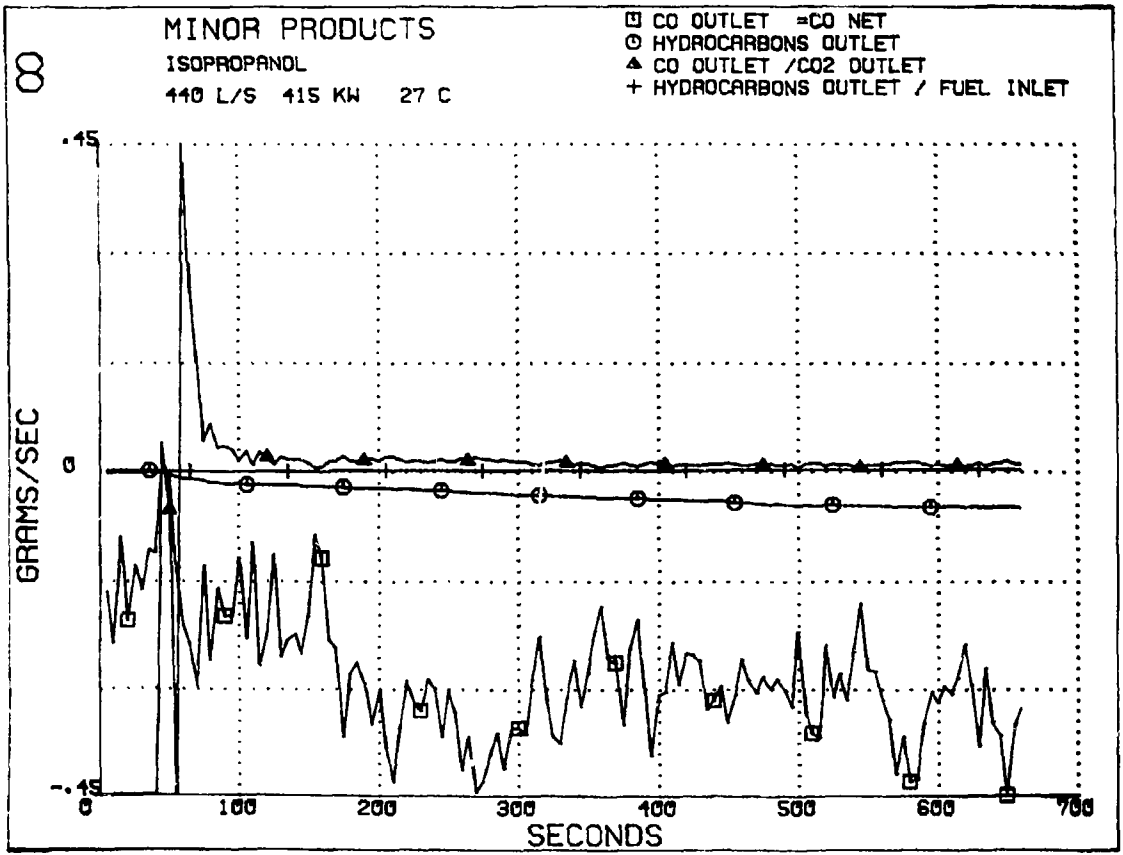
8
MINOR PRODUCTS
ISOPROPANOL
440 L/S 415 KW 27 C
CO OUTLET =CO NET
HYDROCARBONS OUTLET
CO OUTLET /CO2 OUTLET
HYDROCARBONS OUTLET / FUEL INLET
.15
0
-.15
GRAMS/SEC
0
100
200
300
400
500
600
700
SECONDS

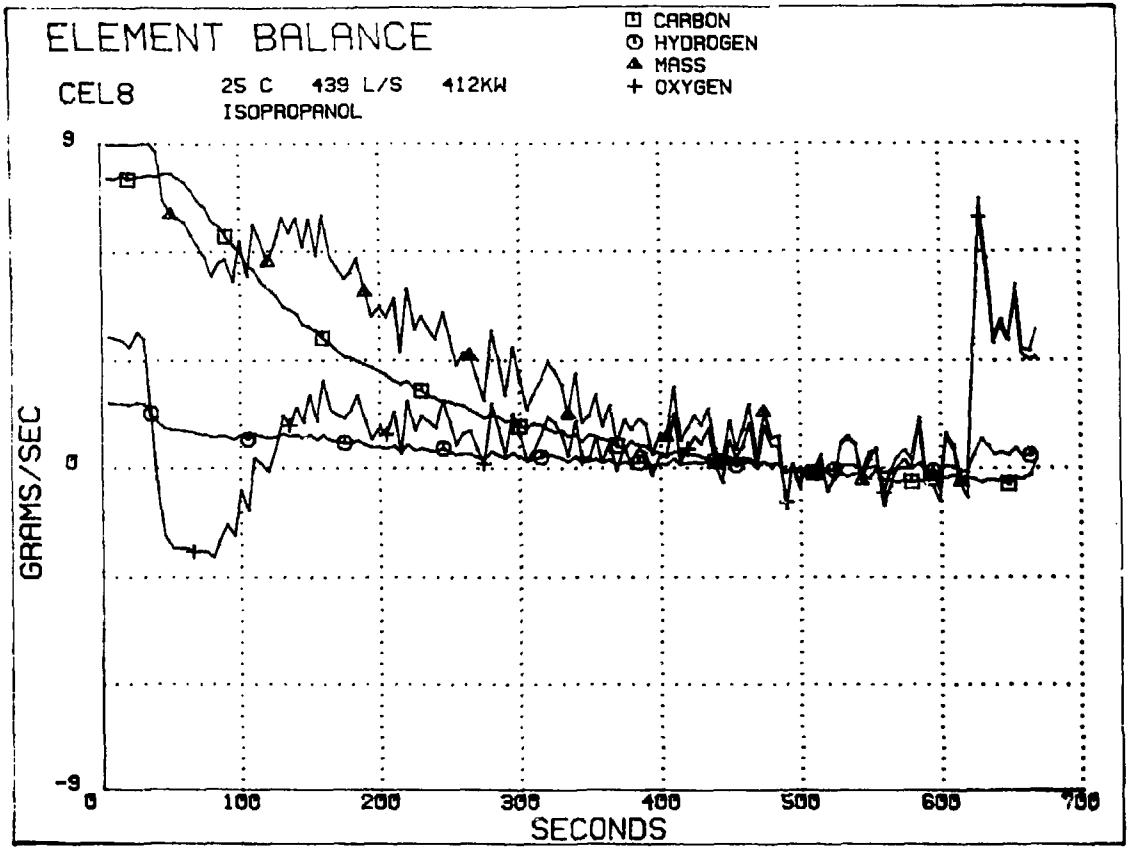
ELEMENT BALANCE
CEL8
25 C 439 L/S 412KW
ISOPROPANOL
CARBON
HYDROGEN
MASS
OXYGEN
9
0
-9
GRAMS/SEC
0
100
200
300
400
500
600
700
SECONDS

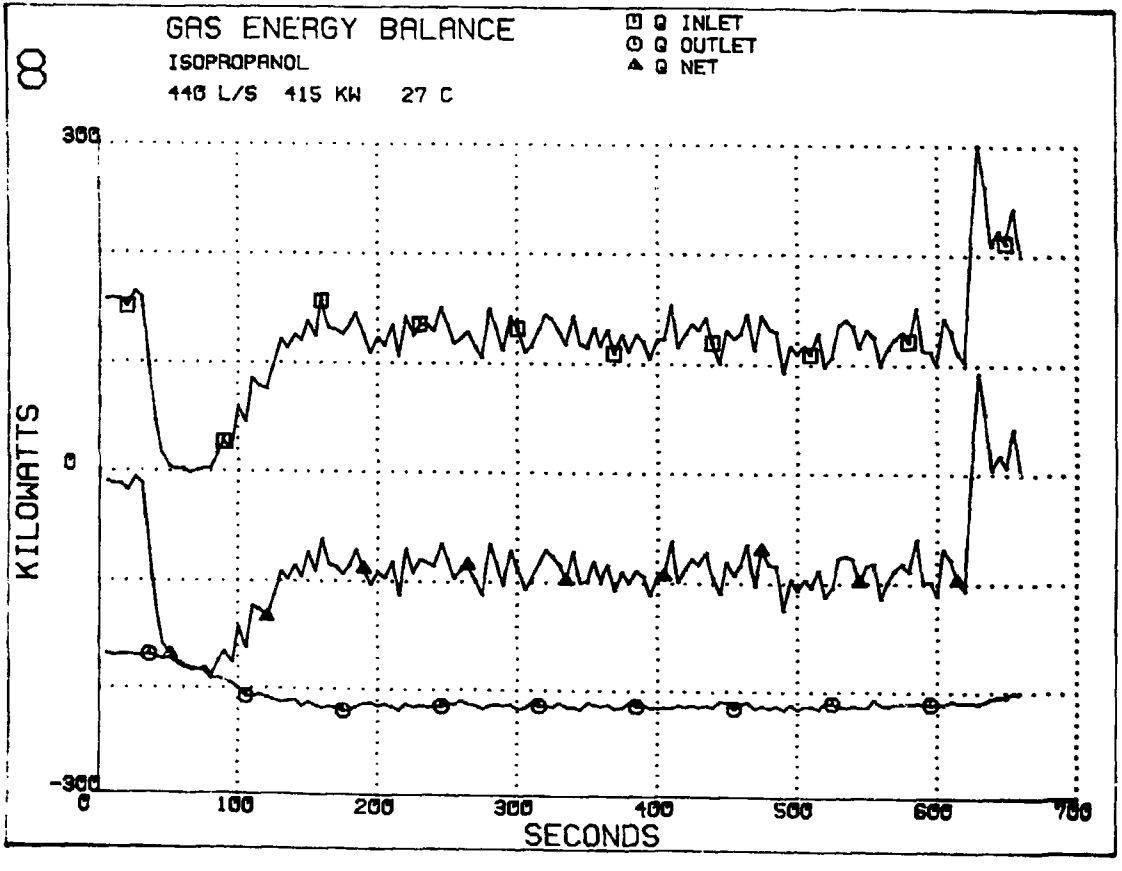
GAS ENERGY BALANCE
ISOPROPANOL
440 L/S 415 KW 27 C
Q INLET
Q OUTLET
Q NET
KILOWATTS
300
0
-300
0
100
200
300
400
500
600
700
SECONDS

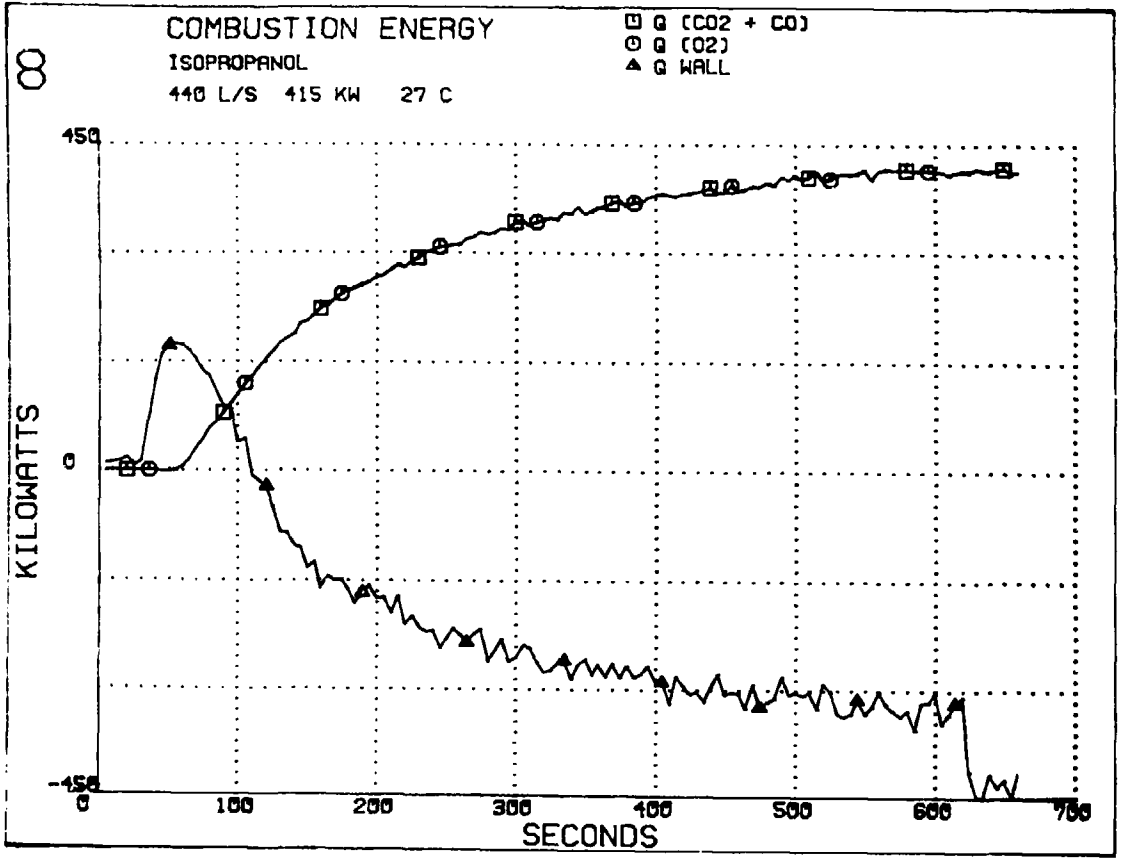
COMBUSTION ENERGY
ISOPROPANOL
440 L/S 415 KW 27 C
Q (CO2 + CO)
Q (O2)
Q WALL
KILOWATTS
450
0
-450
0
100
200
300
400
500
600
700
SECONDS

Table 2

Explanation of Equations and Terms

$Mass_{in}$	Rate of mass coming in inlet duct (grams/sec). Assumes only the pure air enters this inlet duct. The density of inlet gases is found by correcting 1.176 (density of air at 300°K from CRC F-10) by the actual inlet temperature. The measured volume of gases in is corrected by a calibration wall drag factor 1.03. Value should be positive (≈200-500 grams/sec).
$Mass_{out}$	Rate of mass leaving exit duct (grams/sec). Assumes only vitiated air leaves duct. The density is corrected for temperature and the exit air flow is also correct for temperature. Value should be negative (≈200-500 grams/sec).
$Mass_{net}$	Net rate of mass in or out of room (grams/sec). Taken as the total of the masses in ($mass_{in}$ plus $mass_{fuel}$) and mass out. Value should be zero.
N_{2in}	Rate of Nitrogen gas coming in inlet duct (grams/sec). Taken as 76% of the $mass_{in}$. Value should be positive (≈150-350 grams/sec). It is assumed all this exits the room without change.
N_{2out}	Rate of Nitrogen gas leaving exit duct (grams/sec). Calculated from the $mass_{out}$ minus all gas species besides nitrogen. Value should be (≈150-350 grams/sec).
N_{2net}	Net rate of nitrogen gas in or out of test cell (grams/sec). Taken as total of N_{2in} and N_{2out}. Value should be zero.
O_{2in}	Rate of oxygen gas coming in inlet duct (grams/sec). Taken as 23% of the $mass_{in}$. Value should be positive (≈50-100 grams/sec).
O_{2out}	Rate of oxygen gas leaving the exit duct (grams/sec). Taken as O_{2net} minus O_{2in}. Value should be negative.
O_{2net}	Net rate oxygen gas in or out of test cell (grams/sec). Also rate of O_2 consumed by the fire. Calculated from CO_{2net} and CO_{net} by multiplying each by a factor. J1 is the gm O_2 consumed per gm CO_2 produced for a particular fuel and J2 is the gm O_2 consumed per gm CO produced. Value should be positive.
H_2O_{in}	Rate of water vapor coming in inlet duct (grams/sec). Taken as 1% of $mass_{in}$. It is also assumed that all of this exits the room without change. Value should be positive (≈2-4 grams/sec).

H_2O_{out}	Rate of water vapor leaving the exit duct (grams/sec). Since we assume that all H_2O_{in} goes out, H_2O_{out} will equal H_2O_{in} plus the H_2O produced from the fire. We find H_2O_{in} knowing that N_{2in} equals N_{2out} and 1.316% of N_{2in} is equal to the H_2O_{in}. Value should be negative.
H_2O_{net}	Net rate of water vapor coming in or out of test cell (grams/sec). Also rate of H_2O produced by the fire. Taken as total of H_2O_{in} and H_2O_{out}. Value should be negative (≈5-50 grams/sec).
CO_{2net}	Net rate of CO_2 gas produced in test cell (grams/sec). The volumetric % CO_{2out} from to CO_2 analyzer is multiplied by 1.52 (where MW of CO_2 = 44 and MW of air = 29 mass fraction of CO_2 in air) to get % mass CO_{2out} and this is multiplied by $mass_{out}$ to get CO_{2out}; which is equal to CO_{2net} when you assume CO_{2in} equal zero. Value should be negative (≈2-50 grams/sec).
CO_{net}	Net rate of CO gas produced in test cell (grams/sec). The volumetric % CO_{out} from to CO analyzer is multiplied by .97 (mass fraction CO in air) to get % mass CO_{out} and this is multiplied by $mass_{out}$ to get CO_{out}; which is equal to CO_{net} when you assume CO_{in} equal zero. Value should be negative (≈.1-5 grams/sec).
CH_{4net}	Net rate of equivalent methane produced in test cell (grams/sec). The ppm "methane" from the flame ionization hydrocarbon analyzer is multiplied by 1 million and .55 (mass fraction of CH_4 in vitiated air) to convert to % mass "methane"$_{out}$. This is multiplied by $mass_{out}$ to get "methane"$_{out}$; which is equal to "methane"$_{net}$ when you assume "methane"$_{in}$ equal zero. Value should be negative (≈.01-2 grams/sec).
Carbon	Carbon atom balance (grams/sec). Taken as the total of the mass fraction of the carbon containing species going in and out of the test cell. Z1 is the mass fraction of carbon atoms in the fuel. Value should approach zero.
Hydrogen	Hydrogen atom balance (grams/sec). Taken as the total of the mass fraction of all hydrogen containing species going in and out of the test cell. Z2 is the mass fraction of the hydrogen atoms in the fuel. Value should approach zero.
Oxygen	Oxygen atom balance (grams/sec) taken as the total of the mass fraction of all oxygen atom containing species going in or out of the test cell. Z3 is the mass fraction of the oxygen atoms in the fuel. Value should approach zero.
Mass	Mass Balance Check (grams/sec). Taken as $Fuel_{in}$ minus the total of all the net gases. It is an indication of the soot or water entrapment or leaks in the system. Value should approach zero.

Q_{in} — Gas Energy coming in inlet duct (KILOWATTS) .00102 is the heat capacity of pure air in joules/K° • gram. This multiplied by the inlet air temperature and the mass of air in gives Q_{in}. Value should be negative (≈50-150 kw).

Q_{out} — Gas Energy leaving test cell exit vent (KILOWATTS). .00109 is the heat capacity of vitiated air in joules/K° • gram. This is multiplied by the exit air temperature and the mass of air out the outlet to get Q_{out}. Value should be negative (≈100-250 kw).

Q_{net} — Net Gas Energy in or out of test cell via air ducts (KILOWATTS) taken as total of Q_{in} and Q_{out}. Value should be negative (≈50-150 kw).

$Q(CO_2+CO)$ — Heat release rate of fire (KILOWATTS) calculated from CO_2 and CO produced. V1 is the KW released per gram of O_2 consumed. J1 is the grams of O_2 consumed per gm CO_2 produced and J2 is the grams of O_2 consumed per gm CO produced. Value should be equal to the heat release rate calculated from mass of $fuel_{in}$.

$Q(O_2)$ — Heat release rate from fire (KILOWATTS) calculated from O_2 consumed which was calculated from CO_2 and CO produced this calculation assumes all O_2 goes to CO_2. Value should equal $Q\ (CO_2 + CO)$.

Q_{Wall} — Heat Loss to Walls (KILOWATTS) calculated from the heat release rate of the fire minus the net gas energy leaving the test cell. Value should be negative and ≈60%-80% of the fire strength.

THE DOG FILES

Introduction

The dog files were written by Ken Foote with Pat Pagni in September 1981 to analyze data from the large-scale test cell calibration experiments. These programs will analyze data stored in virtual files on a hard disk from Fire Science's PDP-11 under the program EXPT.B99. The analysis includes equations to calculate mass balance, species balance, product balance, gas energy balance, element balance and combustion energy.

The program sequence is FIDO to FANG to ROVER. FIDO retrieves stored data, FANG manipulates it and ROVER plots it. It is important to note that for certain tests the programs FIDO and FANG must be changed to correct for test conditions.

A QUICK RUN THROUGH THE DOG FILES AND HOW-TO LESSON

The dog files are three BASIC programs for manipulating data from LLNL's large scale compartment tests. The program sequence is started by running FIDO.B99 (see Table 3). FIDO asks several questions. The first of which is, "WHAT FILE DO YOU WANT?" You should type in the file name of the test data you wish to analyze. An appropriate response would be "DK1:CEL1" where "DK1:" is the device name the data is stored on and "CEL1" is the file name. The 1981 tests were named CEL1-13.

After asking you for a file to analyze, FIDO will ask you what fuel was used and the fuel flow rate. This information can be found on Tables 4 and 5. The program sets the values of the variables for the density, heat release and atomic composition according to which fuel you input. If you misspell a fuel or enter one that wasn't used, the error message, "ILLEGAL FUEL" will be printed and the program stopped. FIDO will analyze the whole test from start to finish. If you wish to look at only a part of a run changing the values of a and b in line 115 will enable you to do that.

After clearing the screen, FIDO retrieves the raw data (the millivolt readings stored by EXPT.B99), converts them into engineering units and stores them in a large virtual file called PUPPY.D99 [VF1 (6000)]. This data is

stored sequentially. For example, data for channel 70 would be stored in addresses 1-500 and data for channel 71 would be stored in addresses 501-1000, and so on. There are 500 addresses allotted to each channel. Thus, the program can handle up to 500 data points or 2500 s of data if sampling is every 5 s. FIDO analyzes only 11 channels from EXPT: channels 6, 23, 31, 32, 52, 53, 54, 70, 71, 72 and 73 (see Table 6). FIDO, however, has the capacity to access more and different channels with minor modifications. FIDO records the number of data points for each run in address zero of PUPPY for future reference. When all the data has been converted the counting stops, the screen is erased, PUPPY is closed and FIDO chains to FANG.B99.

FANG opens PUPPY and using the data in it calculates various interesting statistics such as mass balance, species balance, product balance, gas energy balance, element balance and combustion energy for that test. Table 6 and 7 will help you follow or change the manipulations. The new values are stored in a new virtual file called SNOOPY.D99 [VF2 (15000)]. Because FANG is slow in doing the manipulations, it counts the data so you can follow its progress. When FANG is completed it erases the screen, closes both PUPPY and SNOOPY and chains to ROVER.B99 to plot the data in SNOOPY.

ROVER asks three main questions. The plot title, the curve numbers and the maximum value of the plot. The appropriate inputs for these questions are on Table 8. If you don't chain directly from FANG to ROVER (such as in a replot), Rover will ask for the file name and the fuel type again. This information is normally chained from FANG to ROVER automatically.

After you input the max value, ROVER will print out the requested plot. Upon completion it copies the plot, clears the screen and returns to ask the main three questions again. ROVER will loop this way indefinitely. To exit the program press <CONTROL C> also lif you make a mistake press <CONTROL C> and RUN to start over.

ROVER uses a string file called BONES.D99 [V5$ (40)]. This file contains the labels for the various curves. There is a program called NEWLBL.B99 (new labels) that will list and change the labels in BONES.

For various tests it will be necessary to change FIDO or FANG to correct for errors in the test conditions. These two corrections are summarized on Table 9. First, it was discovered that the CO analyzer was poorly calibrated for the first 7 runs. So, there is a correction for that. Second, with tests where the exit air flow was approximately 500 l/min, it was decided to have a delay time of 20 s instead of 30 as in the 250 l/min tests. Thus, there is a

4 data point skip (4 X 5 s = 20 s) for the 500 l/min tests, instead of a 6 data point skip (6 X 5 s = 30 s) as in the 250 l/min tests. To make this correction easier there are two entire programs that can replace FANG with these corrections in them. FANG4 is a FANG with a 20-s delay and FANG6 is a FANG with a 30-s delay.

TABLE 3

LIST OF REQUIRED FILES

BASIC PROGRAMS

FIDO	.B99
FANG	.B99
ROVER	.B99
NEWLBL	.B99 (Optional)
FANG6	.B99 (Optional)
FANG4	.B99 (Optional)

DATA FILES

PUPPY	.D99 VF1 (6000)
SNOOPY	.D99 VF2 (15000)
BONES	.D99 VF5$ (40)

TABLE 4

GENERAL INFORMATION

CEL NO.	TYPE OF FUEL	AMBIENT TEMP (°C)	RUN TIME (SEC)	FUEL FLOW (ml/min)	EXIT AIR (l/min)	EST FIRE POWER (kw)
1	Methane	28	1128	160 x 2.214 = 354.2	250	125
2	Methane	30	1777	191 x 2.34 = 446.9	245	130
3	Methane	20	512	94 x 1.92 = 180.5	250	65
4	Methane	25	550	190 x 2.34 = 444.6	465	160
5	Isopropanol	30	691	520	245	205
6	Isopropanol	30	937	1040	230	415
7	Isopropanol	20	890	520	470	205
8	Isopropanol	27	685	1040	440	415
9	Isopropanol	30	865	2080	405	830
10	Isopropanol	32	655	2080	230	830
12	Isopropanol	28	700	520	445	205
		28	1050	1040	420	415
		28	2037	2080	375	830
13	Methanol	32	550	693	440	179
		32	820	1386	430	254
		32	1265	2772	420	750

TABLE 5

VARIABLES FOR FIDO*

Fuel	Formula	D	Z1	Z2	Z3	K1	V1	J1	J2	J3
	$C_xH_yO_z$	ρ (g/cm^3)	$\frac{MW\ C}{MW\ Fuel}$	$\frac{MW\ H}{MW\ Fuel}$	$\frac{MW\ O}{MW\ Fuel}$	$\frac{KJ}{gm\ Fuel}$	$\frac{KJ}{gm\ O_2}$	$\frac{gm\ O_2}{gm\ CO_2}$	$\frac{gm\ O_2}{gm\ CO}$	$\frac{gm\ H_2O}{gm\ CO_2}$
Methane	CH_4	.6647	0.75	0.25	0.0	50.0	12.5	1.45	1.71	.818
Methanol	CH_4O	.787	.375	.125	0.5	20.0	13.3	1.09	1.14	.818
Isopropanol	C_3H_8O	.781	0.6	.133	.267	30.5	12.7	1.09	1.14	.545

Fuel	Formula $C_xH_yO_z$	D (g/cm^3)	$\frac{KJ}{gm\ Fuel\ (CO_2)}$	$\frac{KJ}{gm\ Fuel\ (CO)}$	$\frac{gm\ Fuel}{gm\ O_2\ (CO_2)}$	$\frac{gm\ Fuel}{gm\ O_2\ (CO)}$
Methane	CH_4	.6647	50.0	37.5	0.25	0.33
Methanol	CH_4O	.787	20.0	13.3	1.67	1.00
Isopropanol	C_3H_8O	.781	30.5	19.9	0.42	0.63

TABLE 6

VARIABLES FOR FIDO

Channel		FIDO		VF1(PUPPY)
25	=	P	=	X
54	=	Q	=	X + 500
[illegible]	=	R	=	X + 1000
52	=	S	=	X + 1500
70	=	T	=	X + 2000
71	=	U	=	X + 2500
72	=	V	=	X + 3000
73	=	W	=	X + 3500
5	=	Y	=	X + 4000
51	=	2	=	X + 4500
52	=	20		

VF1(0) - X_n = # of elements

TABLE 7

VARIABLES FOR FANG

VF5$ (BONES)	FANG	VF2(SNOOPY)
Mass inlet	= M1	= I
Mass outlet	= M2	= I + 500
Mass net	= M3	= I + 1000
N_2 inlet	= N1	= I + 1500
N_2 outlet	= N2	= I + 2000
N_2 net	= N3	= I + 2500
O_2 inlet	= O1	= I + 3000
O_2 outlet	= O2	= I + 3500
O_2 net	= O3	= I + 4000
H_2O inlet	= W1	= I + 4500
H_2O outlet	= W2	= I + 5000
H_2O net	= W3	= I + 5500
CO_2 outlet = CO_2 net	= D2 = D3	= I + 6000
CO outlet = CO net	= C2 = C3	= I + 6500
Hydrocarbons outlet	= H2 = H3	= I + 7000
CO outlet/CO_2 outlet	= CO	= I + 7500
Hydrocarbons/Fuel in	= FO	= I + 8000
Carbon	= C8	= I + 8500
Hydrogen	= H8	= I + 9000
Mass	= M8	= I + 9500
Oxygen	= O8	= I + 10000
Q inlet	= Q1	= I + 10500
Q outlet	= Q2	= I + 11000
Q net	= Q3	= I + 11500
Q (CO + CO_2)	= Q4	= I + 12000
Q (O_2)	= Q5	= I + 12500
Q wall	= Q6	= I + 13000

TABLE 8

GUIDE FOR ROVER INPUTS

TITLES	CURVES	MAX VALUES
Mass Balance	0-2	900
Major Species	3-8	600
Major Products	9-12	30
Minor Products	13-16	45
Element Balance	17-20	9
Gas Energy Balance	21-23	300
Combustion Energy	24-26	300

TABLE 9

PROGRAM CHANGES

Program	Line	Change
Offset for uncalibrated CO		
FIDO	633	V = V + .019 (for runs 1-6)
		delete (for runs 8-13)
Time delay for inlet-exit time		
FANG	3140,3160,3180	+ 4 (for 500 liter/min exit) replace with FANG4
		+ 6 (for 250 liter/min exit) replace with FANG6

```
FIDO  12-NOV-81  MU BASIC/RT-11 V01-01D

1 REM FIDO.B99 WRITTEN 10/81 BY KEN FOOTE AS PART OF THE DOG FILES
2 REM TO READ EXPT.B99 VFILES
20 COMMON F1,F2,V1,Z1,Z2,Z3,J1,J2,J3,F$,P$
30 DIM C(11)
50 PRINT CHR$(27),CHR$(12)
100 PRINT "WHAT FILE DO YOU WANT (EX.CEL8)"; \ INPUT P$
105 PRINT "WHAT WAS THE FUEL USED"; \ INPUT F$
115 A=0 \ B=99999 \ REM CAN REPLACE THIS WITH INPUTS FOR A&B
120 PRINT "ENTER THE FUEL FLOW (ML/MIN)"; \ INPUT F
125 IF F$<>"METHANE" THEN 150
130 D=.6647 \ K1=50 \ V1=12.5
135 Z1=.75 \ Z2=.25 \ Z3=0
140 J1=1.45 \ J2=1.71 \ J3=.818 \ GO TO 200
150 IF F$<>"METHANOL" THEN 175
155 D=.787 \ K1=20 \ V1=13.3
160 Z1=.375 \ Z2=.125 \ Z3=.5
165 J1=1.09 \ J2=1.14 \ J3=.818 \ GO TO 200
175 IF F$<>"ISOPROPANOL" THEN PRINT "ILLEGAL FUEL " \ END
180 D=.781 \ K1=30.5 \ V1=12.7
185 Z1=.6 \ Z2=.133 \ Z3=.267
190 J1=1.09 \ J2=1.14 \ J3=.545
200 F1=F*D/60 \ F2=INT(F1*K1)
250 REM                THIS SETS UP WHICH CHANNNELS ARE READ
260 C(1)=23 \ C(2)=54 \ C(3)=53
270 C(4)=52 \ C(5)=70 \ C(6)=71
280 C(7)=72 \ C(8)=73 \ C(9)=6
285 C(10)=31 \ C(11)=32
290 OPEN "PUPPY" FOR INPUT AS FILE VF2(6000) \ N=1000
300 REM            THIS SELECTS AND OPENS EXPT.B99 STORAGE FILES
310 N=N+1 \ N$=STR$(N) \ N$=SEG$(N$,2,4) \ M$="DK1:"+P$+"."+N$
320 OPEN M$ FOR INPUT AS FILE VF1 \ I=-60
```

```
30 I=I+76
340 IF VF1(I+1)=-1 THEN 1000
350 IF VF1(I)=-1 THEN CLOSE VF1 \ GO TO 310
360 IF VF1(I)<A THEN 330
370 IF VF1(I)>B THEN 1000
500 REM                THIS PULLS DATA OFF THE DISC
510 P=VF1(I+C(1)+1) \ Q=VF1(I+C(2)+1) \ R=VF1(I+C(3)+1)
520 S=VF1(I+C(4)+1) \ T=VF1(I+C(5)+1) \ U=VF1(I+C(6)+1)
530 V=VF1(I+C(7)+1) \ W=VF1(I+C(8)+1) \ Y=VF1(I+C(9)+1)
540 Z=VF1(I+C(10)+1) \ Z0=VF1(I+C(11)+1)
600 REM THESE LINES ARE FOR CALIBRATION EQUATIONS
605 P=P*1000 \ P=-1.6+25.544*P-.092367*P^2+1.46670E-03*P^3
607 Y=Y*1000 \ Y=-1.6+25.544*Y-.092367*Y^2+1.46670E-03*Y^3
610 Q=Q*1216
615 R=R*1216
617 S=(S-.016)/1.25000E-03
620 S=168*SQR(ABS(S/248.8))
625 T=T/.05
630 U=-5.88000E-03+11.7*U-4.62*U^2+12.8*U^3
633 U=U+.019
635 V=-3.51000E-03+7.76*V-.476*V^2+2.71*V^3
640 W=W*25000
650 Z=Z*1000 \ Z=-1.6+25.544*Z-.092367*Z^2+1.46670E-03*Z^3
655 Z0=Z0*1000 \ Z0=-1.6+25.544*Z0-.092367*Z0^2+1.46670E-03*Z0^3
675 Z=INT((Z+Z0)/2)
700 REM        THIS STORES DATA IN ENG UNITS IN VFILE PUPPY
710 X=X+1 \ IF X=500 THEN 1000
720 VF2(0)=X \ VF2(X)=P \ VF2(X+500)=Q
730 VF2(X+1000)=R \ VF2(X+1500)=S \ VF2(X+2000)=T
740 VF2(X+2500)=U \ VF2(X+3000)=V \ VF2(X+3500)=W
750 VF2(X+4000)=Y \ VF2(X+4500)=Z
800 GO TO 330
1000 CLOSE  \ PAGE \ PRINT CHR$(27),CHR$(12) \ CHAIN "FANG"

READY
```

```
FANG  12-NOV-81  MU BASIC/RT-11 V01-01D

1 REM FANG.B99 WRITTEN 10/81 BY KEN FOOTE AS PART OF THE DOG FILES
2 REM THIS TAKES DATA FROM FIDO AND CHAINS TO ROVER
20 COMMON F%,P$
1000 OPEN "PUPPY" FOR INPUT AS FILE VF1(6000)
1040 OPEN "SNOOPY" FOR INPUT AS FILE VF2(15000)
1060 VF2(0)=VF1(0)-6 \ VF2(500)=INT(VF1(1500+VF1(0)))
1100 VF2(1000)=VF1(4501) \ VF2(1500)=F2
2000 FOR I=1 TO VF2(0)
3000 REM                              THIS DOES THE MANIPULATION
3020 M1=(352.8/(273+VF1(I+4500)))*(VF1(I+500)+VF1(I+1000))*1.05
3040 M2=-352.8/(273+VF1(I+2))*VF1(I+1502)
3060 M3=M1+M2+F1
3080 W1=.01*M1
3100 N1=.76*M1
3120 O1=.23*M1
3140 D3=.0152*VF1(I+2506)*M2
3160 C3=9.66000E-03*VF1(I+3006)*M2
3180 H3=5.52000E-07*VF1(I+3506)*M2
3200 O3=-(J1*D3+J2*C3)
3220 O2=O3-O1
3240 N2=.99*(M2-O2-H3-C3-D3-J3*D3)
3260 N3=N1+N2
3300 W2=.01316*N2+J3*D3
3320 W3=W1+W2
3340 C0=C3/D3
3360 F0=-H3/F1
3400 Q1=1.02000E-03*(VF1(I+4500)+273)*M1
3420 Q2=1.09000E-03*(VF1(I+4000)+273)*M2
3440 Q3=Q1+Q2
3460 Q4=-V1*(J1*D3+J2*C3)
3480 Q5=V1*O3
```

```
300 Q6=-(Q3+Q4)
3520 C8=Z1*F1+12/44*D3+12/18*C3+12/16*H3
3540 H8=Z2*F1+2/18*W3+4/16*H3
3560 O8=Z3*F1+O3+16/18*W3+32/44*D3+16/28*C3
3580 M8=F1+O3+D3+C3+H3+W3
3600 PRINT I*5;
3700 REM                THIS STORES THE VALUES IN SNOOPY
3720 VF2(I)=M1 \ VF2(I+500)=M2 \ VF2(I+1000)=M3
3730 VF2(I+1500)=N1 \ VF2(I+2000)=N2 \ VF2(I+2500)=N3
3740 VF2(I+3000)=O1 \ VF2(I+3500)=O2 \ VF2(I+4000)=O3
3750 VF2(I+4500)=W1 \ VF2(I+5000)=W2 \ VF2(I+5500)=W3
3760 VF2(I+6000)=D3 \ VF2(I+6500)=C3 \ VF2(I+7000)=H3
3780 VF2(I+7500)=C0 \ VF2(I+8000)=F0
3790 VF2(I+8500)=C8 \ VF2(I+9000)=H8 \ VF2(I+9500)=M8 \ VF2(I+10000)=O8
3800 VF2(I+10500)=Q1 \ VF2(I+11000)=Q2 \ VF2(I+11500)=Q3
3820 VF2(I+12000)=Q4 \ VF2(I+12500)=Q5 \ VF2(I+13000)=Q6
4000 NEXT I
5000 CHAIN "ROVER"

READY
```

```
ROVER  12-NOV-81  MU BASIC/RT-11 V01-01D

1 REM ROVER.B99 WRITTEN 10/81 BY KEN FOOTE AS PART OF THE DOG FILES
2 REM TO PLOT DATA FROM FANG.B99
50 SPD(0) \ PAGE \ PRINT CHR$(27),CHR$(12)
100 IF F$<>"" THEN 150
110 PRINT "WHAT TEST WAS THIS (EX. CEL8)"; \ INPUT P$
120 PRINT "WHAT WAS THE FUEL "; \ INPUT F$
150 PRINT "WHAT IS THE TITLE TO BE"; \ INPUT T$
160 PRINT "WHICH CURVES DO YOU WANT TO SEE?(2 INPUTS 0-26)"; \ INPUT B,C
165 IF ABS(C-B)>8 THEN PRINT "ILLEGAL RANGE (8 CURVES MAX)" \ GO TO 160
170 Y$="GRAMS/SEC" \ IF B>20 THEN Y$="KILOWATTS"
175 PRINT "INPUT THE MAX VALUE OF THE PLOT"; \ INPUT Q
180 Q2=2*Q \ P=600/Q2
200 OPEN "SNOOPY" FOR INPUT AS FILE VF4(15000)
350 REM                              THIS FINDS THE VALUE OF DT      (T3)
355 T0=0 \ T1=VF4(0)*5
360 T2=T1-T0 \ IF T2>48 THEN 370 \ T3=5 \ GO TO 380
370 IF T2>96 THEN 371 \ T3=10 \ GO TO 380
371 IF T2>192 THEN 372 \ T3=20 \ GO TO 380
372 IF T2>480 THEN 373 \ T3=50 \ GO TO 380
373 IF T2>960 THEN 374 \ T3=100 \ GO TO 380
374 IF T2>1920 THEN 375 \ T3=200 \ GO TO 380
375 T3=1000 \ IF T2>4800 THEN 380 \ T3=500
380 T5=0 \ REM T4 AND T5 BRACKET TIME IN MULTIPLES OF DT
385 T5=T5+T3 \ IF T5<=T0 THEN 385 \ T4=T5-T3
390 IF T5>=T1 THEN 395 \ T5=T5+T3 \ GO TO 390
395 T2=T5-T4
500 PRINT CHR$(27),CHR$(12) \ REM              PLOTS PERIMETER
530 PLOT(0,0,0) \ PLOT(0,779,1) \ PLOT(1023,779,1) \ PLOT(1023,0,1)
540 PLOT(0,0,1) \ PLOT(85,650,0) \ PLOT(85,50,1) \ PLOT(985,50,1)
550 REM                    PLOTS VERT & HORIZ GRID
560 FOR I=T4 TO T5 STEP T3 \ X0=85+(I-T4)*900/T2
```

```
50 TEXT(X0-30,33,1,1,I) \ IF I=T4 THEN 590
580 FOR Y0=50 TO 650 STEP 10 \ PLOT(X0,Y0,0) \ NEXT Y0
590 NEXT I
600 FOR Y0=150 TO 650 STEP 100 \ FOR X0=85 TO 984 STEP 90*T3/T2
620 PLOT(X0,Y0,0) \ NEXT X0 \ NEXT Y0
900 REM                          PLOTS TITLES
905 TEXT(480,5,2,1,"SECONDS") \ TEXT(25,250,2,0,Y$)
910 TEXT(50,690,2,1,P$) \ TEXT(40,740,3,1,T$)
915 T1$=STR$(VF4(1000))+" C    " \ T2$=STR$(VF4(500))+" L/S    "
920 T3$=STR$(VF4(1500))+"KW"
925 TEXT(200,700,1,1,T1$+T2$+T3$) \ TEXT(200,675,1,1,F$)
930 TEXT(40,50,1,1,-Q) \ TEXT(40,350,1,1,0) \ TEXT(40,650,1,1,Q)
1000 REM                                  CURVE LABELS
1005 OPEN "BONES" FOR INPUT AS FILE VF5$(40)
1010 FOR I=0 TO C-B \ PLOT(580,767-I*21,0,2,1,I)
1020 I=I+B \ N$=VF5(I) \ I=I-B \ TEXT(600,760-I*21,1,1,N$)
1050 NEXT I \ CLOSE VF5
1100 REM                                THIS PLOTS THE DATA
1120 FOR I=0 TO C-B \ S=S+20*(I+1)+85
1140 FOR J=1 TO VF4(0) \ X0=85+J*900/T2*5
1160 I=I+B \ Y0=50+(VF4(J+I*500)+Q)*P \ I=I-B
1510 IF Y0<50 THEN Y0=50
1520 IF Y0>650 THEN Y0=650
1530 IF X(0)=0 THEN 1600
1540 PLOT(X(0),Y(0),0)
1550 IF X0<S THEN PLOT(X0,Y0,1) \ GO TO 1600
1575 PLOT(X0,Y0,1,2,1,I) \ S=X0+90
1600 X(0)=X0 \ Y(0)=Y0
1900 NEXT J
1950 X(0)=0 \ Y(0)=0 \ S=0
2000 NEXT I \ CLOSE
3000 PRINT CHR$(27),CHR$(23) \ PRINT CHR$(27),CHR$(12) \ GO TO 150

READY
```

```
NEWLBL  12-NOV-81  MU BASIC/RT-11 V01-01D

1 REM THIS SETS THE LABELS USED FOR THE DOG FILES
2 REM WRITTEN 7/81 BY KEN FOOTE
7 PRINT CHR$(27),CHR$(12)
10 OPEN "BONES" FOR INPUT AS FILE VF5$(40)
15 FOR I=0 TO 30 \ PRINT I,VF5(I) \ NEXT I \ CLOSE
20 PRINT "WHICH ONE IS THE FIRST TO BE CHANGED"; \ INPUT A
25 PRINT "WHICH ONE IS THE LAST  TO BE CHANGED"; \ INPUT B
30 IF A=69 THEN 200
40 PRINT CHR$(27),CHR$(12)
50 OPEN "BONES" FOR INPUT AS FILE VF5$(40)
55 FOR I=A TO B
59 PRINT  \ PRINT
60 PRINT "ELEMENT (";I;") USED TO BE          ";VF5(I)
65 PRINT "NOW ELEMENT (";I;") IS            "; \ INPUT L$
75 VF5(I)=L$
100 NEXT I
200 CLOSE

READY
```

APPENDIX C

SPECKLER'S METHOD FOR A TWO-LAYER TEMPERATURE PROFILE

Dr. Ken Speckler has developed a method for forming a two-layer room temperature profile from real data. This important accomplishment links and compares real data and current fire growth models, via constraining air temperature gradients into a hot- and cold-layer analogy of the gradient.

Given room height (h_r), upper layer temperature (T_U) and measured values of temperature ($T(y)$) as a function of height, Speckler predicts the layer interface height (h_l) and the lower-layer temperature (T_L). The equations for h_l and T_L are derived from equations for the conservation of mass in the room and the conservation of area under the $T(y)$ curve. This last condition isn't completely justified, yet it seems reasonable. Speckler's full derivation is at the end of this appendix. Essentially his equations can be reduced to:

$$h_l = h_r \left(\frac{-(a-1)(b-1)}{a+b-2} \right)$$

$$T_L = T_U \left(\frac{(a+b-2)}{(b-1)} + 1 \right)$$

where $a = \int_0^{h_r} \frac{T(y)}{h_r T_U} dy$ normalized area under the curve $\frac{T(y)}{T_U}$

$$b = \int_0^{h_r} \frac{T_U}{h_r T(y)} dy$$ normalized area under the curve $\frac{T_U}{T(y)}$

For our tests, we constructed a thermocouple (TC) rake with 10 TC's evenly spaced approximately 45 cm apart starting 20 cm above the floor. The room height (h_r) was 4.5 meters, thus we were able to assume that each TC was in the middle of a region h_r/n ($n = 10$) and was a representative temperature over its entire region h_r/n. We then took the value of $\underline{a}$ as the average of the temperatures (K°) of the rake divided by T_U. The value of $\underline{b}$ was found similarly by averaging the inverse of the temperatures (K°) and multiplying by T_U.

T_U was determined by first finding the average temperature (T_A) of all the rake TC's. The T_U was taken as the average of all the temperatures greater than T_A.

These simple assumptions proved to be adequate when compared to more complicated analysis of the data (i.e., full integration of the temperature curve to find the true area under the curve T(y) and more subjective determination of T_U).

Speckler's Derivation

From conservation of the mass in the room

$$(1) \qquad m = \int_0^{h_r} \rho A \, dy$$

assuming $\frac{P}{R}$ is constant $\rho = \frac{P}{RT}$ so,

$$(2) \qquad m = \int_0^{h_r} \frac{AP}{RT(y)} \, dy$$

rearrange

$$(3) \qquad \frac{mR}{AP} = \int_0^{h_r} \frac{1}{T(y)} \, dy$$

our equivalent two layer model of this mass equation is

$$(4) \quad \frac{mR}{AP} \text{ equal } = \frac{h_1}{T_L} + \frac{h_r - h_1}{T_U}$$

if the model is good $\frac{mR}{AP} = \frac{mR}{AP}$ equal so combine 3 and 4

$$(5) \qquad \frac{h_1}{T_L} + \frac{h_r - h_1}{T_U} = \int_0^{h_r} \frac{1}{T(y)} \, dy$$

multiplying by $\frac{T_U}{h_r}$ we get

$$(6) \qquad \frac{T_U \, h_1}{T_L \, h_r} + 1 - \frac{h_1}{h_r} = \int_0^{h_r} \frac{T_U}{h_r \, T(y)} \, dy$$

Define $y' = y/hr$ to normalize

$$(7) \qquad \frac{T_U}{T_L}\frac{h_1}{h_r} + 1 - \frac{h_1}{h_r} = \int_0^1 \frac{T_U}{T(y')}\, dy'$$

Rearranging

$$(8) \qquad \frac{T_U}{T_L}\frac{h_1}{h_r} = \frac{h_1}{h_r} - 1 + \int_0^1 \frac{T_U}{T(y')}\, dy'$$

multiplying by $\frac{h_r}{h_1}$ we get,

$$(9) \qquad \frac{T_U}{T_L} = 1 - \frac{h_r}{h_1} + \frac{h_r}{h_1}\int_0^1 \frac{T_U}{T(y')}\, dy'$$

From the conservation of area under the curve T(y)

$$(10) \qquad T_L h_1 + T_U (h_r - h_1) = \int_0^{h_r} T(y)\, dy$$

Dividing by $h_r\ T_U$ we get,

$$(11) \qquad \frac{T_L}{T_U}\frac{h_1}{h_r} + 1 - \frac{h_1}{h_r} = \int_0^{h_r} \frac{T(y)\, dy}{h_r T_U}$$

Again we define $y' = y/h_r$ to normalize.

$$(12) \qquad \frac{T_L}{T_U}\frac{h_1}{h_r} + 1 - \frac{h_1}{h_r} = \int_0^1 \frac{T(y')\, dy'}{T_U}$$

Rearranging and multiplying by $\frac{h_1}{h_r}$ we get

$$(13) \qquad \frac{T_L}{T_U} = \frac{h_r}{h_1}\int_0^1 \frac{T(y')\, dy'}{T_U} + \frac{h_1}{h_r} - 1$$

To simplify let:

$$a = \int_0^1 \frac{T(y)'\, dy}{T_U} = \text{normalized area under the curve } T(y')$$

$$b = \int_0^1 \frac{T_U\, dy'}{T(y')} = \text{normalized area under the curve } 1/T(y')$$

$$X = \frac{h_l}{h_r}$$

$$Y = \frac{T_L}{T_U}$$

Thus 13 becomes

$$(13a) \qquad Y = \frac{1}{X} \quad (a + (X - 1))$$

Rearranging

$$(13b) \qquad Y = \frac{(a + X - 1)}{X}$$

Rearranging

$$(13c) \qquad Y = \frac{(a - 1)}{X} + 1$$

and 9 becomes,

$$(9a) \qquad \frac{1}{Y} = 1 - \frac{1}{X} + \frac{b}{X}$$

substituting 13b for Y

$$(14) \qquad \frac{1}{\frac{(a + X - 1)}{X}} = 1 - \frac{1}{X} + \frac{b}{X}$$

Rearranging we get

$$(15) \qquad 1 = \frac{(X - 1 + b)}{X} \frac{(a + X - 1)}{X}$$

multiplying by X^2 we get

$$(16) \qquad X^2 = (X - 1 + b)\ (a + X - 1)$$

multiplying out gives us

(17) $X^2 = X^2 - 2X + aX + bX + ab - a - b + 1$

Regrouping

(18) $X^2 = X^2 + X(a - 1) + X(b - 1) + (a - 1)(b - 1)$

subtraction X^2 to both sides

(19) $0 = X(a - 1) + X(b - 1) + (a - 1)(b - 1)$

subtract $(a - 1)(b - 1)$ from both sides

(20) $-(a - 1)(b - 1) = X(a - 1) + (b - 1)$

Regrouping give us

(21) $-(a - 1)(b - 1) = X(a - 1 + b - 1)$

dividing by $(a - 1 + b - 1)$ and summing gives us

(22) $X = \dfrac{-(a - 1)(b - 1)}{(a + b - 2)}$

Taking 22 and substituting X from the definition of X and rearranging gives

(23) $b_1 = b_r \quad \dfrac{-(a - 1)(b - 1)}{a + b - 2}$

Taking 13c and substituting Y from the definition of Y and X from 22 gives

(24) $\dfrac{T_L}{T_U} = \dfrac{(a - 1)}{\dfrac{-(a - 1)(b - 1)}{a + b - 2}} + 1$

Rearranging gives

(25) $T_L = T_U \quad \dfrac{(a - 1)(a + b - 2)}{-(a - 1)(b - 1)} + 1$

(26) $T_L = T_U \quad \dfrac{-(a + b - 2)}{(b - 1)} + 1$

```
LAYER  11-NOV-81  MU BASIC/RT-11 V01-01D

1 REM LAYER.B99  WRITTEN 11/81 BY KEN FOOTE
2 REM IT TAKES REK DATA AND CALCULATES LAYER HEIGHT AND TEMPS
50 PRINT "WHAT FILE DO YOU WANT (EX.  REK.2)"; \ INPUT F$ \ F$="DK1:"+F$
60 PRINT "WHAT IS THE FIRST TIME YOU WANT TO SEE"; \ INPUT S0
70 PRINT "WHAT IS THE LAST TIME YOU WANT TO SEE"; \ INPUT S1
100 PRINT CHR$(27),CHR$(12) \ OPEN F$ FOR INPUT AS FILE VF1(20000)
110 IF S1>=VF1(4) THEN S1=VF1(4)
120 FOR J=S0/5*11+5 TO S1/5*11+5 STEP 11
130 R0=0 \ R1=0 \ R2=0 \ C=0 \ H0=4.5
140 PRINT VF1(J);
150 FOR I=1 TO 10
160 PRINT VF1(J+I); \ R0=R0+VF1(J+I) \ R1=R1+(1/(VF1(J+I)+273))
170 NEXT I
200 REM T UPPER IS TAKEN AS THE AVG. OF ALL TEMP ABOVE MEAN
210 M=R0/10 \ M1=R1/10 \ PRINT  \ PRINT "M =";M,
220 E=0 \ IF VF1(J+10)<40 THEN E=5
230 FOR I=1 TO 10 \ IF VF1(J+I)<M+E THEN 250
240 R2=R2+VF1(J+I) \ C=C+1 \ PRINT VF1(J+I);
250 NEXT I \ PRINT
300 IF C=0 THEN H=H0 \ T0=VF1(J+10) \ T1=VF1(J+1) \ GO TO 500
320 T0=R2/C+273
340 REM         THIS CALCULATES THE AREA AND NORMALIZES IT
360 A=(M+273)/T0 \ B=M1*T0
400 REM THIS CALCULATES THE LAYER HEIGHT AND THE LOWER TEMP
420 X=-(A-1)*(B-1)/(A+B-2) \ Y=(A-1)/X+1
440 T1=INT(T0*Y-273) \ T0=INT(T0-273) \ H=INT(H0*X*100)/100
500 PRINT "T LOWER =";T1;"    T UPPER =";T0;
510 PRINT "                      LAYER HEIGHT =";H
520 PRINT  \ PRINT  \ NEXT J \ CLOSE

READY
```

APPENDIX D

- Smoke Dilution System
- Smoke Detector Survey

SMOKE DILUTION SYSTEM

Contrary to our expectations, the aerosol dilution system described in the 2nd and 3rd progress reports of FY 1981 proved to be nearly useless. Consisting of a porous tube concentrically installed in an impervious cylinder, aerosol-laden air (Q_S) flowing axially through the tube is diluted by clean air (Q_D) passing radially through the porous tube. Fire dilution ratio in the combined flow (Q_T) is defined by relative radial-to-axial-flow rates. Q_D momentum allegedly forms an air sheath on the inner surfaces that prevents particulate contact with the wall, but allows for diffusion of pure air into Q_S as shown schematically in Fig. 1. However, if $Q_S + Q_D$ becomes turbulent at some distance down the tube, particulate intrudes through the surface boundary layer and interacts with the walls, thus changing aerosol characteristics. Fig. 2 shows dilution ratios Q_S versus pressure for five sizes of monodispersed aerosols ranging in diameter from 0.364 microns to 3.0 microns. Obviously dilution effectiveness is aerosol-size dependent which is an unacceptable state for analysis.

The method we plan to try next is shown schematically in Fig. 3.

Employing flow transducers used at the University of Minnesota, dilution would be controlled by the amount of dilution air Q_{D2} and air pressure to drive Q_{D1}. Sample inlet tube would be sized to allow isokinetic sampling in the sample stream. The outlet would be open to atmosphere and a sample drawn from it at an isokinetic velocities.

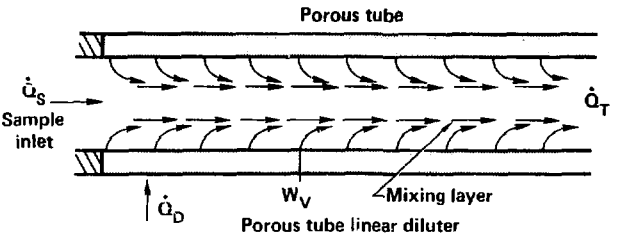

Figure 1.

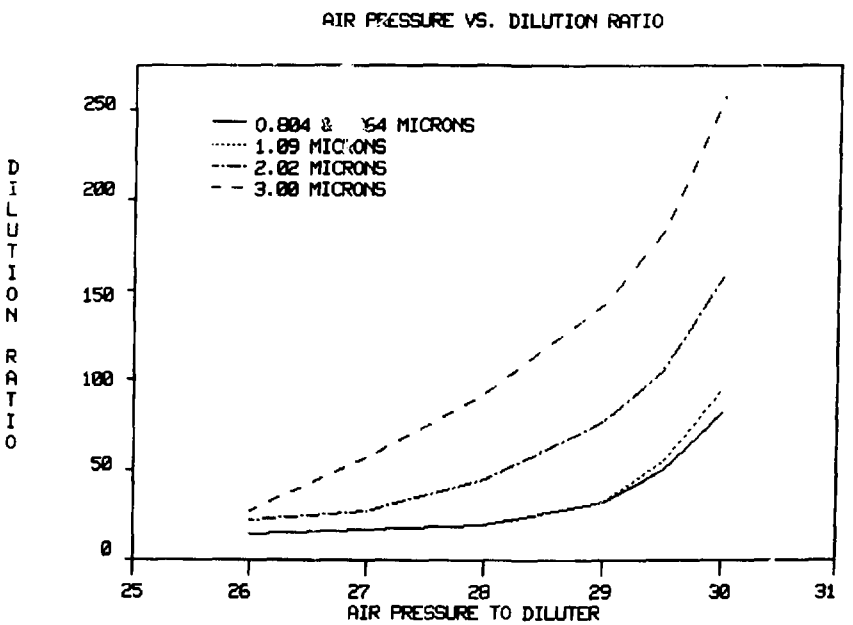

Figure 2.

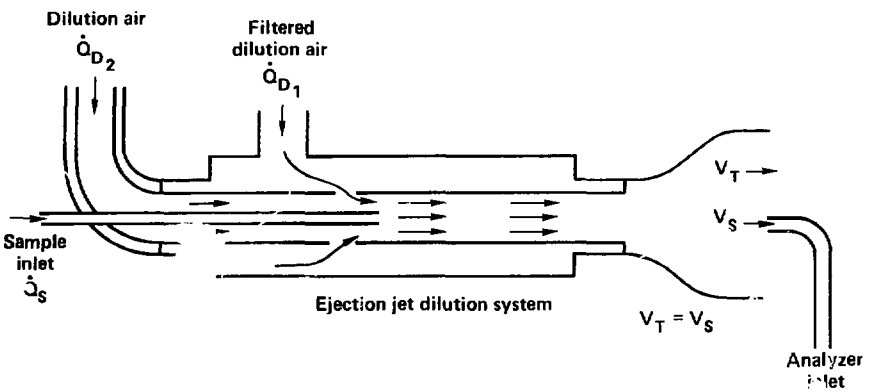
Dilution air
$\dot{Q}_{D_2}$
Filtered
dilution air
$\dot{Q}_{D_1}$
V_T
V_S
Sample
inlet
$\dot{Q}_S$
Ejection jet dilution system
$V_T = V_S$
Analyzer
inlet

Figure 3.

SURVEY OF COMMERCIAL FIRE DETECTORS

The following table condenses state-of-the-art information about the operation and charcteristics of commercially available fire detectors. These data were collected from contemporary reports and brochures representing the range of international manufacturers of smoke and fire detectors.

The survey shows us that commercial detector fabricators are not actively seeking business in special markets such as high-energy-research laboratories. We will not be able to buy "off-the-shelf" detectors that discriminate between smoke aerosols from different burning materials. Thus, our next task will be to directly contact the manufacturers, determine the direction of their research efforts, and to assess their capability to produce individual detection equipment to our specifications.

MAJOR TYPES	SUBGROUPS	INDIVIDUAL DETECTORS	METHOD OF OPERATION	COMBUSTION PRODUCT BEST DETECTED	ADVANTAGES	DRAWBACKS
RADIANT ENERGY						
	Infrared		Infrared component of flame detected by any one of several types of photocells.	Flames	Wide scanning range, respond to shielded signals.	Expensive, require maintinance. Subject to false alarms due to shock. Slow response from smoldering fires.
	Ultraviolet		Ultraviolet flame component detected by various sensing elements.	Flames	Insensitive to sun or artificial light, wide viewing range.	
SUBMICROMETER PARTICLE COUNTING						
	Particle Ionization		Measurement of the variation in electrical charge due to the presence of ionized particles to determine submicrometer particle concentration.	Flames and smoke.	High sensitivity.	Care must be taken to choose proper alarm thresholds to prevent false alarms.
	Condensation Nuclei		Photoelectric measurement of water condensation particles.	Flames and smoke.	Variable sensitivities for various conditions.	
ULTRASONIC			Air movements, caused gases from a fire, disturbs the standing wave pattern of an ultrasonic oscillator and is monitored by an ultrasonic receiver.	Hot gases.	Fairly large area can be monitored.	Can only be used when protected premises are unoccupied.
COMBINATION						
	Photoelectric/ Ionization		Incorporates both photoelectric and ionization chambers in single unit.	Both open flame and smoke fires.	The advantages present in single -stage photoelectric and ionization detectors are present in the combination units.	More expensive than single units. Requires some maintenance. Must be used in clean area.

MAJOR TYPES	SUBGROUPS	INDIVIDUAL DETECTORS	METHOD OF OPERATION	COMBUSTION PRODUCT BEST DETECTED	ADVANTAGES	DRAWBACKS
AERSOL & GAS		Obscuration	Beam of light energy projected across protected area to photosensing receiver, smoke present cuts down on light present, setting off alarm.	Aerosol and gases produced during fires.	Less expensive than ionization types. Not subject to false alarms from humidity and shock. Good response to smoldering fires. Good reliability if maintained. Resetting type.	Possible false alarms due to dust or powders. Slow response to clean fires.
		Scattering	Photosensing device placed out of light beam path, smoke particles present scatter the light causing contact with photosensing device setting off alarm.			More expensive than heat detectors. Slow response to clean fire. Maintenance required.
		Light Attenuation	Beam of light projected to receiver, (photocell/ relay assembly), is reduced by smoke.	Smoke	Good for protection of large open areas.	Slow response due to length of light path. Exposure to light can damange photocells.
	Solid State		Response with large decrease in resistance when exposed to reducing or combustible gases.	Reducing or combustible gases, hydrogen, carbon monoxide, methane, propane, alcohol, volatile oil and acetylene.	Self-restoring	Contamination of sensor. False alarms due to bug spray, cleaning fluids and other commonly used items.
	Resistance Bridge		Decrease of resistance on high resistance grid due to adsorption of aerosol and gaseous products, setting off alarm.	Gases and aerosols.	Able to compensate for slow changes in ambient conditions.	Difficulty with false alarms from moisture and airborne contaminants.
RADIANT ENERGY			Response to infrared or ultraviolet bands.	Smoldering or flaming combustion.	Fast response, good reliability.	Relatively expensive.

MAJOR TYPES	SUBGROUPS	INDIVIDUAL DETECTORS	METHOD OF OPERATION	COMBUSTION PRODUCT BEST DETECTED	ADVANTAGES	DRAWBACKS
RATE OF RISE						
		Pneumatic	Expansion of gases within closed system generates mechanical forces setting off alarm.	Convected thermal energy evolved during combustion.	Fairly inexpensive. Both continuous line and spot type available. Self restoring.	False alarms due to steam leaks, unvented combustion heaters and forced air heating units.
		Thermoelectric	Voltage generation between thermocouples at different temperatures and variations in rate of resistance change with temperature.	" "	Not subject to false alarms, good reliability, little maintenance required.	
AEROSOL AND GAS						
	Ion Chamber		Radioactive material in the sensing chamber gives off a minute electrical current. Smoke particles upon entering the chamber lower the current which is sensed by the circuitry sounding the alarm.	Good for detecting fires with an open flame and little visible smoke present.	Highly sensitive, low electrical stress resulting in low maintainance, radioactive source, with long half-life, never needs replacing.	Easily fooled subject to false alarms from humidity, shock and air velocity.
	Photoelectric		Aerosols generated during fire affect the propagation of light passing through the detector.	Smoke particles present during combustion	Fairly maintenance free,battery periodically replaced, and less occasionally the LED used as the light source detector.	Slow response to hot clean flame. Must be maintained and installed in clean atmosphere to prevent possible false alarms.

MAJOR TYPES	SUBGROUPS	INDIVIDUAL DETECTORS	METHOD OF OPERATION	COMBUSTION PRODUCT BEST DETECTED	ADVANTAGES	DRAWBACKS
CONVECTED ENERGY			Response to thermal energy generated in fire.	All of the following are designed to respond to the convected thermal energy evolved during combustion.	High reliability, low maintenance, and freedom from false alarms.	Slow response to smoldering or slow burning fires.
	Fixed Temperature		Response when operating element reaches preset temperature.	" "	Generally the least expensive type detectors.	
		Eutectic Metal	Activates alarm when metal used reaches its melting point.	" "	Good reliability, good freedom from false alarms.	Must be replaced after activation.
		Glass Bulb	Bulb breaks due to pressure increase causing contacts to close.	" "	Little maintenance, temperature of activation controllable.	Bulb must be replaced.
		Continuous Line	Thermoplastic insulator melts, allowing two steel wires to make contact, setting off alarm.	" "	Some types can be used to determine location of fire, easy installation.	Fused section must be replaced each time.
		Bimetal	Different coefficients of expansions of two metals cause stress, setting off alarm.	" "	Automatic restoration when temperature drops below operation point.	Lack of rapid positive action, prone to false alarms due to vibration.
	Rate of Rise		Operates when temperature change per minute exceeds approximately 15°F (8.33°C).	Convected thermal energy.	Compensates for non-fire ambient temperature changes. Faster reacting than fixed temperature types.	Not fast responding to smoldering or slow burning fires.

MAJOR TYPES	SUBGROUPS	INDIVIDUAL DETECTORS	METHOD OF OPERATION	COMBUSTION PRODUCT BEST DETECTED	ADVANTAGES	DRAWBACKS
COMBINATION						
	Rate of Rise/ Fixed Temperature		Rate of rise function is usually a vented hemispherical air chamber and a flexible diaphragm. Fixed temperature element is either a bimetal strip of leaf spring restrained by eutectic metal.	Heat evolved during combustion.	Quick response to rapidly developing fires by rate of rise and response to slow developing smoldering fires by fixed temperature.	More expensive than single units. Response time to slow burning or smoldering fires slower than rapid developing fires.
	Resistance Bridge/ Ion Chamber		Each detection element has its own bridge circuit which triggers one electronic gate. When a fire signal is present from both gates the detector sound the alarm.	Gases, aerosols and open flame fires.	Sensitive yet not overly prone to false alarms if care is taken with proper placement of units.	False alarms due to common items such as cooking, dust, powder and aerosol sprays.
	Ultraviolet/ Infrared		A predetermined deviation from the prescribed ambient set off alarm.	Flaming fires.	Wide scanning range, response to a shielded signal.	Prone to false alarm signals when used near flashing lights or lights with UV radiation.

U.S. Government Printing Office: 1982/9-587-002/4097

Technical Information Department · Lawrence Livermore National Laboratory
University of California · Livermore, California 94550

First Class Mail